



UNIFORMED SERVICES UNIVERSITY, SCHOOL OF MEDICINE GRADUATE PROGRAMS
Graduate Education Office (A 1045), 4301 Jones Bridge Road, Bethesda, MD 20814



DISSERTATION APPROVAL FOR THE DOCTORAL DISSERTATION IN THE EMERGING
INFECTIOUS DISEASES GRADUATE PROGRAM

Title of Dissertation: "Defining key entry events for Crimean-Congo hemorrhagic fever virus in mammalian cells."

Name of Candidate: Aura Garrison
Doctor of Philosophy Degree
August 10, 2012

DISSERTATION AND ABSTRACT APPROVED:

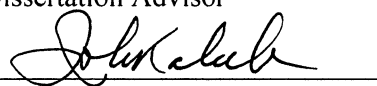
DATE:


Dr. Christopher Broder
DEPARTMENT OF EMERGING INFECTIOUS DISEASES
Committee Chairperson

8/15/12


Dr. Connie Schmaljohn
DEPARTMENT OF EMERGING INFECTIOUS DISEASES
Dissertation Advisor

8/10/12


Dr. Johnan Kaleeba
DEPARTMENT OF MICROBIOLOGY AND IMMUNOLOGY
Committee Member

8/10/12


Dr. Robert Doms
DEPARTMENT OF MICROBIOLOGY, University of Pennsylvania
Committee Member

8/10/12



UNIFORMED SERVICES UNIVERSITY, SCHOOL OF MEDICINE GRADUATE PROGRAMS
Graduate Education Office (A 1045), 4301 Jones Bridge Road, Bethesda, MD 20814



FINAL EXAMINATION/PRIVATE DEFENSE FOR THE DEGREE OF DOCTOR OF PHILOSOPHY
IN THE EMERGING INFECTIOUS DISEASES GRADUATE PROGRAM

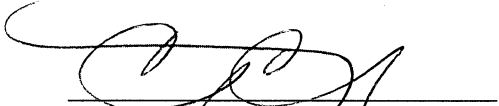
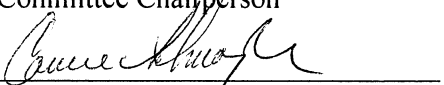
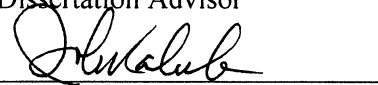
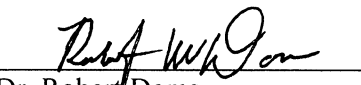
Name of Student: Aura Garrison

Date of Examination: August 10, 2012

Time: 1:00pm

Place: A2015

DECISION OF EXAMINATION COMMITTEE MEMBERS:

	PASS	FAIL
 Dr. Christopher Broder DEPARTMENT OF EMERGING INFECTIOUS DISEASES Committee Chairperson	<input checked="" type="checkbox"/>	<input type="checkbox"/>
 Dr. Connie Schmaljohn DEPARTMENT OF EMERGING INFECTIOUS DISEASES Dissertation Advisor	<input checked="" type="checkbox"/>	<input type="checkbox"/>
 Dr. Johnan Kaleeba DEPARTMENT OF MICROBIOLOGY AND IMMUNOLOGY Committee Member	<input checked="" type="checkbox"/>	<input type="checkbox"/>
 Dr. Robert Doms DEPARTMENT OF MICROBIOLOGY, University of Pennsylvania Committee Member	<input checked="" type="checkbox"/>	<input type="checkbox"/>

The author certifies that the use of any copyrighted material in the dissertation manuscript entitled:

**"Defining key entry events for Crimean-Congo hemorrhagic fever virus in
mammalian cells."**

is appropriately acknowledged and, beyond brief excerpts, is with the permission of the copyright owner.

A handwritten signature in cursive script, reading "Aura Rae Garrison".

Aura Rae Garrison
Emerging Infectious Diseases Graduate Program
Uniformed Services University

ABSTRACT

Defining key entry events for Crimean-Congo hemorrhagic fever virus in mammalian cells.

Aura Garrison, Ph.D., M.S., 2012

Thesis Supervisor: Dr. Connie Schmaljohn, Chief Scientist, United States Army Medical Research Institute of Infectious Diseases

Crimean Congo hemorrhagic fever virus (CCHFV) is an arthropod-borne virus in the genus *Nairovirus* within the family *Bunyaviridae* that causes significant morbidity and mortality in humans. Little is known about CCHFV-host cell interactions, in part due to the requirement for Biological Safety Level 4 containment for studies using infectious virus. Entry studies on other members of the family *Bunyaviridae* indicate that most of the viruses enter by clathrin-mediated endocytosis (CME). However, a clathrin-independent mechanism was described for one virus within the family, which was a cell-dependent phenomenon. All bunyaviruses that have been studied also require endosomal acidification for entry, with some entering through early endosomes (EE) and others through late endosomes (LE).

The goal of this study was to define key cellular entry events for CCHFV. To substantiate earlier work indicating that CCHFV uses CME for entry, we interrupted CME with the clathrin-specific inhibitor Pitstop 2. Pitstop 2 completely blocked CCHFV replication, providing evidence that CCHFV uses CME for entry. In addition, siRNAs to

a protein complex specific for clathrin coated pits, the AP-2 complex, reduced CCHFV replication. Together, these data indicate that CCHFV enters cells by CME.

To explore the pH-dependency of CCHFV entry we compared the sensitivity of CCHFV to various concentrations of ammonium chloride, which prevents the acidification of endosomes, to two control viruses with known EE or LE entry mechanisms. The sensitivity of CCHFV to such treatment was more similar to the EE dependent control virus than the LE-dependent virus. A pH sensitivity assay showed that CCHFV infectivity was inactivated at pH 6.0, which is also consistent with EE entry. Finally, using dominant negative Rab5 and Rab7 GTPase proteins, which are necessary for EE and LE trafficking, respectively, we showed that CCHFV requires Rab5 but not Rab7 for infectivity. Collectively our data are consistent with CCHFV entry through EE, not LE.

Our findings provide confirmatory and novel information concerning two cellular entry events for CCHFV. The data also add to the overall knowledge of the early replication mechanisms of viruses in the family *Bunyaviridae*, and provide clues that could be useful for identifying antiviral targets.

**Defining the mechanism of Crimean-Congo hemorrhagic fever virus entry in
mammalian cells.**

by

Aura Rae Garrison

Dissertation submitted to the Faculty of the
Emerging Infectious Diseases Graduate Program
Uniformed Services University of the Health Sciences
in partial fulfillment of the requirements for the degree of
Doctor of Philosophy 2012

Dedication

I thank the past and present members of Dr. Connie Schmaljohn's lab, particularly Louis Altamura, Lesley Dupuy, and Michelle Richards for all of the laughter and support they have given to me. I also owe a special debt of gratitude to my mentor Dr. Connie Schmaljohn for allowing me to pursue a doctoral degree in her lab, and providing me with tremendous support throughout this endeavor. I would also like to thank Dr. Eleanor Metcalf for all of her guidance along the way. I would also like to thank my graduate school committee members for all of their guidance and advice along the way: Dr. Christopher Broder, Dr. Robert Doms, Dr. Johnan Kaleeba, and Dr. Connie Schmaljohn.

I would also like to thank the other graduate students in the EID program who have made this a wonderful and growing experience. I would like to thank in particular Kenny Lin, Stephanie Petzing and Rachel Vonck for their friendship, encouragement, and laughter throughout my graduate school journey. Additionally, I would like to thank Dr. Dennis Bente, at UTMB, for his advice and encouragement as we shared the trials and tribulations of working with CCHFV.

I would especially like to thank my son, Xavier, for the countless joy he brings to my life. Last but not least, I thank my husband, Jeff, for always encouraging me, making me laugh, and for being so patient through all of this.

Table of Contents

Chapter 1: Introduction	11
Historical Perspective.....	11
Vectors and Animal Hosts	12
Emergence of CCHFV	15
Disease in Humans	18
Treatment and Prevention.....	20
Molecular Biology of Viruses in the Family Bunyaviridae.....	21
Structure, genome and encoded proteins.....	23
Attachment	28
Internalization	31
Uncoating.....	38
Aims and hypotheses	48
Chapter 2: Materials and Methods.....	49
Cells, viruses, and pseudoviruses.....	49
Determining CCHFV growth kinetics to increase yield	50
Monoclonal antibodies, immunofluorescence, and imaging	51
HCI statistics.....	52
CCHFV and clathrin heavy chain co-localization	53
CME inhibition with Pitstop 2	54
siRNA-mediated knockdown.....	54
Lysosomotropic drug assay.....	56
Dominant negative blockage of CCHFV entry and fusion.....	57
Flow Cytometry.....	58
Trypsin-sensitivity of CCHFV binding to 293T cells	59
Fc-tagged protein cloning and purification.....	60
Non-permissive cell line infection and analysis	62
Chapter 3. Development of High Content Screening Assay	64
Introduction	64
Results.....	66
Analysis of results and conclusions.....	75
Chapter 4: Clathrin-dependent entry of CCHFV	77

Introduction	77
Results	78
Analysis of Results and Conclusions	89
Chapter 5: Endosomal Trafficking of CCHFV	93
Introduction	93
Results	94
Analysis of Results and Conclusions	103
Chapter 6: Additional CCHFV entry studies	105
Introduction	105
Results	107
Analysis of Results and Conclusions	118
Chapter 7: Discussion	120
Preface	120
Experimental results in the context of the project aims.	121
Contributions to the field of bunyavirus entry	123
Unanswered questions	125
Limitations of the study	127
Future directions of research	129
Conclusions	134
References	135

List of Tables

Table 1. NCI-59 cell line library and CCHFV replication.	111
Table 2. List of 25 common plasma membrane proteins genes expressed in permissive cells with low or no expression in non-permissive cells.	114

List of Figures

Figure 1: Geographical distribution of CCHFV as of January 2012.	16
Figure 2. Clinical and laboratory course of CCHFV	19
Figure 3. Bunyavirus structure.	24
Figure 4. Bunyavirus genome strategies.	26
Figure 5. Replication cycle of viruses in the family Bunyaviridae.	30
Figure 6. Clathrin coated pit formation.	34
Figure 7. The mechanism of action and binding domain of Pitstop 2.	40
Figure 8. Class II fusion.	46
Figure 9. Growth kinetics of CCHFV IbAr 10200 in CER and HepG2 cells.	67
Figure 10. A schematic of the HCI assay used to study CCHFV entry events with transfected cells expressing GFP, and IFA staining of the viruses used in this study.	70
Figure 11. HCI parameters in A549 and 293 T cells.	72
Figure 12. The effect of MOI on VSV-eGFP and VACV-eGFP infection in A549 cells.	73
Figure 13. Parameters of control virus HCI in 293T cells.	74
Figure 14. Co-localization of CCHFV and transferrin with clathrin in A549 cells.	80
Figure 15. Co-localization of CCHFV and clathrin heavy-chain in HepG2 cells.	81
Figure 16. CCHFV has minimal co-localization with caveolin in HepG2 cells at 60 minutes post infection.	82
Figure 17. CCHFV uses AP-2 to enter A549 cells.	86
Figure 18. CCHFV entry is mediated by the clathrin-dependent pathway.	88
Figure 19. CCHFV entry is acid-dependent.	95
Figure 20. Threshold of pH inactivation.	97
Figure 21. CCHFV is Rab 5 dependent.	100
Figure 22. CCHFV is not Rab 7 dependent.	102
Figure 23. Trypsin treatment decreases CCHFV attachment to 293T cells.	109
Figure 24. Flow cytometry confirmation of non-permissive cell lines for CCHFV infection.	113
Figure 25. CCHFV GN-Fc production and binding to 293T cells.	117

Chapter 1: Introduction

Historical Perspective

Crimean-Congo hemorrhagic fever virus (CCHFV), a member of the *Nairovirus* genus in the family *Bunyaviridae*, is a viral pathogen of interest because of its high mortality rate, transmissibility, and extensive geographic distribution. The first reported outbreak of Crimean-Congo hemorrhagic fever (CCHF) occurred from 1940 to 1945 when approximately 200 Soviet soldiers were infected in Crimea. The causative agent was identified in 1967 when Russian and Pakistani scientists isolated a virus from newborn mouse brain and newborn rat brain tissues after intracranial injection of patient sera; the virus was termed Crimean hemorrhagic fever (CHF) virus [1, 2] (reviewed in [3]). In 1968, American scientists were investigating virus strains from patients in the Congo and Uganda, which was registered in 1969 as Congo virus in the Catalogue of Arthropod-borne Viruses of the World [1-4]). In 1969, work by both Russian and American scientists revealed that the two viruses were antigenically indistinguishable, and disputes over naming the virus began [5]. The Soviet scientists insisted on keeping the name CHF virus, but as a compromise the designation CHF-Congo virus was suggested. The name Crimean-Congo hemorrhagic fever virus (CCHFV) was suggested by Darwish et al. in 1978, as they thought the name CHF-Congo was awkward, and the designation CCHFV was generally accepted by the 1980s [3, 6].

CCHFV has the widest distribution of any tick-borne virus causing human disease, and is found in over 30 countries throughout parts of Europe, the Middle East, Asia, and Africa [7, 8]. Although CCHF outbreaks occur only sporadically, CCHFV has recently received renewed attention because of increased cases and the potential for its

use for biological warfare or bioterrorism. Accordingly, CCHFV is listed as a Select Agent on the Centers for Disease Control (CDC) registry, and as a Category C Biological Disease Threat by the National Institutes of Allergy and Infectious Diseases (NIAID) because of its potential for high morbidity and mortality and its major health impact [9].

Vectors and Animal Hosts

CCHFV circulates in a tick-vertebrate host-tick cycle, and causes either no or very mild disease in the natural vertebrate hosts. CCHFV has been isolated from over 31 species of ticks and 1 species of biting midge. Ticks in the family *Ixodidae* are the only known competent vectors for CCHFV; thus, the isolation of CCHFV from other arthropods does not imply that they are also CCHFV-competent vectors, as CCHFV might have simply been present in a recent blood meal. CCHFV was isolated from *Hyalomma* spp. ticks in the 1970s and they are recognized as the primary vector for CCHFV. These ticks are able to transmit the virus transstadially (as the tick matures from the larvae and nymph stage to the adult stage), transovarially (from mother to eggs), horizontally (while feeding on the same host), and venereally [3, 10].

Ticks in the larvae and nymph stages typically feed on small mammals, such as hares, hedgehogs, and mice. These mammals serve as amplifying hosts and are important for the transstadial transmission, and for maintaining the virus in nature. One epidemiological study of small animals found CCHFV antibodies in 3% of 274 small mammals in northern Iran [11]. Adult ticks feed on large mammals such as cattle, sheep, goats, domestic dogs, baboons, and gazelles, and these animals can also serve as amplifying hosts [12-15].

In laboratory studies, numerous species of wild-caught or laboratory-bred small animals have been found to be capable of supporting CCHFV replication without suffering apparent disease. Shepherd et al. experimentally infected 11 species of African small wild or laboratory mammals with two African strains of CCHFV, SPU 4/81 and SPU4/54, which were respectively isolated from a fatal human case and non-fatal human case. In this experiment only hares of the genus *Lepus* developed viremias high enough to be considered an amplification host but as the authors note, this species alone would be insufficient to maintain the virus in nature. In southern Africa these hares are only fed upon by one of three *Hyalomma* spp. of ticks in the region, *Hyalomma truncatum*, thus they would not serve as amplification hosts to the other *Hyalomma* species in which CCHFV has been isolated. Most of the infected small animals studied developed detectable antibody responses and the virus cleared within seven days [16]. The results of the study by Shepherd et al. contrasted with those found in a previous study by Soviet scientists comparing 12 CCHFV strains from the former Soviet Union, Africa, and Pakistan [17]. In this study, higher viremias were detected in all of the animals (adult white mice, cotton rats, guinea pigs, rabbits, Syrian hamsters), and they cleared the virus within 7 days. All of the adult animals developed antibody responses to the infection, and all of the newborn small animals (white mice, white rats, and cotton rats) succumbed to infection. Shepherd et al. surmised that the differences in viremias in the adult animals were due to the differing routes of infection, subcutaneous (Shepherd) versus intracranial and peripheral (Smirnova), and adaptations of the virus that increased virulence due to more passages in mouse brains in the work by Smirnova et al. [16]. Both studies revealed that most small animals are capable of replicating the virus at least to very low levels, as

indicated by antibody responses, which supports the theory that small mammals can serve to maintain the virus in nature. Although reptiles and birds, with the exception of ostriches, appear to be resistant to infection by CCHFV, migratory birds may contribute to the spread of the disease, as they may transport infected ticks across large geographical areas [15]. Viremia and antibody responses were detected in all of the large animals tested (sheep, rhesus macaque monkeys, donkeys, calves, patas monkeys, and baboons) but only mild disease was observed in laboratory-infected sheep, calves, and baboons, with only the baboons and sheep developing neutralizing antibody responses to CCHFV [13, 18, 19]. The lack of significant pathogenesis in all of the mammalian species tested, other than newborn mice, rats and guinea pigs, underscores the difficulty in developing an animal model to mimic CCHF pathogenesis in humans for the study of therapeutics and vaccines.

Humans are considered accidental hosts of CCHFV. Although human infections generally result from tick-bite transmission of CCHFV, humans can also contract CCHF through exposure to virus in infected animal blood or tissues during animal slaughter, crushing of infected ticks, and through nosocomial infection. For example, a human outbreak of CCHF occurred among workers at an ostrich abattoir in 1996 in South Africa, which led to a 30 day pre-slaughter quarantine period rule in South African ostrich export facilities [20]. Nosocomial infections of hospital workers has occurred on numerous occasions, with the highest risk for contracting CCHFV associated with procedures to treat gastrointestinal bleeding and emergency surgical procedures performed on patients that have not yet been diagnosed with CCHFV [21].

Emergence of CCHFV

Since the early 2000s, the annual number of documented CCHF cases in endemic regions has drastically increased, and the disease has been recognized in an increasing number of countries (**Fig. 1**). Most notably, reported cases of CCHF in Turkey have risen from 20 in 2002 and 2003, to over 1,300 in 2008 [22]. Similarly, after almost 27 years without any reported human cases, 1,300 clinical cases of CCHF were diagnosed in the Russian Federation from 2000 to 2009. In Greece, an assumed nonpathogenic strain of CCHFV, AP-92, was isolated in 1975 from *Rhipicephalus bursa* ticks. Seroprevalence studies conducted from 1981-1988 and from 2009-2010 revealed that 1.1% and 4.2% respectively of the human population in Greece had antibodies to CCHFV, presumably to the AP-92 strain [23, 24]. The first clinical case of CCHF, which was fatal, was recorded in Greece in 2008 [25, 26]. This case resulted in one additional fatal contact case. The CCHFV strain responsible for these two fatal cases differed significantly from the AP-92 strain, and resembled strains associated with severe disease that circulate in the Balkan Peninsula, Russia, and Turkey. The first fatal case of CCHF ever reported in India occurred in 2010. A nosocomial outbreak of three additional fatal cases resulted from contact with the first patient, and one familial contact contracted the disease and survived [27, 28]. Further cases of CCHF associated with tick bites have been reported in India since then, which have also resulted in nosocomial outbreaks [29]. Because of the potential for human-to-human transmission of CCHFV, community outbreaks and nosocomial outbreaks are a significant public health concern throughout the endemic disease region. Secondary cases are reported to often be more severe with higher mortality than primary cases [5].

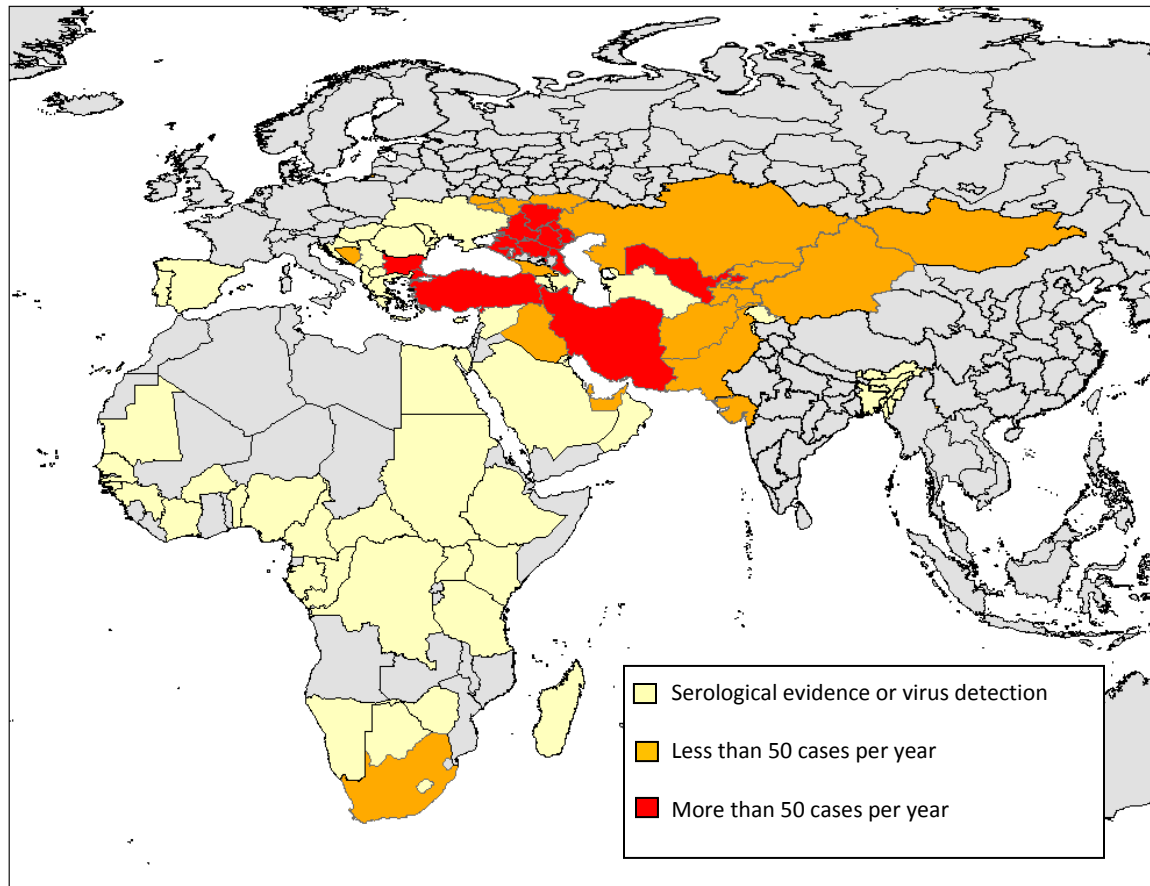


Figure 1: Geographical distribution of CCHFV as of January 2012. Yellow = serological evidence or virus detection. Orange = less than 50 cases per year. Red = more than 50 cases per year.

Re-printed with kind permission from Dennis Bente (University of Texas Medical Branch) (personal communication).

There is either a perceived emergence of CCHFV due to an increase in diagnostic capabilities, and increased disease surveillance and reporting, or an actual emergence of the disease in Europe, which is a point for debate. The numbers of reported cases have increased in endemic regions and the disease has been reported in countries recently that are not considered endemic. A serosurvey was conducted in an outbreak region in Turkey that found 10% of the population had antibodies to CCHFV that increased with the patient age. In addition, these investigators also estimated that 88% of CCHFV infections were subclinical [30]. The increased number of individuals with CCHFV specific antibodies among subjects age 60 and above suggested that the virus has been circulating for decades in Turkey, and only recently (2002) has it been recognized in the country. Additional and continued serosurveys in regions where CCHFV cases occur are needed to resolve whether or not the actual incidence of CCHFV infections are increasing, or if the perceived increase is due to a better recognition and diagnosis of the disease. There are several theories attributed to the possible emergence of CCHFV in Europe, based on several studies aimed at assessing the impact of climate change and vegetation features on the spread of vector-borne viruses [22, 31]. The geographical distribution of the virus coincides with the range of its *Hyalomma* tick vector; consequently, increasing either the range or number of ticks carrying CCHFV impacts human exposure to the virus. Factors implicated in expansion and distribution of the *Hyalomma* tick vectors include changes in climate, land use, agricultural practices, hunting practices, and livestock movement, all of which could increase the interactions between ticks and animals that can serve as viral amplification hosts. Estrada-Pena et al. found that high fragmentation of land, which can lead to greater contact between the

vector and the animal reservoir, had the highest correlation with CCHFV cases in Turkey between 2003 and 2008 [22]. Likewise, an increase in the tick vector population or an expansion into areas inhabited by humans also increases the probability that ticks carrying CCHFV can feed on humans, resulting in viral emergence [7, 21].

Disease in Humans

The disease course of CCHFV occurs in four phases: incubation, pre-hemorrhagic, hemorrhagic, and convalescence. After infection, the incubation phase usually lasts for about 3-7 days, and the timing probably depends on the route of exposure and the viral dose (**Fig. 2**) [3, 32]. Following the incubation phase there is a pre-hemorrhagic phase that lasts from 1-7 days and results in a rapid onset of acute febrile illness with severe fever, headache, nausea, diarrhea, muscle aches, photophobia, and other non-specific flu-like symptoms [3, 5, 32]. Soon after the onset of illness, the circulating virus can be detected in blood by reverse transcriptase polymerase chain reaction (RT-PCR). Patients with high levels of circulating virus (e.g., 10^9 genomes per ml of plasma) have a poorer prognosis than those with lower circulating virus levels.

As patients progress to the hemorrhagic phase, which typically lasts from 1-3 days, viremia decreases. Hemorrhages, ranging from petechiae to large areas of ecchymosis to profuse bleeding, are often more pronounced in CCHF than in other viral hemorrhagic diseases [21]. In severe cases, the coagulation cascade is disrupted and the patient rapidly progresses and succumbs to infection due to disseminated intravascular coagulation, bleeding, multi-organ failure, and shock [33, 34]. Mortality rates of 10%-70% have been reported for various CCHF outbreaks and it is not clear if the large range is due to

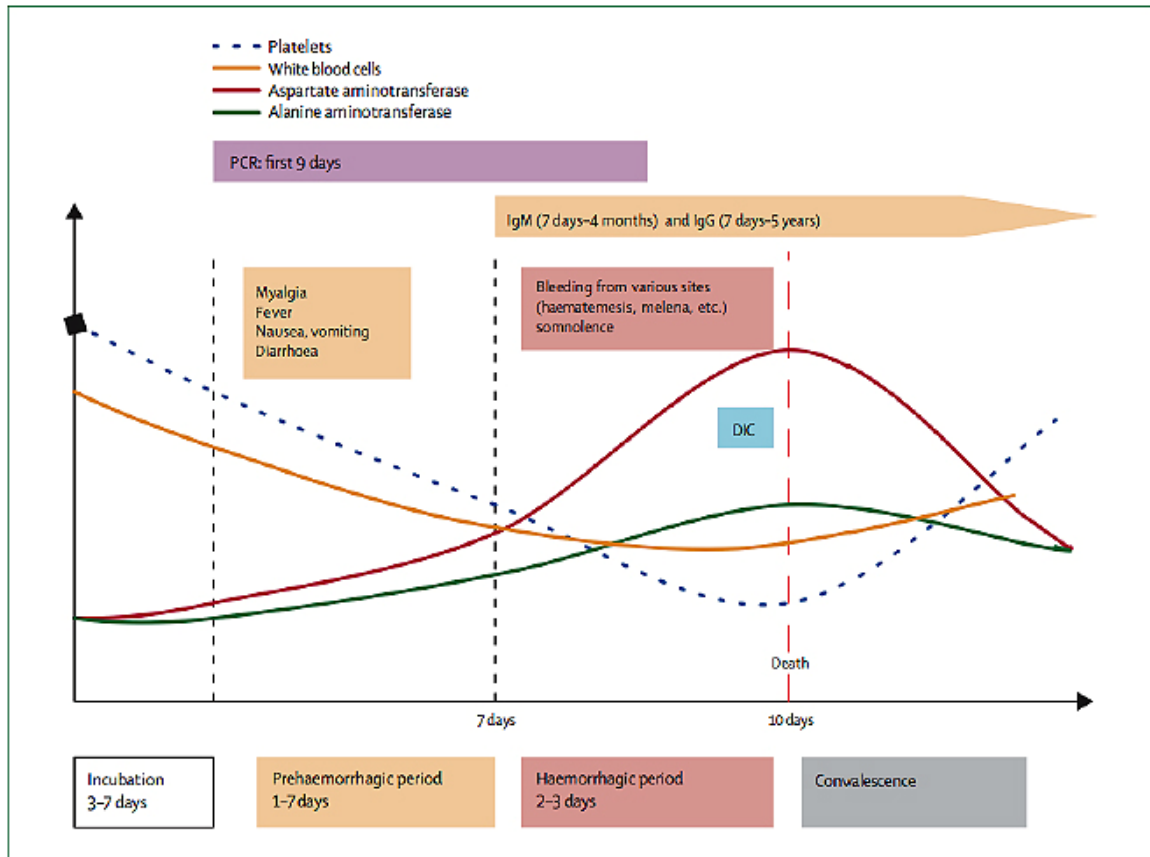


Figure 2. Clinical and laboratory course of CCHFV

From [21]. Reprinted with permission Elsevier.

differences in the virus itself, or to other factors such as route of exposure or dose of the infecting virus (reviewed in[35])[36]. Clinical laboratory features of CCHF include thrombocytopenia, an increase in serum aspartate and alanine aminotransferase levels, and depending on sample collection time, either an increase or decrease in the total white blood cell count. Additionally, there is a prolongation of prothrombin and partial thromboplastin times, a fall in the fibrinogen level, and lymphocytopenia. One hallmark of CCHF is hemophagocytosis, which is the destruction of platelets, some leukocytes, and erythrocytes by reactive histiocytes [37-39].

An early marker of survival is the development of an IgM response starting at about 7 days post infection, which is generally absent in fatal cases [21]. In patients that survive, the convalescent phase begins about 10-20 days after symptoms first appear, and is characterized by sequelae that may last up to a year or more. These sequelae can include severe weakness, bradycardia, headache, polyneuritis, dizziness, nausea, loss of memory, poor appetite, sweating, complete hair loss, and hearing loss. Following convalescence, CCHFV-specific IgG can be detected for several years after infection in these patients.

Treatment and Prevention

The treatment for CCHF is primarily supportive therapy to prevent dehydration, as well as constant monitoring of blood volume and blood chemistry for the replacement of blood components when necessary. Some observational studies have shown that patients who are given the antiviral drug ribavirin very early in the disease course have a higher rate of survival [40]; however, other observational studies have not found ribavirin to increase survival. Although data from statistically controlled studies are not available, ribavirin remains the only treatment option other than supportive therapy given to

patients suspected to have contracted CCHFV [41]. There is no proven safe and effective vaccine available for CCHFV, although there is an inactivated mouse-brain derived CCHFV vaccine used on a small scale in some areas of Eastern Europe [3, 42]. Research into CCHFV vaccines is severely hindered as there is an absence of an immune-competent animal model for CCHFV. There are two lethal CCHFV models in adult mice with defective interferon responses [43], [44]. Neutralizing antibodies were elicited in immune-competent mice in response to a DNA vaccine containing the M segment [45], but further evaluation in the STAT-1 knockout animal model was inconclusive (unpublished data, USAMRIID).

To prevent CCHFV infection, persons living in endemic areas are advised to use personal protective measures to avoid tick bites when the tick vectors are most active, in the spring and fall. They should regularly examine and remove ticks from clothing and skin, as well as use repellent. In endemic areas, persons in contact with livestock and other animals are also advised to take practical measures such as using repellent, and wearing gloves and other protective clothing to avoid exposure to infected tissue and blood [46]. As nosocomial outbreaks are a real concern, it is advised that patients suspected to have CCHFV infections be isolated if possible and hospital staff should use barrier techniques when in contact with the patient. Universal precautions should be used when handling patients' body fluids in particular.

Molecular Biology of Viruses in the Family Bunyaviridae

The family *Bunyaviridae* is made up of over 300 viruses and includes four genera (*Hantavirus*, *Nairovirus*, *Orthobunyavirus*, and *Phlebovirus*) of animal viruses and one

genus (*Tospovirus*) of plant viruses. Except for hantaviruses, bunyaviruses are arthropod-borne, with vectors that include including mosquitoes, culicoid flies, sandflies, ticks, and thrips. Hantaviruses are carried by persistently infected rodents and are spread through aerosolized rodent excreta (reviewed in[35]).

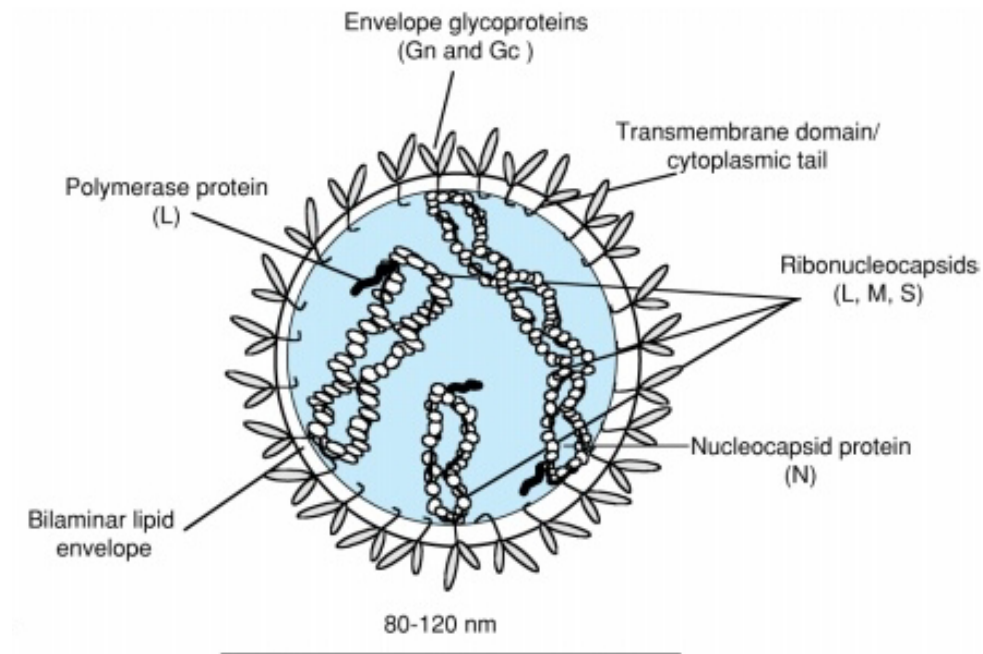
The family *Bunyaviridae* includes a number of important human or animal pathogens, although many members are not known to be pathogenic. Several orthobunyaviruses, such as California encephalitis virus (CEV), La Crosse virus (LACV), and Jamestown Canyon virus (JCV), cause encephalitis in humans. Phleboviruses can also cause human disease, such as Rift Valley fever virus (RVFV), which causes a range of disease manifestations from a mild febrile illness, retinitis, encephalitis, hepatitis, to a fatal hemorrhagic fever [47]. Other phleboviruses that cause human diseases include sandfly fever Sicilian virus (SFSV) and sandfly fever Naples virus (SFNV), which both cause febrile illnesses and encephalitis and meningitis [48]. Hantaviruses are classified on their geographical distribution and their ability to cause two types of human disease. Old World hantaviruses (e.g. Hantaan virus, HTNV, and Seoul virus, SEOV) cause hemorrhagic fever with renal syndrome (HFRS) which presents with renal dysfunction, thrombocytopenia, and hemorrhage [49]. New World hantaviruses (e.g. Sin Nombre virus, SNV, Andes Virus, ANDV) cause hantavirus pulmonary syndrome, which presents with lesser renal involvement than HFRS, acute respiratory failure, thrombocytopenia, and reactive lymphocytosis [49]. Among the nairoviruses, CCHFV and Nairobi sheep disease (NSDV) virus are the most significant human and livestock pathogens, respectively [35, 50]. NSDV causes acute hemorrhagic gastroenteritis in sheep and goats [51]. The family also includes significant plant pathogens in the genus *Tospovirus* such as

tomato spotted wilt virus (TSWV), which infects over 925 plant species, including many important crop species. Crop losses due to TSWV can amount to more than a billion dollars annually (reviewed in[35]).

Structure, genome and encoded proteins

Bunyavirus virion particles have a diameters ranging from 90-140 nm and contain spike-like projections of 5-10 nm (**Fig. 3**) [35, 52, 53]. The bunyavirus genome consists of three segments of single strand RNA designated as large (L), medium (M) and small (S), which respectively minimally encode the four structural proteins: the viral RNA dependent RNA polymerase (RdRP), two envelope glycoproteins (G_N and G_C), and the nucleocapsid protein (N) [35], [54]. Phleboviruses and tospoviruses also encode nonstructural proteins in virus-sense RNAs; thus, these viruses have ambisense gene segments (**Fig. 4A**). For most bunyaviruses the mRNA of the M segment contains a single continuous ORF that is co-translationally cleaved in the ER to form mature G_N and G_C . There is a great diversity in the size of the mature glycoproteins among the genera, which is shown in Figure 4A. All bunyaviruses, with the exception of hantaviruses, have a non-structural protein coded in the M segment (NS_M). Nairoviruses have the most complex processing among the bunyaviruses as the M polyproteins requires processing through a series of glycoprotein intermediates to generate the mature glycoproteins (**Fig. 4B**) [55-57]. First, the M polyprotein is co-translationally cleaved, presumably by a signal peptidase, into Pre G_N (140kDa) and Pre G_C (85kDa). The serine protease subtilisin-kexin isoenzyme-1/site-1-protease (SKI-1/S1P) then releases the mucin-GP38 domain of the N-terminus of Pre G_N , which is then further processed by furin to generate

A.



B.

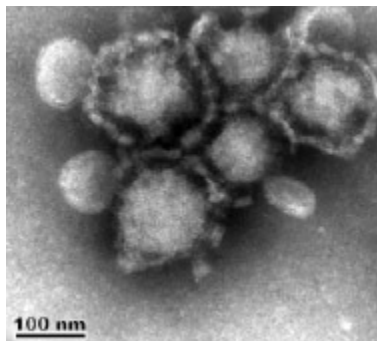
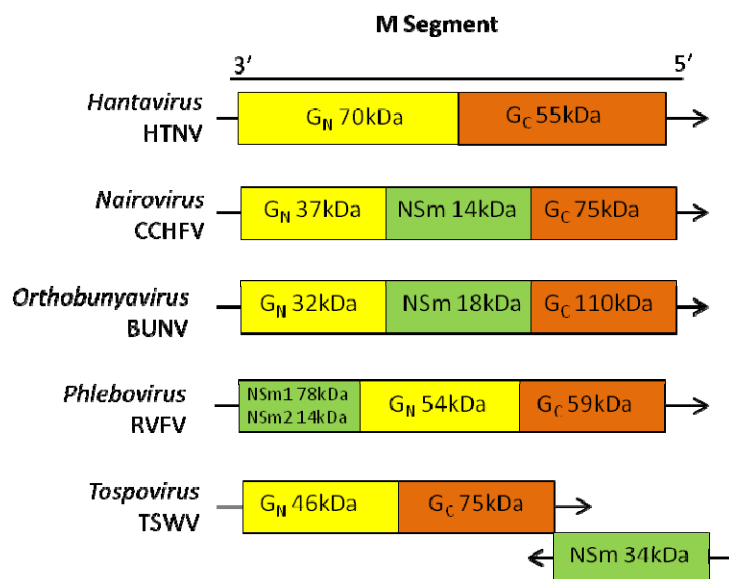


Figure 3. Bunyavirus structure. A. General bunyavirus virion structure. B. Electron micrograph image of negatively stained CCHFV.

A. From the book *Fields Virology*, Fifth Edition, 2006, figure 49.1, page 1747, chapter 49: *Bunyaviridae*, Schmaljohn and Nichol [35]. Reprinted with permission from Wolters Kluwer Health.

B. From [53]. Reprinted with permission from the American Society for Microbiology.

A.



B.

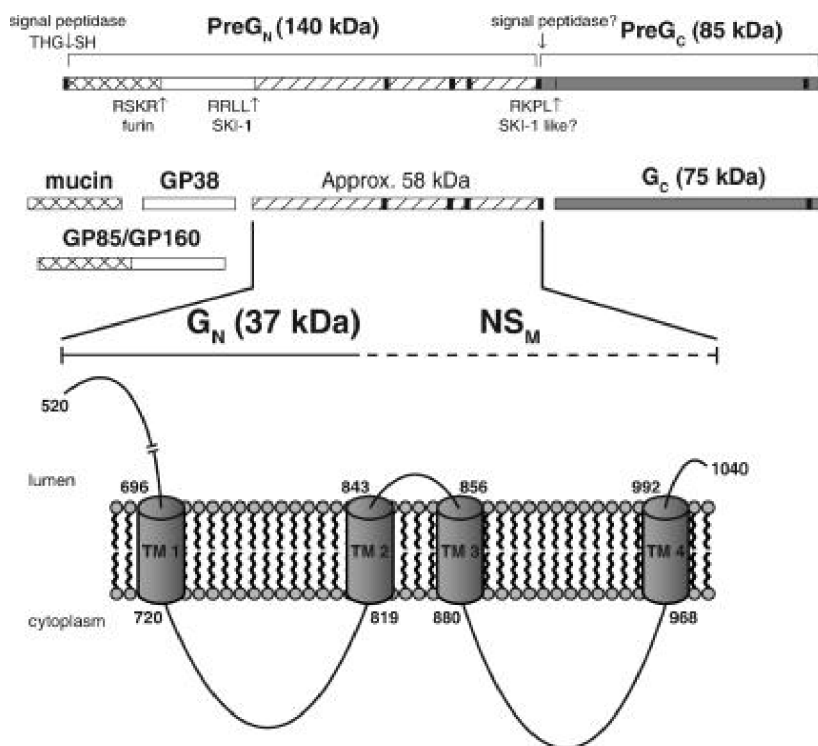


Figure 4. Bunyavirus genome strategies. A. Coding strategies of genome segments of the family *Bunyaviridae*. B. A schematic of the CCHFV M segment-encoded polyprotein processing is shown, with known and suspected cleavage sites indicated. Signal peptidase is thought to generate the N terminus of the polyprotein and may also liberate PreG_C as indicated [55]. The mucin-GP38 domains are liberated by SKI-1 cleavage following the RRLL cleavage site to generate the N terminus of G_N at amino acid 520 [54, 55]. A second cleavage event, perhaps also mediated by SKI-1 or a similar protease, produces the N terminus of G_C at residue 1041 following the sequence RKPL [55]. Further cleavage by furin following the RSKR motif separates the mucin-like domain from GP38 [58]. The region defined by the N termini of G_N and G_C encodes a 58-kDa polypeptide having four predicted transmembrane domains, indicated by black bars. Since mature G_N is approximately 37 kDa, an additional C-terminal processing site may exist between G_N and G_C, leading to the generation of an NS_M protein. The uncertain boundaries of this putative NS_M protein are indicated by a dashed line. The cylinders labeled TM 1 to TM 4 represent the four predicted transmembrane helices between the ectodomains of G_N and G_C. Amino acid boundaries for each helix were predicted with TMHMM 2.0 [59].

Figure 4B is from [57]. Reprinted with limited editing with permission from American Society for Microbiology.

the secreted glycoproteins GP38, GP85, GP160, and possibly a mucin-like protein [55, 56, 58]. NS_M separates from the C-terminus of G_N, releasing the 37kDa mature G_N [57].

The glycoprotein spikes on the surfaces of the virions are proposed to be composed of either hetero- or homo-oligomeric dimers or trimers of G_N and G_C. Cryo-electron microscopy (Cryo-EM) studies of RVFV and cryo-EM and cryo-electron tomography (cryo-ET) studies of HTNV have provided some evidence that the spikes are composed of G_N-G_C heterodimers [60, 61]. To date, crystal structures have not been reported for the glycoproteins of any bunyavirus; however, cryo-ET studies of the phleboviruses, Uukuniemi virus (UUKV) and RVFV, and the hantavirus, HTNV, and a cryo-EM study of the orthobunyavirus LACV revealed that these bunyaviruses have plasticity in their glycoprotein lattices [52, 60-63]. Phleboviruses appear to be the most structured of the bunyaviruses, having a T=12 icosohedral glycoprotein lattice structure, while HTNV and a nonpathogenic hantavirus Tula virus, lacked the icosohedral symmetry but the glycoproteins are instead organized into tetrameric spikes [60, 61].

These microscopy studies also revealed conformational changes in the glycoprotein spikes of UUKV and LACV in response to a drop in pH from pH 7.0 to pH 6.0, or from pH 7.0 to pH 5.4, respectively. For UUKV the glycoprotein spikes were measured at approximately 13 nm in height at pH 7.0, and approximately 8 nm in height at pH 6.0, indicating a conformational shift. Additional evidence that bunyavirus glycoproteins undergo conformational changes in response to pH includes that G_C of the orthobunyaviruses CEV, BUNV and LACV, the glycoproteins of the hantavirus HTNV, as well as the phlebovirus RVFV, promote cell-cell fusion at low pH [64-68]. G_C of CEV also shows altered detergent binding and altered protease cleavage patterns in response to

low pH indicating that the glycoprotein undergoes conformational changes at low pH [69]. It was also found that G_C of LACV forms oligomers upon low pH treatment, as well as changes as antigenic changes that showed altered monoclonal binding to G_C in response to low pH as compared to native G_C [70]. This conformational change is thought to have a functional significance for viral entry, in particular for virus fusion with the host membrane. All of the bunyaviruses studied to date appear to undergo fusion with cells in response to a low pH trigger, which will be discussed further in the *Uncoating* section below.

Similar microscopy and biochemical studies have not been reported for CCHFV, probably in part due to the requirement for a Biosafety level 4 (BSL-4) containment laboratory to work with infectious virus, and because the virus grows to very low titers in cell culture systems tested so far. For these same reasons, most steps in the replication process of CCHFV have remained undefined. In addition, the glycoproteins of CCHFV, when over-expressed in cells, do not traffic to the cell surface [71], so similar cell-cell fusion experiments described above have not been reported to characterize the conformational changes in the glycoproteins in response to pH. A recent publication describing the production of soluble G_C and G_N of CCHFV [72], as well as my own work described in Chapter 6, may be useful for the biochemical analysis of the glycoproteins in response to low pH.

Attachment

Although very little is known about CCHFV attachment and entry, a few studies with viruses in other genera of the family *Bunyaviridae* provide direction for dissecting CCHFV attachment. In general, the first step in bunyavirus entry requires an interaction

between cell surface receptors and the viral envelope proteins, G_N and/or G_C (**Fig. 5**). Host cell receptors have not been identified for most viruses in the family; however, pathogenic and nonpathogenic hantaviruses were shown to use $\beta 3$ and $\beta 1$ integrins, respectively, to enter endothelial cells [73, 74]. Other interactions reported include binding to dendritic cell-specific intercellular adhesion molecule-3-grabbing non-integrin (DC-SIGN) for UUKV and RVFV, but as these viruses also infect cells that do not express DC-SIGN, there must be additional unidentified receptors for these viruses [75].

For the orthobunyaviruses CEV, LACV, and Tahnya virus, G_C appears to be the main viral attachment protein required for entry into mammalian cells, mosquito cells, and mosquitoes [76-81]. For phleboviruses and hantaviruses, the presence of neutralizing and hemagglutination-inhibiting sites on both G_N and G_C suggest that both proteins may be involved in attachment [35, 67]. Although it is possible that both are directly involved, it is more likely that both are essential due to conformational requirements that depend on dimerization of G_N and G_C .

A receptor study for CCHFV suggested that nucleolin is a possible entry factor [72]. Data obtained in my research studies, presented in Chapter 6, indicate that the cell receptor for CCHFV is sensitive to trypsin. Additionally, we identified for the first time several cell lines that do not support the productive replication of CCHFV. These cell lines, which are described in Chapter 6, may prove to be valuable tools for future studies on specific receptors for CCHFV.

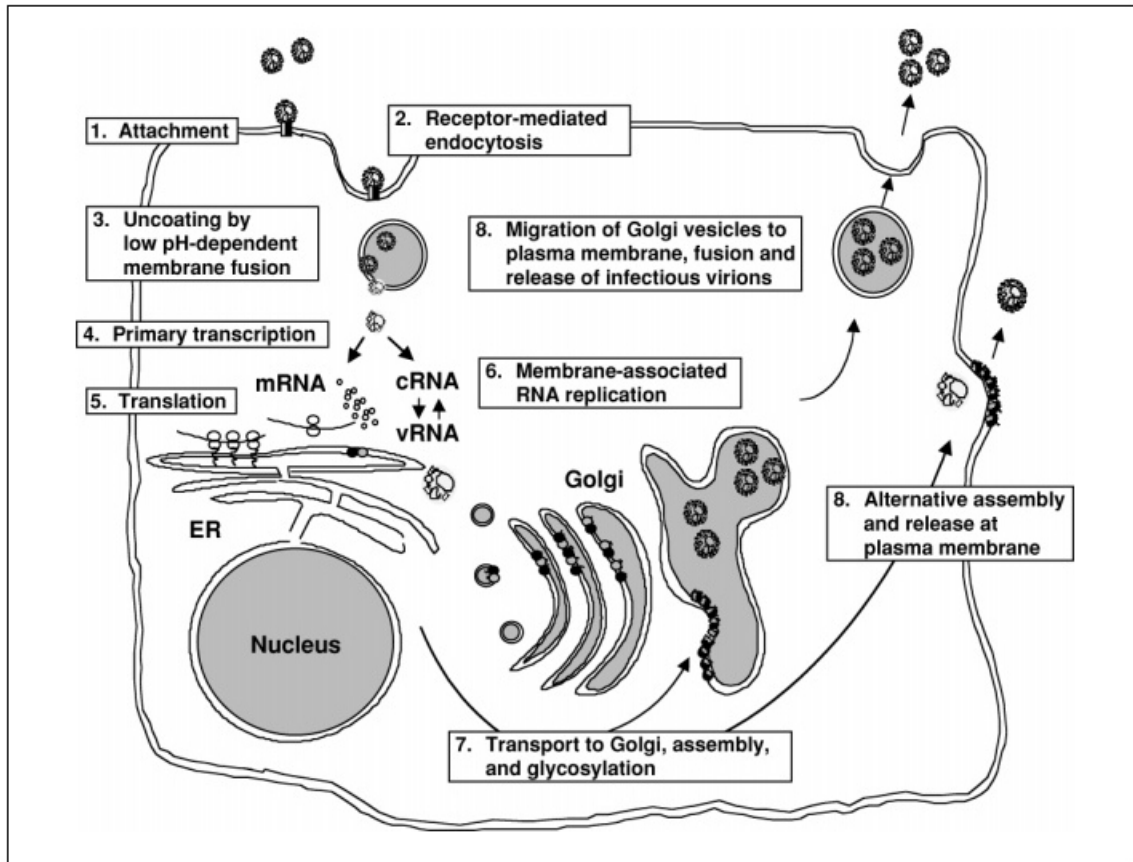


Figure 5. Replication cycle of viruses in the family Bunyaviridae. Steps in the replication cycle are: 1. Attachment, mediated by interaction of viral proteins and host receptors; 2. Receptor-mediated endocytosis; 3. Uncoating, by fusion if viral membranes with endosomal membranes following vesicle acidification; 4. Primary transcription of viral-complimentary mRNA species using viral RNA-dependent RNA polymerase; 5. Translation of L, M, and S mRNAs, cotranslational cleavage of the M segment polyprotein, and dimerization of G_N and G_C in the ER; 6. Genome replication; 7. Morphogenesis with transport of the structural proteins to the Golgi, glycosylation of G_N and G_C , and budding into the Golgi cisternae; 8. Exocytosis with migration of Golgi vesicles containing viruses to the cell surface, fusion of vesicle membranes with the plasma membrane, and release of infectious virions. Some viruses in some cell types can bud into intracellular vesicles and also from the plasma membrane. ER, endoplasmic reticulum, \square receptor, \bigcirc N, \bullet G_N and G_C .

From the book *Fields Virology*, Fifth Edition, 2006, figure 49.3, page 1752, chapter 49: *Bunyaviridae*, Schmaljohn and Nichol [35]. Reprinted, with minimal editing, with permission from Wolters Kluwer Health.

Internalization

After attachment to host cell receptors, enveloped viruses are internalized either by fusing directly with the plasma membrane, or through endocytosis (**Fig. 5**). Several endocytic pathways have been described, such as clathrin-mediated endocytosis (CME), caveolar/raft-mediated endocytosis, macropinocytosis, or other less well-characterized mechanisms that are clathrin- and caveolae-independent [82, 83]. CME is the best studied of the endocytic pathways and is a crucial component of the normal intracellular transport of molecules from the plasma membrane to early endosomes [84, 85]. The CME pathway is also the main entry mechanism for a variety of viruses including Semliki Forest virus, adenoviruses, hepatitis C virus, influenza virus, and the dengue viruses [75, 86-88]. There is also continually expanding evidence that numerous bunyaviruses enter cells via clathrin-mediated endocytosis, and in some cases the entry mechanism may be cell-type dependent.

The CME pathway is initiated by the binding of cargo to AP-2, which is considered the core plasma membrane adaptor for clathrin, or by binding to cargo-specific protein adaptors that bind directly to AP-2 [89](reviewed in [90]). Next, the clathrin cages assemble on the cytoplasmic face of the plasma membrane (**Fig. 6a**). These cages are composed of three 190-kDa clathrin heavy chains, three 25-kDa light chains, and several host proteins including AP-2, cargo specific protein adaptors (i.e. disabled homology-2, Dab2, autosomal recessive hypercholesterolaemia, ARH), EPS15, and other accessory proteins [91-95]. Dab2 has been found to initiate clathrin pit formation in the absence of AP-2 as well, although this is cargo specific, as integrin β CME uptake is impaired in the absence of AP-2 but transferrin uptake by CME is not [96]. There is some

redundancy in the pathway to allow for nucleation of clathrin in response to specific cargo in the absence of AP-2. The clathrin cages form invaginations in the plasma membrane called clathrin-coated pits, which are then pinched from the plasma membrane, with the help of the GTPase dynamin, to form free clathrin-coated vesicles (**Fig. 6a**) [97]. Viruses that have defined entry mechanisms, such as vesicular stomatitis virus (VSV), have been valuable tools in the study of proteins, lipids, and kinases involved in clathrin-mediated endocytosis because they are efficient, reproducible and easily measurable. In one particular study utilizing VSV as the CME cargo, and a genome wide siRNA knockdown screen of kinases, the researchers identified 50 different kinases that were implicated to be involved in assembly and regulation of CME, respectively [98]. Many of the kinases that were revealed to be involved in CME include those in the mTOR pathway, which regulates cell growth in response to nutrient and maintains or stimulates CME. The mTOR pathway appears to regulate CME at multiple steps in the pathway as even kinases in the mTOR pathway blocked VSV infection as well as transferrin internalization, trafficking, and recycling. Four G-protein receptor linked kinases also inhibited both VSV and transferrin uptake, indicating that these kinases are not only involved in the internalization of G-protein coupled receptors, but they also are involved in general control over CME. Although blocking clathrin uptake completely in cells is extremely detrimental, since a loss of function of AP-2 and clathrin leads to embryonic lethality [99](reviewed in[90]), small molecule targeting of regulators of CME may prove to be useful short-term treatments for acute infections caused by viruses that use the CME pathway for entry. Cyclin-dependent kinase inhibitors have been investigated since 1997 to inhibit cancers as well as viral infections (reviewed in [100-

102]), and thirteen kinase inhibitors are approved in the United States for cancer treatment (reviewed in [103, 104]). In a recent study, the general kinase inhibitor genistein increased the survival rates in Syrian golden hamsters infected with the arenavirus Pirital virus [105]. Two C-Jun N-terminal kinase inhibitors also decreased the replication of avian influenza and human pathogenic influenza A virus in both cell culture and in a mouse model [106]. In addition, two kinase inhibitors genistein and tyrphostin AG1478 inhibited the induction or infection with the hemorrhagic fever viruses Lassa virus (LACV), EBOV, and Marburg virus (MARV) in cell culture [107].

After clathrin, AP-2 is the second most abundant protein in clathrin-coated vesicles and is considered the core of clathrin-coated pit formation as it binds not only to clathrin, but also to most of the accessory proteins (**Fig. 6b**) [90, 108]. The AP-2 adaptor complex is a heterotetramer of 2 large adaptins (subunit AP2 α 1 or AP2 α 2 and subunit AP2 β 1), a medium adaptin (AP2 μ 2), and a small adaptin (AP2 σ 1) [109]. Other cargo specific adapters, such as the fibrinogen adaptor Disabled-2, have been reported to be able to replace AP-2 in clathrin-coated pit formation, although one study indicated that AP-2 is essential and that clathrin-coated pit formation is completely abrogated in the absence of this protein [110-113]. Once the vesicle is formed, the clathrin coat is quickly disassembled from the vesicle, releasing it for transport to the early endosome (EE) [114].

There are several methods that can be used to determine if clathrin is involved in the entry pathway of a virus. The most direct approach is to visualize the interaction between clathrin and viruses using microscopy. Clathrin structures have a distinct morphology, which permits co-localization of viruses and clathrin-coated vesicles by electron microscopy, or immunoelectron microscopy [91](reviewed in[83]). Co-localization

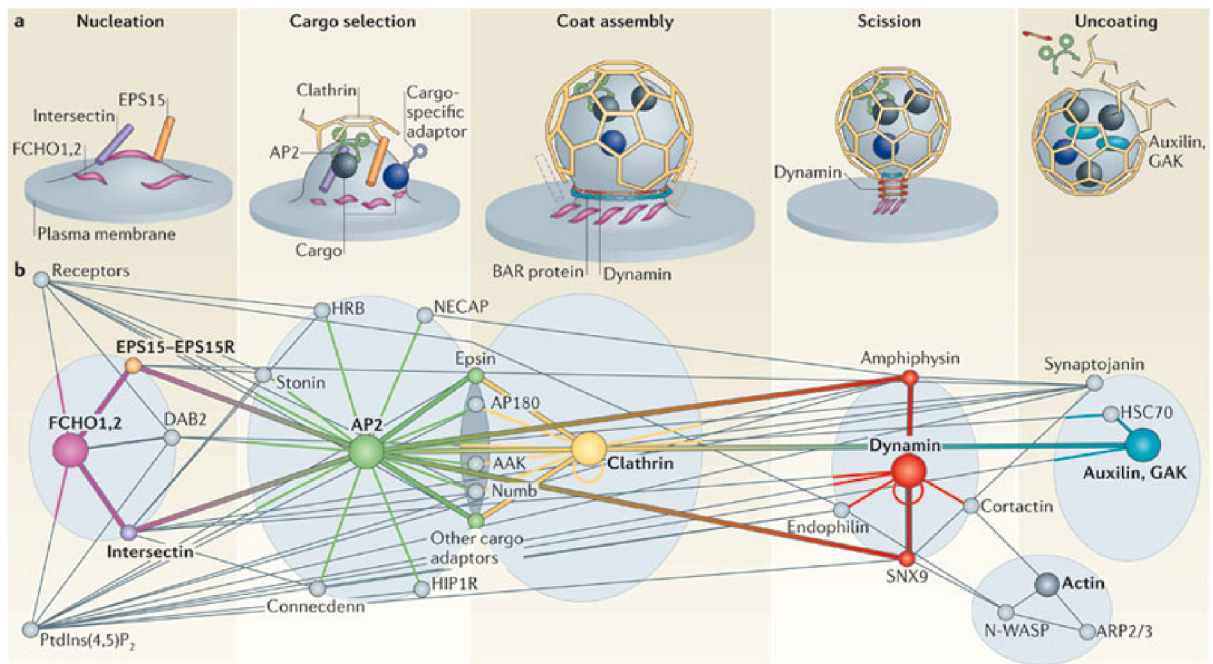


Figure 6. Clathrin coated pit formation. **A.** The proposed five steps of clathrin-coated vesicle formation. **Nucleation:** FCH domain only (FCHO) proteins bind phosphatidylinositol-4,5-bisphosphate (PtdIns(4,5)P₂)-rich zones of the plasma membrane and recruit EPS15–EPS15R (EGFR pathway substrate 15–EPS15-related) and intersectins to initiate clathrin-coated pit formation by recruiting adaptor protein 2 (AP-2). **Cargo selection:** AP-2 recruits several classes of receptors directly through its μ -subunit and σ -subunit. Cargo-specific adaptors bind to AP-2 appendage domains and recruit specific receptors to the AP-2 hub. **Coat assembly:** clathrin triskelia are recruited by the AP2 hub and polymerize in hexagons and pentagons to form the clathrin coat around the nascent pit. **Scission:** the GTPase dynamin is recruited at the neck of the forming vesicle by BAR domain-containing proteins, where it self-polymerizes and, upon GTP hydrolysis, induces membrane scission. **Uncoating:** auxilin or cyclin G-associated kinase (GAK) recruit the ATPase heat shock cognate 70 (HSC70) to disassemble the clathrin coat and produce an endocytic vesicle containing the cargo molecules. Synaptojanin probably facilitates this by releasing adaptor proteins from the vesicle membrane through its PtdIns lipid phosphatase activity. The components of the clathrin machinery are then freed and become available for another round of clathrin-coated vesicle formation. **B.** The clathrin network. The protein–protein interactions underlying the different stages of vesicle progression are shown. Major hubs are obvious because of their central location in the network and the large number of interacting molecules. They are essential for pathway progression and are denoted by the central colored circles. Possible pathways of progression between hubs are shown with thicker lines.

A and B are from [90]. Figure A and B and the figure legend were reprinted with permission from Nature Publishing Group. The figure legend is reprinted with minimal editing.

studies of the clathrin heavy-chain and viral proteins can also be carried out utilizing confocal microscopy with specific tagged markers. These direct studies are attractive in that there is no disruption of the normal processes of the cells with the use of inhibitors of the pathways, as described below, but they require large amounts of virus and precise timing as the clathrin-coated vesicles formation and disassembly is rapid and the co-localization events can be missed.

Another common method for studying clathrin-mediated entry is to disrupt clathrin-coated pit formation by treating cells with compounds such as chlorpromazine or sucrose. Although this method can provide an initial dissection of entry, both compounds have been shown to cause other effects in cells, thus the results are not completely specific for clathrin entry. For example, chlorpromazine is a cationic amphiphilic drug and a calmodulin inhibitor that is thought to inhibit CME through the reverse translocation of AP-2 and clathrin to intracellular vesicles; therefore, clathrin lattices form on endosome membranes but do not form at the cell surface [115]. Chlorpromazine has been shown to also inhibit phagocytosis in neutrophils and macrophages, as well as prevent the degranulation of neutrophils [116], [117]. In addition, the efficacy and cytotoxicity of chlorpromazine was found to be cell-type dependent. For example, the drug did not inhibit the CME uptake of transferrin in COS-7 cells, and minimally inhibited transferrin uptake in ARPE-19, Vero, and COS-7 cells in comparison to HUH-7 cells [118]. In ARPE-19 cells the use of chlorpromazine strongly increased the uptake of the caveolae specific cargo LaCler [118]. Hypertonic sucrose inhibits CME by removing membrane associated clathrin lattices so they no longer form clathrin-coated pits or clathrin-coated vesicles [119]. However, hypertonic sucrose treatment was found to be nonspecific in

that it decreased both clathrin-coated pits as well as non-coated invaginations on fibroblasts [120-122].

A specific method of examining the role of CME in virus entry is the use of clathrin-specific siRNA. Clathrin is an abundant protein and most published reports describe the need to use high concentrations of siRNA as well as to perform sequential transfections of siRNA to achieve substantial depletion of clathrin proteins [75]. Additionally, since siRNA has variable off-target effects that are cell line dependent and the expression of non-specific target genes vary among cell lines, the use of clathrin-dependent and clathrin-independent controls are necessary for these types of experiments for clarity [123]. Even if disruption of clathrin is shown to impact viral entry, additional studies are required to demonstrate that CME is indeed the entry mechanism, because clathrin is not only involved in viral entry. Clathrin also plays functional roles in the transport of vesicles from the *trans*-Golgi network (TGN) to other parts of the cell, such as the transport of hydrolases to the lysosome, and is involved in the formation of the mitotic spindle (reviewed in [90])[124, 125]. To confirm that a virus enters via a clathrin-dependent manner the association with other proteins integral to CME, such as AP-2 or EPS15, with viral entry can be measured.

These methods have been used for studying the entry of various bunyaviruses. For example, HTNV replication decreased in cells treated with chlorpromazine or sucrose [87]. HTNV virus particles also co-localized with the clathrin heavy-chain as measured by confocal microscopy. In addition, the expression of a dominant negative dynamin plasmid, a critical component of CME, decreased HTNV infection. Likewise, the orthobunyavirus Oropouche virus (OROV) was also found to associate with clathrin-

coated vesicles by transmission electron microscopy and confocal microscopy [88]. LACV was also found to enter cells by CME as G_C co-localized with the clathrin-heavy chain and the perturbation of CME with numerous inhibitors including a dynamin inhibitor, several clathrin inhibitors, and a dominant negative EPS15 decreased LACV replication [126]. Only one entry study on CCHFV or any other nairovirus has appeared to date. CCHFV infected cells treated with sucrose or chlorpromazine had reduced levels of N protein compared to untreated cells [127]. Viral RNA synthesis and protein expression were both partially inhibited after treatment with clathrin-specific siRNAs. Although these data support CME entry of CCHFV, additional supportive evidence is necessary as discussed above.

Although CME appears to be a common entry mechanism for many bunyaviruses, it is apparently not used exclusively by all viruses in the family. Studies with UUKV showed viral entry occurs primarily via non-coated vesicles by electron microscopy in A549 cells [75]. Consistent with this finding, only a small decrease in UUKV infection was observed with the use of clathrin heavy-chain specific small interfering RNA (siRNA) to inhibit CME in A549 cells. However, other studies using EM and confocal microscopy based co-localization experiments found that UUKV entered DC-SIGN expressing cells mainly through a clathrin-dependent mechanism [128].

In our research, we used several of these methods to gain insight into the cellular entry mechanism of CCHFV. We performed several microscopy studies aimed at identifying an interaction between CCHFV and clathrin. These co-localization studies require highly concentrated virus in order to achieve a significant number of viruses to image virions within the rapidly assembling and disassembling clathrin-coated vesicles;

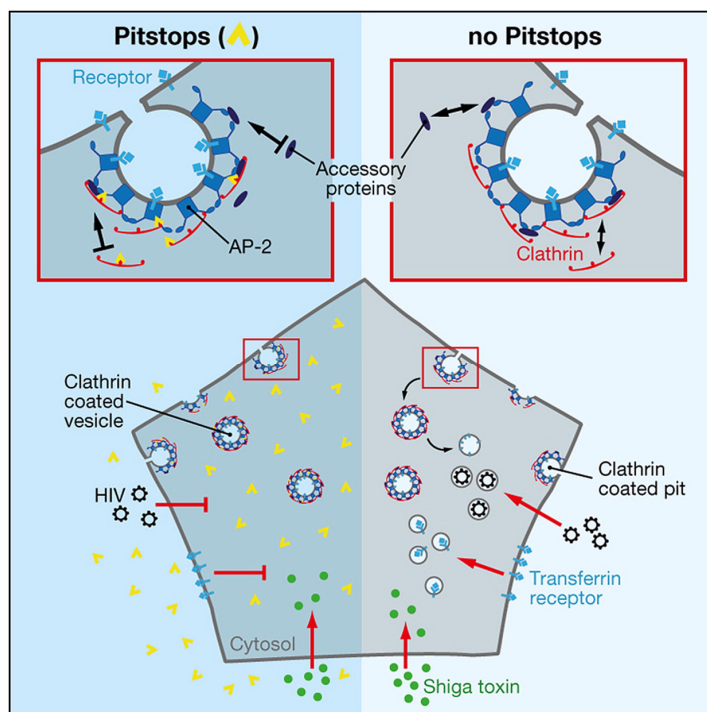
therefore, my results using these methods were not conclusive, as will be discussed further in Chapter 4. We also tested various methods of disrupting clathrin pit formation, as will be described in Chapter 4, including specific siRNAs for two subunits of AP-2 complex, AP2A2 and AP2M1.

I also present results in which we used a new method for identifying CME of a virus, with an amphiphilic clathrin specific compound, Pitstop 2. This compound binds to the terminal domain of the clathrin heavy-chain, thereby preventing the interaction of the clathrin heavy chain and numerous ligands thus halting the dynamics of clathrin-coated vesicles (**Fig. 7**) [114]. In the presence of Pitstop 2, clathrin-coated pits are still able to form on the cell surface, but as the terminal domain cannot interact with accessory proteins, the vesicles are inhibited from pinching off into clathrin-coated vesicles, thus the cargo is prevented from entering the cells. Pitstop 2 rapidly and completely prevents the formation clathrin-coated vesicles. The drug effects are also quickly reversible by performing several washes and adding fetal bovine serum to the cell culture medium, which sequesters any remaining drug. The rapid effects and reversibility of the drug avoids the off-target effects that can result from the long-term inactivation of clathrin. In the results that I present in Chapter 4, we provide additional evidence for CME entry of CCHFV.

Uncoating

Upon entry, enveloped viruses that replicate in the cytosol typically require fusion between the viral membrane and the host membrane to release the genome into the cytosol. Viruses are classified as pH-dependent or pH-independent for fusion. For pH-

A.



B.

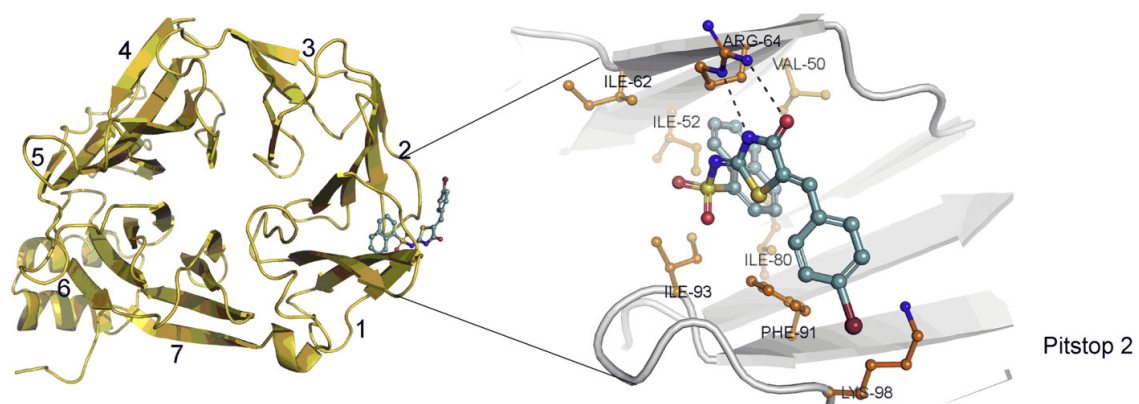


Figure 7. The mechanism of action and binding domain of Pitstop 2. A. A schematic of the steps in clathrin-coated vesicle formation that are inhibited by Pitstop 2. B. The ribbons in the figure to the left represent the clathrin terminal domain with Pitstop 2, shown in ball-and-stick mode, in the binding domain. On the right is a close-up view of the binding site for Pitstop 2. Bidentate hydrogen bonds at 3.0 Å distance are formed between the guanidinium group of Arg64 and O and N atoms of the central portion of Pitstop 2. The aromatic ring of Phe91 is located in the same position as in the inhibitor-free form of the clathrin TD and stacks against the edge of the bromobenzene of Pitstop 2.

From [114]. Figures and legend reprinted with permission from Elsevier.

dependent viruses, the acidic environment in endosomal vesicles can trigger a conformational change in the viral glycoproteins that allows direct fusion or attachment of the fusion glycoprotein to its receptor, virus-host membrane mixing, and eventual fusion. The required pH necessary to trigger fusion will typically correlate to the pH of either EE (pH ~6.2), as with VSV, or the late endosome (LE) (pH ~5.5), such as the dengue viruses (reviewed in [82])[129-132]. In some cases the acidic pH is sufficient to trigger fusion of the virus with the host membrane. Some viruses, such as Ebola virus (EBOV) and Severe acute respiratory syndrome (SARS) coronavirus, also require acid-dependent endosomal proteases [133, 134]. Other viruses, such as avian leukosis virus, require interaction with a specific receptor for fusion to occur (reviewed in [135])[136].

Vesicle trafficking is coordinated by the interactions of numerous regulatory GTPases called Rabs (Ras related to brain), which are members of the Ras superfamily of small GTPases. Rab GTPases are localized on the cytosolic face of vesicles throughout the cell (reviewed in Stenmark, 2009). Rab GTPases switch between active states, in which they are GTP-bound, and inactive states, in which they are GDP-bound. The GDP for GTP exchange is catalyzed by a guanine exchange factor (GEF), and the active Rab GTPase is recognized by multiple effector proteins. GTPase-activating protein (GAP) then releases an inorganic phosphate and the Rab GTPase is converted back to the GDP-bound inactive state. Active Rab GTPases have numerous functions in vesicle trafficking such as sorting receptors into budding vesicles, uncoating of vesicles by recruiting phosphoinositide kinases or phosphatases, recruiting motor adaptors to vesicles to facilitate the transport along cytoskeletal tracts, or vesicle tethering to cell membranes (reviewed in [137])[138, 139]. For their role in endosome trafficking, for example,

vesicles are transported from internalization vesicles, such as clathrin-coated vesicles, to early endosome by the interactions of Rab5a with AP2 to coordinate the uncoating of the clathrin-coated vesicles [140]. From the early endosomes, the vesicles are either sorted to recycling endosomes to transport cargo back to the cell surface, through the regulatory functions of Rab4, or sorted to the degradative pathway through late endosomes and then lysosomes, through the activity of Rab7. Rab GTPase proteins interact with the motor proteins dynein or dynactin to move the vesicles towards the microtubule organizing center (MTOC), or with kinesin-1 to recycle endosomes to the cell surface along microtubules [141-145]. Rab GTPase proteins that are of particular interest for virus entry studies are Rab5, which is associated with the EE, and Rab 7, which is associated with LE and lysosomes.

Several methods are commonly used to identify which endosomal compartment a virus uses for fusion. Lysomotropic agents, such as the weak bases ammonium chloride and chloroquine, or the vacuolar-type H⁺ ATPase inhibitor bafilomycin A, rapidly prevent the protonation of endocytic vesicles and are often used to determine if a virus is pH dependent. These compounds provide useful but inconclusive evidence of pH-dependency, as they can cause indirect-effects that may reduce virus uptake, such as defects in receptor cycling and the inhibition of endosomal maturation (reviewed in [146]). A more reliable and direct method for identifying pH dependency is to show co-localization of the virus or viral proteins with an EE marker, such as Rab5 or EEA-1, or a LE marker, such as Rab7 or LAMP-1, utilizing microscopy [75, 147-149]. This method depends on the presence of a sufficient amount of virus for the co-localization events to be quantifiable, and they also require exact timing as viruses rapidly traffic through these

vesicles after entry, typically within 5 minutes for EE and 10-20 minutes for LE [75, 110, 150].

Another means to gain insight into which endosomal compartment a virus uses for fusion and uncoating, and also to help determine if low pH alone is sufficient to induce fusion, is to identify the fusion pH threshold of a virus. Typically, this can be accomplished by performing a fusion-from-without experiment in which confluent monolayers of cells are exposed to virus at a large multiplicity of infection (MOI) of virus at 4°C, treated with low pH buffers for several minutes, then warmed to 37°C [75, 151]). The low pH treatment will trigger a conformational change in the viral glycoproteins such that they will fuse with more than one cell at their plasma membranes, and the close proximity of the cells will allow for membrane mixing and fusion between cells. A fusion index can be calculated based on comparing the number of cells present versus the number of nuclei at each pH using microscopy. For some viruses it is also possible to perform virus independent cell-cell fusion assays in which viral glycoproteins are expressed on an effector population of cells that also contain a T7 RNA polymerase and then mixing these with target cells containing a reporter under the control of a T7 promoter. Once the pH is lowered to the critical point to induce fusion, the contents of the effector and target cells will mix and production of the reporter is detected, syncytia formation can also be measured in the absence of a reporter [152-154]. A fusion bypass experiment can also be used to determine the pH threshold of a virus [155]. For this, virus is first allowed to attach to cells at 4°C, the cells are then rapidly warmed and briefly treated with a low pH buffer to induce virus fusion with the plasma membrane directly. NH₄Cl is then added to prevent virus infection through endosomal acidification

[155]. The pH threshold in this type of experiment would be determined as the pH that triggered the virus fusion directly with the plasma membrane.

A method for studying trafficking through the EE and LE involves the use of dominant negative Rab GTPases that are specific for EE and LE [110, 156-160]. Rab5 and Rab7 dominant negative proteins contain single amino acid changes that prevent the exchange of GTP for GDP on the protein, thus maintaining the proteins in an inactive state so they can no longer bind to their effectors. When these mutant proteins are over-expressed in cells they elicit a dominant negative effect over the wild-type protein; thus, rendering the endogenous protein ineffective. A virus that requires either the EE or LE for trafficking will be adversely affected by the over-expression of the dominant negative protein specific for that compartment.

It appears that in general bunyaviruses require vacuolar acidification for fusion with mammalian cell membranes, and either G_N or G_C serves as the fusion protein, but that they do not all require the same endosomal compartment for fusion [52, 65, 66, 70, 75, 87, 88, 127, 128]. Bunyaviruses are theorized to undergo class II fusion (**Fig. 8**), which is based solely on predictive modeling that shows possible homology to class II fusion proteins of other viruses [161, 162]. The predicted secondary structures of the G_C proteins of bunyaviruses indicate that there may be high β -sheet content, which is found in class II fusion proteins. In addition, in all of the bunyaviruses for which studies were performed, the G_N and G_C proteins form heterodimers in the ER, which is another hallmark of class II fusion [161-163]. Comparative molecular modeling of the hantavirus ANDV G_C , combined with binding studies with a putative class II fusion peptide in G_C , serves as preliminary evidence that G_C of hantaviruses are involved in fusion between the

virus and the cell membrane [162]. Class II fusion occurs when the viral fusion protein is activated by a trigger, such as a decrease in the pH, which causes a conformational change in the fusion protein and the glycoproteins shift from heterodimers to homotrimers (**Fig. 8**). A hydrophobic fusion loop within the fusion protein is exposed and inserted into the host membrane, which brings the two membranes in close proximity and allows for membrane mixing and fusion (reviewed in [164]). It appears that the G_C proteins of two orthobunyaviruses, LACV and Tahyna virus, also serve as their fusion proteins. The proximal two-thirds of G_C was determined to be critical for cell-cell fusion and mutagenesis of these regions decreased the pH threshold below that of the wild-type viruses [65, 66].

UUKV, HTNV, and OROV have been reported to require the LE for fusion. For HTNV, co-localization with both the EE marker EEA-1, as well as the late endosome (LE) marker LAMP-1 was observed in confocal immunofluorescence studies, indicating that the virus enters the LE for fusion [87]. UUKV was also associated with LE-dependent fusion in studies using dominant negative Rab5 and 7 GTPases, fusion-from-without, and fusion bypass experiments that identified a fusion index of 5.2 and below [75]. UUKV also was shown to co-localize with the LE marker LAMP-1. Likewise, OROV was shown to co-localize with the LE marker Rab7 by confocal microscopy [88]. In contrast, LACV and RVFV appear to require the EE for fusion. LACV was found to require Rab5 but not Rab 7 for entry, and RVFV glycoproteins promote syncytia formation in a cell-cell fusion assay at pH 6.2 and below which is consistent with the early endosome [126, 165].

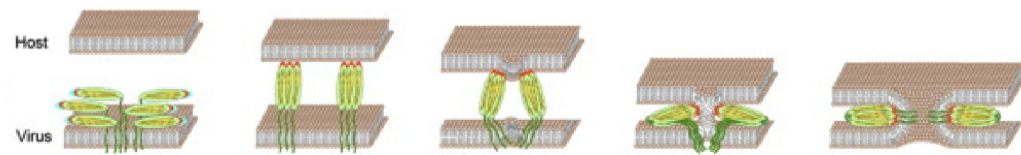


Figure 8. Class II fusion. Hydrophobic fusion loops are contained within a structure containing β sheets. After activation, such as a decrease in pH, and a shift from heterodimers to homotrimers (not shown), the fusion loops are exposed and inserted into the opposing membrane. Folding back occurs presumably by interaction between different domains of the protein that drive membrane fusion. α helices, light and dark blue cylinders; transmembrane domains, dark green; fusion loops, orange; β sheets, light green ellipses.

From [164]. Figure and legend reprinted with minimal editing with permission from Elsevier.

As of this writing there are no published reports describing CCHFV trafficking through intracellular endosomes, and the requirements for fusion have not been described. In my research, we have investigated both of these important steps in CCHFV replication and have described in Chapter 4 for the first time the pH requirements as well as the endosomal trafficking conditions necessary for fusion.

Aims and hypotheses

Hypothesis: Crimean-Congo hemorrhagic fever virus enters cells by clathrin mediated endocytosis and uses an endosomal compartment for fusion in order to gain entry into the cytosol for replication.

Specific Aim 1: To confirm that CCHFV enters through CME.

Specific Aim 2: To identify the endosomal compartment used by CCHFV to gain entry to the cytosol for replication.

Chapter 2: Materials and Methods

Cells, viruses, and pseudoviruses

A549 cells (ATCC# **CCL-185**) were maintained in F12-K medium (Gibco) with 10% fetal bovine serum (FBS)(ThermoScientific/Hyclone, Logan, UT). HEK 293T (ATCC# HB-8065), HepG2 (ATCC# CRL-11268), chicken embryo related (CER)(USAMRIID, Fort Detrick, Frederick, MD) cells were maintained in Eagle's minimal essential medium (EMEM)(Invitrogen, Carlsbad, CA) with 10% FBS. All cell lines were maintained at 37°C and 5% CO₂ during incubations. Cells were plated on poly-D-lysine coated black 96 well clear bottom plates (Greiner Bio One, Monroe, NC) for all experiments. The viruses used in this study include: CCHFV strain IbAr 10200 (USAMRIID collection), Vesicular stomatitis virus expressing enhanced green fluorescent protein (VSV-eGFP) which was a generous gift from John Connor (Boston University), vaccinia virus Western Reserve-GFP (VACV-eGFP) which was a generous gift from Arthur Goff (made at USAMRIID, personal communication), Ebola Zaire virus (EBOV)(USAMRIID collection), and Ebola Zaire virus expressing eGFP (EBOV-eGFP)(USAMRIID collection) [166]. The CCHFV seed was propagated in chicken embryo related cells (CER)(USAMRIID) in EMEM containing 5% fetal bovine serum and had a titer of 2×10^6 plaque forming units per ml (pfu/ml). VSV-eGFP, EBOV, and EBOV-eGFP were propagated in Vero cells in EMEM. All viruses, except for VACV-eGFP, were collected from clarified cell culture supernatants. VACV-eGFP was harvested from cell culture supernatant and cell lysates. CCHFV, EBOV, and EBOV-eGFP were handled in Biosafety Level 4 containment at USAMRIID. The Nipah virus

(NiV) lentivirus based pseudovirus expressing red fluorescent protein (RFP) was a generous gift from Robert Doms (University of Pennsylvania) [167]

Determining CCHFV growth kinetics to increase yield

The method used to propagate CCHFV IbAr 10200 produced virus titers of approximately 1×10^5 pfu/ml harvested from the supernatant of SW-13 cells (ATCC#CCL-105). To determine the optimal time to harvest CCHFV from cell supernatant and cell lysates, we performed a growth kinetics experiment in two cell lines, CER and HepG2, which resulted in increased CCHFV titers than SW-13 cells. The rate of CCHFV IbAr 10200 was determined by measuring the virus in the cell lysates and supernatants of infected CER and HepG2 cells at 12-hour intervals after infection. The harvested virus was plaqued on 90-95% confluent monolayers of CER cells in 6-well plates. Virus dilutions were made, the media was removed from the cell monolayer, and 100 μ l of each diluted inoculum was added to the cells and incubated at 37°C for 30 minutes. Two ml of a primary overlay containing Basal Medium Eagle with Earle's Salts (EBME)(Invitrogen), 4%[vol/vol] L-glutamine (Invitrogen), 5% FBS, 1%[vol/vol] DMSO (Sigma, St. Louis, MO), and 0.8%[wt/vol] SeaKem ME agarose (Lonza, Walkersville, MD) was then added to each well and incubated at 37°C for 4 days. A secondary overlay was added to each well, with the addition of 2.5% neutral red (Gibco/Invitrogen) to the primary overlay recipe listed above, and the cells were incubated overnight at 37°C. The plaques were counted the following day.

Monoclonal antibodies, immunofluorescence, and imaging

For all high content imaging (HCI) experiments, CCHFV N was detected using a mouse monoclonal antibody 9D5, which was produced by Jonathan Smith (formerly USAMRIID) (Altamura, 2007). EBOV GP was detected using a mouse monoclonal antibody 6D8 [168]. The cells were permeabilized using 0.1% Triton-x 100 (Sigma-Aldrich) for 5 minutes at room temperature, then the cells were washed twice in PBS. A blocking solution containing 3% bovine serum albumin in PBS (Sigma-Aldrich) was added to the cells, and they were incubated at room temperature for 30-60 minutes, to block non-specific epitopes. The primary antibodies were diluted to 1ng/ μ l, and 100 μ l was added to each plate and incubated for one hour. The cells were then washed twice in PBS. For CCHFV N protein and EBOV G protein detection in all experiments, either an Alexa-488 or Alexa-568 tagged goat anti-mouse secondary antibody (Invitrogen) was used. The secondary antibody was added to each well at a concentration of 2ng/ μ l and the plates were incubated at room temperature for one hour, then the cells were washed three times in PBS. The cell nuclei were stained with 1 μ g/ml of Hoechst (Invitrogen), and the plasma membranes were stained with 500ng/ml of CellMask Deep Red (Invitrogen).

High content data was acquired and analyzed on either an Operetta (PerkinElmer, Waltham, MA, USA) high-throughput, wide-field fluorescence microscope reader (Perkin Elmer, Waltham, MA 02451) using the non-confocal setting with a 20X objective, or on the Opera confocal reader (model 5025-Quadruple Excitation High Sensitivity (QEHS), Perkin Elmer) with a 10x air objective. On the Operetta images in the Blue (Hoechst), Green (GFP or Alexa488), Red (Cherry/RFP or Alexa568) and Far

Red (Cell Mask Deep Red) channels were sequentially acquired by a single charged coupled device (CCD) camera. For each field of acquisition, a single imaging plane was automatically set by using an infrared laser based autofocus unit. The excitation light was provided by a 300W Xenon lamp and images were acquired using a 20X long working distance objective. The settings for the excitation (EX)/emission (EM) filters used for the different channels were as follows: Blue EX 360-400, EM 410-480; Green EX 460-490 EM 590-640; Red DM EX 560-580, EM 590-640; Far Red EX 620-640, EM 650-700. Image analysis was performed on the fly by using the Harmony 3.0 software package (PerkinElemer). On the Opera confocal reader the first exposure utilized the 488 nm or 568nm, and 640 nm lasers to excite the viral and cell body fluorophores, respectively. The emission light was split by a 580 nm short pass dichroic mirror and collected on separate cameras through 562/40 nm and 690/70 nm band pass filters. The second exposure used a 425 nm long pass to steer the UV (350 nm) to the sample to excite the nuclear stain. The visible emission was directed to the non-confocal camera by a 475 nm long pass filter with the emission defined with a 450/50 nm band pass filter.

HCI statistics

For each HCI assay, the statistics were performed in excel as described previously to determine the robustness of each assay [169]. The % coefficient of variance (%CV) was calculated to determine the reproducibility between replicates within a plate as follows: $(\text{mean} \div \text{standard deviation of the mean}) \times 100$. A %CV of less than 5% was considered optimal, and a higher %CV was acceptable provided the Z' -value was within the acceptable range as described below. The Z' -values were calculated for the development of each assay to assess the assay quality using the standard deviation of the

infected wells (σ_{c+}) and the standard deviation of the negative (mock) controls (σ_{c-}) using the following equation: $Z' = 1 - \frac{(3\sigma_{c+} + 3\sigma_{c-})}{(\mu_{c+} - \mu_{c-})}$. Z' -values between 0.5 and 1.0 were indicative of a high quality assay.

CCHFV and clathrin heavy chain co-localization

HepG2 and A549 cells were seeded on coverslips in 24 well plates. Once the monolayers were 60-80% confluent they were infected on ice with CCHFV at an MOI of 10-30 for 15 minutes (HepG2) or 60 minutes (A549), or 35 μ g/ml of transferrin conjugated to FITC (A549 cells). The plates were then placed at 37°C to slowly warm, and fixed in 10% formalin at 1, 5, 10, 15, and 30 minute time-points (A549) or 15, 30, 45, and 60 minute time-points (HepG2). After 24 hours of fixation, the plates were removed from BSL-4. The cells were permeabilized with 0.1% Triton-X 100 (Pierce Biotechnology) and stained for CCHFV G_C with a mouse monoclonal antibody 11E7 (USAMRIID), clathrin-heavy chain with rabbit anti-clathrin heavy chain (Abcam, Cambridge, MA) or caveolin with rabbit anti-caveolin-1 (Abcam). An Alexa-488 conjugated anti-mouse antibody (Invitrogen) was then used to detect 11E7 bound to CCHFV G_C, and an anti-rabbit Alexa-568 conjugated anti-rabbit antibody (Invitrogen) was used to detect either the bound clathrin-heavy chain or caveolin primary antibody. The nuclei were stained with Hoechst, and actin filaments were stained with Alexa-647 conjugated phalloidin. The coverslips were mounted onto glass slides with Fluoromount-G mounting fluid (SouthernBiotech, Birmingham, AL). Images were captured with a Leica TCS SP5 confocal microscope and overlaid using Leica Application Suite software.

CME inhibition with Pitstop 2

The effect of Pitstop 2 (Abcam), which inhibits clathrin-coated vesicle dynamics, on CCHFV entry was assessed. A549 cells were treated at 37°C with Pitstop 2 at concentrations ranging from 3.75µM to 25µM in a maximum of 0.1% DMSO. DMSO concentration matched control and media alone controls were also used for each virus. The drug or controls were added to cells in triplicate for 15 minutes at 37°C. The cells were then infected with CCHFV, VACV-eGFP, or VSV-eGFP in the presence of the drug at 37°C for 1 hour. Unbound virus was washed away with PBS (Cellgro, Manassas, VA), and the cells were incubated for an additional 6 hours for VSV-eGFP, or 24 hours for CCHFV and VACV-eGFP in the presence of the drug. Infected cells were fixed in 10% buffered formalin for 24 hours prior to staining. CCHFV N protein was detected as described above. The plates were read and analyzed on the Operetta reader, and normalized to the DMSO matched control. At least 6,000 cells were scored per experimental point for each virus to determine the percent of infection. The cell viability was determined by comparing the overall cell number per experimental point to the DMSO matched controls. All concentrations of DMSO showed no toxicity when compared to media alone.

siRNA-mediated knockdown

For the inhibition of proteins involved in CME, siRNAs were used to inhibit the expression of subunits of AP-2. A549 cells were reverse transfected in 96 well plates (20,000 cells per well) with 40nM of small interfering RNA (siRNA) targeting AP2A1 (ON-TARGET Plus), AP2A2 (ON-TARGET Plus), AP2M1 (ON-TARGET Plus), or

Non-Targeting Control (Thermo Scientific/Dharmacon, Lafayette, CO) or in the absence of siRNA using HiPerfect (Qiagen). Each siRNA was diluted to 2 μ M working stocks prior to use. In each well of a poly-D-lysine coated 96 well clear-bottom plate, 40nM of each siRNA (4.5 μ l) was diluted in triplicate in Optimem (Gibco/Invitrogen) to a final volume of 25 μ l. A master mix of 0.75 μ l of HiPerfect and 24.25 μ l of Optimem per well was prepared and added to each well containing siRNA, or control wells, and mixed well by pipetting. A549 cells were then added to each well, 20,000 cells per well, and the siRNA and cells were mixed well by rocking the plate. Cells were infected 48 hours post transfection, and replicate plates were used for cellular mRNA extraction and qRT-PCR analysis. Total cellular RNA was extracted from the siRNA transfected A549 cells using an RNeasy extraction kit (Qiagen, Valencia, CA) per the manufacturer's instructions. Total mRNA from each sample was diluted to 5ng/ μ l, and 25ng of each total mRNA was used in each qRT-PCR reaction, in triplicate. Gene target mRNA was detected using AP2A1 and AP2M1 primer/probe20X reaction sets (Applied Biosystems, Carlsbad, CA) and TaqMan® Reverse Transcription Reagents (Applied Biosystems), and normalized to a housekeeping gene control, PPIB. The samples were run and analyzed on the 7900HT Fast Real-Time PCR System (Applied Biosystems) using the following cycling profile: 1 cycle at 50°C for 30 minutes, 1 cycle at 95°C for 10 minutes, followed by 40 cycles at 95°C for 15 minutes and 60°C for 30 minutes. The $\Delta\Delta C_T$ was calculated for each sample and normalized to the PPIB housekeeping control for each sample. The percentage of mRNA knockdown for each siRNA target was calculated in comparison to the non-targeting siRNA control.

Lysosomotropic drug assay

293T cells were pre-treated with ammonium chloride at concentrations of 1-25 μ M, or media alone for 60 minutes prior to infection with VSV-GFP, CCHFV, or EBOV-GFP for 16, 24, and 48 hours respectively. The infected cells were then fixed in 10% buffered formalin for 24 to 72 hours prior to staining. CCHFV N protein was detected using the N-specific mouse monoclonal antibody 9D5, and an Alexa-488 goat anti-mouse secondary antibody as described above. The nuclei and cytoplasm were also stained as described above, and the plates were read and analyzed on the Operetta reader. The percent of infection was determined in each experimental point and normalized to the mock control for each virus.

pH Sensitivity assay

Low pH buffers ranging from pH 4.5 to pH 7.0 were prepared from EMEM (Cellgro) without FBS, 200 mM 2-(N-morpholino)ethanesulfonic acid (Sigma-Aldrich) was added, and the pH was adjusted with sodium hydroxide or hydrochloric acid. CCHFV, NiV, and VSV were pre-treated with the low pH buffers for 15 minutes at 37°C prior to neutralization to a pH of 7.2-7.4. Neutralizing buffers were made from EMEM with 100 mM Trizma pH 8.0 (Sigma-Aldrich), and pH adjusted with sodium hydroxide. After the virus dilutions were neutralized, 293T cells were infected with the neutralized virus samples for 2 hours in replicates of 6. Unbound virus was then washed away with PBS and replaced with EMEM with 10% fetal bovine serum. The infections continued for 7 hours for VSV, 16 hours for NiV pseudovirus, and 24 hours for CCHFV. CCHFV N protein was detected utilizing 9D5 antibody and an Alexa-488 goat anti-mouse secondary

antibody as described above. The nuclei of the cells and the cytoplasm were stained as described above and the plates were read and analyzed on the Operetta reader. The percent of infection in greater than 20,000 cells was determined per experimental point and normalized to the pH 7.0 treated virus data.

Dominant negative blockage of CCHFV entry and fusion

Transfections of wild-type (WT) and dominant negative (DN) Rab proteins were performed in 293T cells to determine their effects on CCHFV entry. Rab5 WT and DN were tagged with GFP in pEGFP-C1 and were kindly provided by Robert Davey (Texas Biomedical Research Institute). Rab7 WT and DN were tagged with DsRed in pDsRed-C1 (Clontech, Mountain View, CA) and were kindly provided by Richard E. Pagano [170]. Negative controls used in all experiments included pEGFP-C1 (Clontech) or pDsRed-C1 (Clontech), and pcDNA3.1 (Invitrogen). 293T cells were plated at a density of 1×10^4 cells per well in a 96 well poly-D-lysine coated black clear-bottom plate 24 hours before transfection. Each plasmid was transfected at a concentration of $0.05 \mu\text{g}$ per well using Fugene HD (Promega, Madison, WI) following the manufacturer's protocol for 293T cells. Fugene HD was added at a 3:1 ratio of Fugene HD to DNA, and incubated for 5 minutes before adding the mixture to the cells. Twenty-four hours post transfection the cells were infected with CCHFV, EBOV, or EBOV-eGFP as a control. For the infection the medium was removed from the cells and the diluted virus was added in a volume of $50 \mu\text{l}$ per well at an MOI of 2 for CCHFV, and an MOI of 2.5 for EBOV or EBOV-eGFP. The plates were incubated with virus at 37°C for 1 hour, then the inoculums were removed and $100 \mu\text{l}$ of fresh medium was added. CCHFV plates were fixed in 10% buffered formalin 24 hours post infection, EBOV plates were fixed at 48

hours post infection. The cells were fixed in 10% formalin for 24 to 72 hours prior to bringing them out of the BSL-4 laboratory. Immunofluorescence was then carried out to detect CCHFV N and EBOV GP using monoclonal antibodies 9D5 and 6D8 respectively. An Alexa-568 goat anti-mouse secondary (Invitrogen) was then used to detect the monoclonal antibodies for GFP transfected cells, or Alexa-488 goat anti-mouse (Invitrogen) for DsRed expressing cells. The nuclei of the cells and the cytoplasm were stained as described above and the plates were read and analyzed on the Operetta or Opera reader.

Flow Cytometry

A flow cytometry based infectivity assay was optimized in 293T cells. Two-million cells per well were infected in 12 well plates with CCHFV IbAr 10200, at a range of MOIs from 5 to 0.5, in final volume of 2 ml/well. The infected cells were incubated for 24 hours at 37°C. 293T cells were then resuspended and fixed in 500µl of 10% buffered formalin and allowed to fix for 24 hours prior to immunofluorescent staining. HepG2 wells were trypsonized to remove them from the plate, then pelleted in a microcentrifuge (Eppendorf, Hauppauge, NY) at 3,000 rpm, followed by resuspension and fixation in 500µl of 10% buffered formalin. For immunofluorescent staining of the cells, the cells were first washed in PBS, then 100µl of proteinase K (DAKO) was added and the cells were incubated at room temperature for 10 minutes to retrieve the epitopes, by breaking the protein cross-links caused from formalin treatment [171]. The cells were then washed twice with PBS, and permeabilized with 0.2% saponin in PBS with 1% FBS for 5 minutes at room temperature. The cells were washed twice in PBS, and then non-specific epitopes were blocked by incubating the cells with a blocking buffer (PBS with

0.1% Tween-20 and 10% FBS) for 1 hour. The primary antibodies 9D5 (to CCHFV N protein) or an IgG2a isotype matched negative control to VEE E1 were diluted to 1ng/ μ l, and 100ul was added to each sample and incubated for one hour. The cells were then washed twice in PBS. An Alexa-488 tagged goat anti-mouse secondary antibody (Invitrogen) was used to detect the bound primary antibody. The secondary antibody was added to each well at a concentration of 2ng/ μ l and the cells were incubated at room temperature for one hour, then the cells were washed twice in PBS and resuspended in 500 μ l of PBS with 1%FBS and read on a FACScalibur flow cytometer (BD Biosciences, San Jose, CA).

Trypsin-sensitivity of CCHFV binding to 293T cells

293T cells were treated with 0.4mg/ml of trypsin (Sigma-Aldrich) in HBSS for 15 minutes at 37°C then washed twice with PBS. Trypsin treated 293T cells and non-treated control cells were then incubated with CCHFV IbAr 10200 at a MOI of 10 for 90 minutes at 4°C. The cells were washed four times in PBS to remove any unbound virus, the cells were resuspended in 250 μ l of PBS and lysed in 750 μ l of Trizol LS (Invitrogen, Carlsbad, CA), and then the samples were removed from BSL-4 containment. The total RNA was extracted by the following method: 200 μ l of chloroform (SIGMA) was added to the lysed cells and mixed vigorously and incubated at room temperature for 2 minutes, then centrifuged at 12,000 g at 4°C for 15 minutes to separate the aqueous and organic phases. The aqueous phase was transferred to a clean 1.5ml tube and 500 μ l of isopropyl alcohol was added and in the mixture was incubated at room temperature for 10 minutes. The samples were then centrifuged at 12,000 g at 4°C for 10 minutes to pellet the RNA. The pellet was washed in 1 ml of 75% ethanol and centrifuged at 7,500 g for 5 minutes,

then the pellet was air dried and resuspended in 20 μ l of RNase/DNase free water. Viral RNA was detected by qRT-PCR as previously described [172]. Briefly, 5 μ l of the extracted sample was added to 15 μ l of master mix which contained 1.25 μ M of the forward primer (5'-GGAGTGGTGCAG GGAATT TG-3'), 1.25 μ M of the reverse primer (5'-CAGGGCGGGTTGAAA GC-3'), 100nM of the TaqMan-MGB probe (5'-6FAM-CAAGGCAAGTACATCAT-MGBNFQ-3'), and 0.25 units per reaction of SSII RT/Platinum® Taq Mixture (Invitrogen, Carlsbad, CA). The qRT-PCR reactions were run on the 7500 Real-Time PCR System (Applied Biosystems, Carlsbad, CA) using the following cycling conditions: 50°C for 15 minutes, followed by 1 cycle at 95°C for 5 minutes, and 45 cycles at 94°C for 0 seconds, 55°C for 20 seconds, and 68°C for 5 seconds. Fluorescence was read in Channel 1 with a gain of 8/2 at the end of each 68°C step. Analysis of the real-time RT-PCR data was performed with SDS 2.0 software (Applied Biosystems, Carlsbad, CA).

Fc-tagged protein cloning and purification

Fc-tagged CCHFV glycoprotein genes were cloned and expressed for use in co-precipitation studies with CCHFV permissive cell lines. The G_N ectodomain gene region of CCHFV was amplified from a codon optimized CCHFV M segment in pCAGGS was a generous gift from Robert Doms (University of Pennsylvania). The G_N ectodomain region was amplified using the 5' primer (5'-CCCGCTAGCAGCGAGGAGC-3'), and the 3' primer containing a flexible linker (GGGGSGGGG) and a stop codon, both primers contained external BglII sites. The resulting PCR amplicon was gel purified and cloned into the BglII site of the pFUSE-Fc (Invivogen, San Diego, CA) cloning site. The resulting plasmid, G_N-pFUSE-Fc, was sequenced to ensure the correct orientation of the

G_N insert in the pFUSE-FC plasmid, and the expression product was verified in cell supernatants by western blot using the G_N specific monoclonal antibody 4093 (which was a generous gift from Louis Altamura).

To produce the Fc-tagged G_N ectodomain protein, 10 T150 flasks (Corning) of 293T cells in DMEM (Gibco) with 10%FBS, once 90% confluent, were transfected with 60μg of G_N-pFUSE-Fc DNA per flask with Lipofectamine 2000 (Invitrogen) per the manufacturers' protocol. Six hours following transfection, the medium was removed and replaced with 293 SFM II medium (Gibco). Forty-eight hours post transfection, the supernatant was removed from the flasks and clarified first by centrifugation for 15 minutes at 3,500 x g, then by filtration through a 0.22μm filter (Millipore). The clarified supernatant was pH adjusted to 7.5 with 1M Tris (pH 7.5) (SIGMA) to a final concentration of 50mM Tris, and one protease inhibitor cocktail tablet (Roche) was added per 50 ml of supernatant, and 300mM NaCl was added. The supernatant was cooled to 4°C prior to purification.

The cooled supernatant was purified using a HiTrap Protein A column (GE Healthcare) on the Akta Explorer 100 Air FPLC (GE Healthcare), the Protein A column was equilibrated with PBS containing 0.5M NaCl at pH 7.5, then the cooled supernatant was passed through the column. The column was washed with PBS containing 0.5M NaCl, and the bound G_N-Fc protein was eluted with a linear gradient of 3M MgCl₂ or 0.1M glycine and 5ml fractions were collected. To determine the fractions that were to be concentrated and dialyzed, 20μl of each fraction, in a 4X loading dye (Invitrogen) containing reducing agent, was run on a 10% Bis-Tris gel using MOPS buffer (Invitrogen). The gel was stained with silver stain using the Silver Stain Plus kit (Bio-

Rad) per the manufacturer's protocol. The fractions containing G_N-Fc were either dialyzed using a 12ml Slide-A-Lyzer cassette with a molecular weight cutoff of 10,000 (Pierce) against PBS at 4°C, with a total of 3 PBS exchanges, or concentrated and exchanged for PBS using a Centriprep-20 column (Millipore, Billerica, MA). For dialyzing, the first two PBS exchanges were at 2 hour intervals, and the third was overnight. The dialyzed G_N-Fc was then concentrated using a Centriprep-20 column, and quantified using a NanoOrange protein quantitation assay (Invitrogen) per the manufacturer's protocol. The G_N-Fc protein was aliquoted and stored at -80°C.

The G_N-Fc was analyzed by flow cytometry to determine if it would bind to 293T cells. Three percent FBS was added to the G_N-Fc protein samples and 293T cells were incubated with the protein for 90 minutes at 4°C on a rocker. The cells were then washed twice in cold PBS. Bound G_N-Fc was detected with an Alexa-488 conjugated goat anti human antibody (Invitrogen), the secondary antibody was incubated with the cells at 4°C for 45 minutes. The cells were washed twice with cold PBS and fixed with Cytofix (BD Biosciences), and then run on the FACScaliber flow cytometer.

Non-permissive cell line infection and analysis

The 55 human cell lines listed in Chapter 6 were tested for CCHFV IbAr 10200 replication to identify non-permissive cell lines. Two rounds of testing were conducted to identify the non-permissive cells by microscopy using an immunofluorescence assay (IFA). For the first round of testing, cells were infected with CCHFV at a MOI of 1 for 48 hours in duplicate in 24 well plates containing coverslips. CCHFV infected CER cells (chicken embryo-related cells) were used as a positive control. The cells were fixed for

24 hours in 10% buffered formalin and stained for CCHFV N as described above in the *Flow cytometry* section. The coverslips were mounted onto glass slides with Vectashield mounting media containing Dapi (Vector Labs) to stain the nuclei. Suspension cell staining was done in 1.5ml tubes, and spot slides were made by drying the resuspended cells onto glass slides, and coverslips were mounted on top of the spots with the mounting media listed above. The cells were examined on a fluorescent microscope first using a 10X magnification objective, then under a 20X magnification objective and scored for CCHFV N staining.

The second round of testing was performed as described above, but cells were harvested on days 3, 5, and 7 post infection. HL-60, Jurkat, and Molt-4 cells were then infected and harvested on days 2 and 3 post infection and analyzed by flow cytometry as described above.

Chapter 3. Development of High Content Screening Assay

Introduction

Automated microscopy and image analysis algorithms were first developed in the mid-1990s. Since then, major advances in microscopy equipment and methods, as well as in image processing have led to the development of high-content screening (HCS) and imaging (HCI). For entry studies, immunofluorescent imaging of viral proteins to assess the effect of inhibitors on entry was manually analyzed, which was laborious and could lead to observational bias. Automated image analysis can reduce some of the bias provided great care is taken in optimizing the assays to ensure that the analysis can reliably distinguish between infected and uninfected cells. HCS/HCI provided researchers with the tools to replicate human observations with less labor, while providing objective and quantitative measurements of cell-based assays for statistical analyses. Multiple parameters can be measured within single cells simultaneously and on a large scale in response to virus infection, drugs, or other stimuli. HCS has been used to perform large screens of small molecules, drugs, kinase inhibitors, and siRNA to assess pathways involved in virus entry and identify potential anti-viral compounds. A large scale screen was performed against EBOV and Marburg virus (MARV) and identified a novel anti-oxidant that has broad spectrum anti-viral activity, NSC 62914 [173, 174]. In another study a screen 1280 compounds identified numerous compounds that inhibited RVFV, which provided insight into the entry mechanism of the virus, such as its dependence on protein-kinase C epsilon early in entry [175]. A genome wide kinase siRNA screen was performed to identify kinases involved in CME and caveolin-dependent endocytosis utilizing VSV and simian virus 40 (SV40) respectively as cargo [98]. Not only did this

kinase screen provide insight into the pathways involved in endocytosis, it also provided potential anti-viral targets that can be explored with small molecule inhibitors. HCS has provided the means to perform much larger screens than was possible by traditional methods, such as plaque yield reduction assays. These large screens are useful as an initial identification of inhibitors, but traditional methods, such as plaque yield reduction assays can be used to confirm potential inhibitors. Although the study presented here did not include large scale screens, the use of HCI allowed for a large number of replicates per experimental condition, robust statistical analysis to ensure it was specific and sensitive, and minimized the subjectivity of analysis.

The basic principles of HCI involve dividing the image into pixels and applying segmentation algorithms able to assign pixels to distinct objects in the cell (e.g., the nucleus, cytoplasm, organelles, and labeled proteins) (**Fig. 10**) (reviewed in [176]). Numerous viral entry studies have been published. Most studies use a basic readout for imaging-based assays, the fluorescent intensity of antigens or over-expressed fluorescent reporters [98, 177-179]. Other, more complex assays include the scoring of morphological features in response to stimuli, live-cell analysis for visualizing protein-protein interactions, and time-resolved live imaging for visualizing dynamic processes such as cell division.

Although some aspects of any HCI assay are similar, specific parameters must be identified and optimized to consistently produce the desired readout for the new assay being developed. To minimize or negate the effects of the many variables encountered in this type of bioassay, which can lead to poor reproducibility, care must be taken to optimize each new assay with regards to cell density, virus MOI, and staining [173]. To

determine the quality of the assay, statistical equations for signal-to-noise ratio, percent coefficient of variation (%CV) (which measures screening data variability), and Z' -values (which defines the power of an assay to discriminate between a negative control and a positive control) are applied [14, 173, 176, 180]. A %CV of less than 5% is ideal, but may be difficult to achieve for all viruses, as some viruses infect in distinct foci which can lead to variability and a larger %CV between replicates. A Z' -value between 0.5 and 1.0 are indicative of a robust assay, and indicate that there is a reliable distinction between positive and negative cells. In this Chapter, I describe a sensitive and specific 96-well HCI assay that we optimized for use with CCHFV infections, as well as for infections with control viruses and a pseudovirus. In subsequent chapters I detail its' use in accomplishing the goals of this project with regard to defining early cellular entry events for CCHFV.

Results

Increasing CCHFV yield for HCI: The methods used to propagate CCHFV prior to this study, in SW13 cells and harvesting at 4 to 5 days post infection, would yield virus titers with a maximum of 10^5 pfu/ml. This low virus titer was insufficient for cell culture based immunofluorescence entry assays, as a single round of replication is ideal for studying the effect of a drug on entry as opposed to egress. To increase CCHFV titers we infected CER and HepG2 cells in T25 flasks were infected with CCHFV at an MOI of 0.003, and harvested and combined virus from the cell supernatant and cell lysates at 12 hour time points. The virus was then titered by plaque assay on CER cells. Between 36 and 48 hours, the maximum virus yield (1×10^7 pfu/ml) was reached in both cell lines, which was a high enough titer to be used for HCI assay development (**Fig. 9**). The virus yield had a

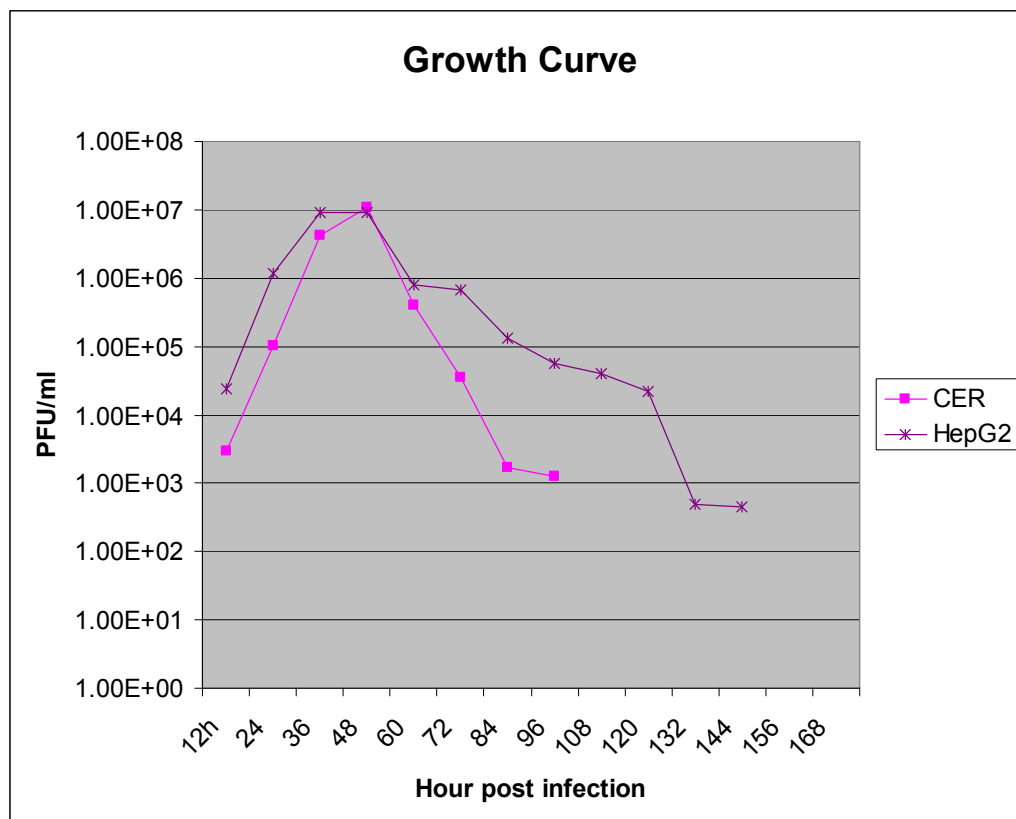


Figure 9. Growth kinetics of CCHFV IbAr 10200 in CER and HepG2 cells. CCHFV was harvested at 12 hour time-points from both the cell supernatants and the cell lysates, which were combined, and the virus was titered by plaque assay. Forty-eight hours was determined to be optimal for virus growth in both cell lines, and was used to make a large stock of virus that was used for this study.

sharp decline after 48 hours post infection which was consistent with earlier studies showing that CCHFV is inactivated rapidly at 37°C [53]. The CCHFV stocks used throughout the study were harvested from supernatant alone, which had titers ranging from 2×10^6 pfu/ml and 1×10^7 pfu/ml, because it was thought that the lysate added significantly more cellular debris, which might influence subsequent infections in cell-culture.

Optimization of CCHFV infection assays: The seeding density of A549 and 293T cells and CCHFV inoculums and incubation times were optimized in 96 well plates to achieve 50%-60% infection in order to enable discrimination between treatments that inhibited or increased infection. In addition, the 50-60% infection rate decreases the variability within a well and between replicates, which is calculated by the %CV, when analyzing a subset of the well as CCHFV typically infects in distinct foci. A lower infection rate would require the analysis of a larger subset of cells to reduce the variability. Our previous work established that in most cell lines CCHFV proteins can be detected in infected cells by immunofluorescent antibody staining 24 hours after infection. Consequently, we chose this time as the baseline for optimizing cell density and multiplicity of infection to achieve the target number of infected cells.

We compared two seeding densities and four MOI in two cell types. We selected these parameters for testing based on results of assays developed by my co-workers for the filoviruses, EBOV and MARV, as well as preliminary testing of CCHFV in several cell lines based on four seeding densities (data not shown) [173]. The analysis shown for each experiment was derived from a single plate with each experimental parameter in triplicate (**Fig10**). The statistical analysis of these parameters indicated that with an

increased virus MOI the coefficient of variance (%CV) decreased while the Z' value increased (**Fig. 11**). Thus, the overall quality of the assay improved with an increase of the MOI. The optimal parameters among those that we tested for the HCI in A549 cells were cells seeded at a density of 40,000 cells/well, and a CCHFV infection at MOI of 2. These parameters resulted in a CV <5% and a Z' value of 0.9, yielding 48% of the cells showing detectable infection (**Fig. 11**). A higher virus MOI did not significantly increase the percent of infected cells nor did it improve the quality of the assay; therefore, an MOI of 2 was used for CCHFV for all subsequent studies in A549 cells. As there was little difference between HCI assay results with A549 seeding densities of either 40,000 cells per well or 80,000 cells per well, both were considered acceptable (**Fig. 11A**).

A higher percentage of infected cells were required for the studies that we performed in 293T cells (described in Chapter 5). For the 293T cell HCI, of the parameters that we tested, the same conditions as chosen for A549 cells resulted in the higher infection target for 293T cells; i.e., 40,000 cells per well, CCHFV MOI of 2, resulting in 86% detectable cell infection with a %CV=5 and a Z' factor of 0.9 which (**Fig. 11B**).

Application of the CCHFV HCI assays: We used the HCI conditions identified for A549 cells to determine if drugs or siRNAs influenced CCHFV infection (Chapters 4 and 5). The 293T cell HCI assay was used to identify virus infection in cells that are transfected with wild- type and dominant-negative tagged Rab GTPase proteins (Chapter 5), to determine the effect of these over-expressed proteins on CCHFV infection, and to examine the pH dependent nature of the virus. The cytotoxicity of the drugs, transfected

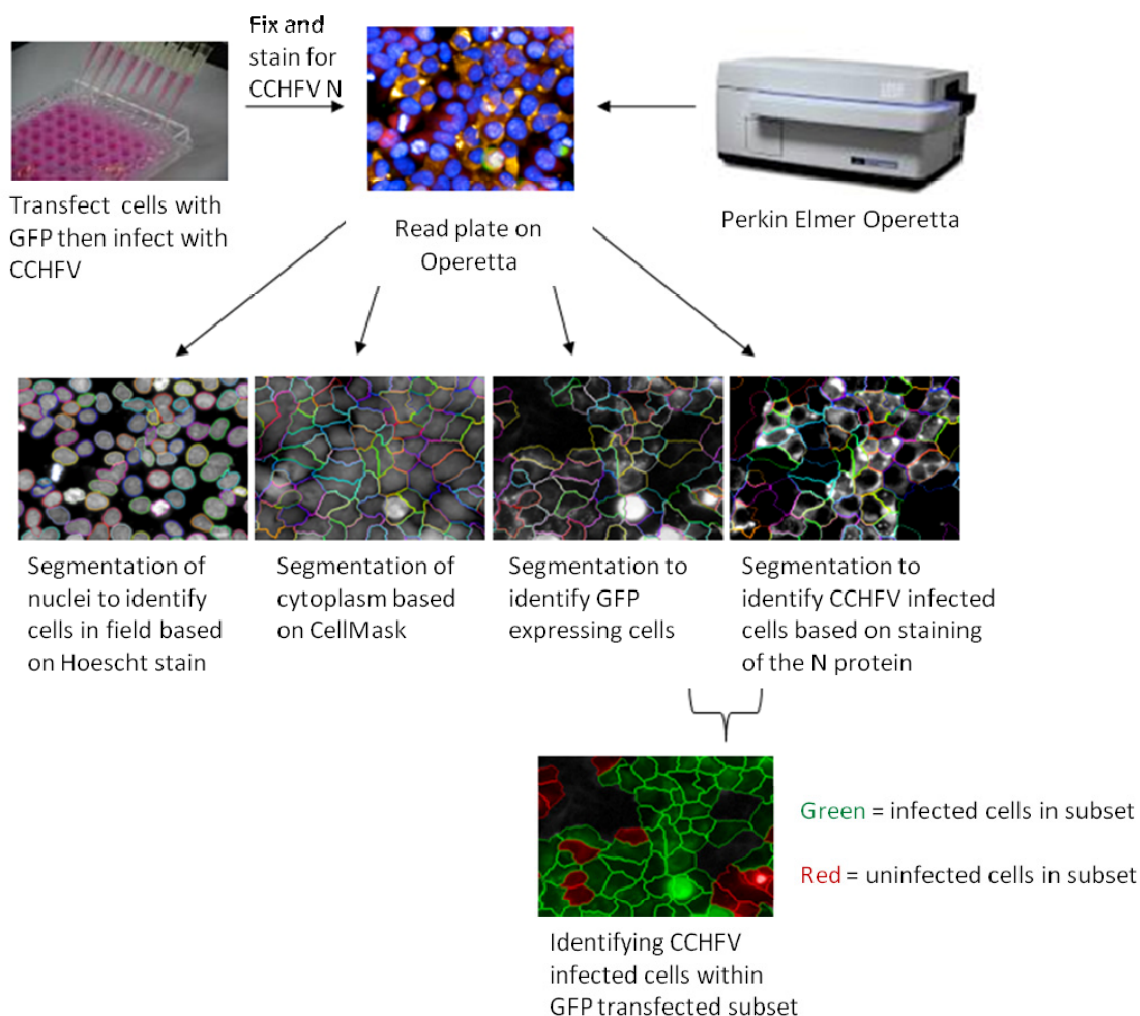
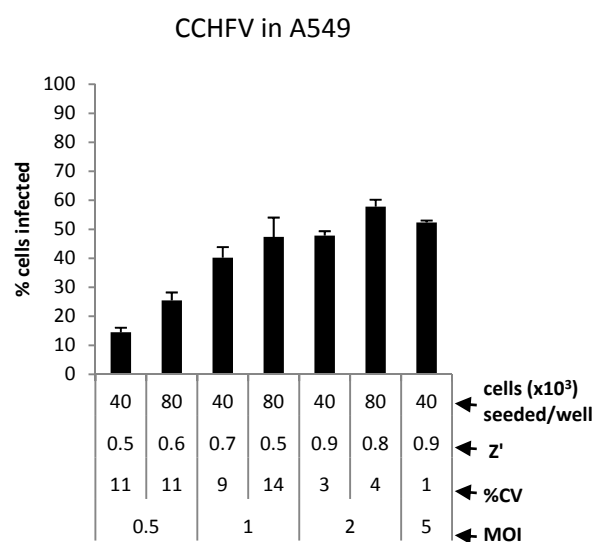


Figure 10. A schematic of the HCI assay used to study CCHFV entry events with transfected cells expressing GFP, and IFA staining of the viruses used in this study. In this example HCI assay, we seeded cells in a 96 well plate, transfected with a GFP expressing plasmid, then infected with CCHFV 24 hours later. The plate was fixed 24 hours after infection, and the viral protein was fluorescently stained as described in the Materials and Methods. Images were captured on the Operetta instrument, and using standard algorithms that use custom parameters the nuclei were identified by Hoechst staining, to determine the cell number within each field. Next, the cell membrane was defined using the CellMask stain image. The transfected cells were identified as those cells that express GFP above the mock control and the virus-infected cells were identified as those stained with Alexa-568 above the mock control. In the last panel the virus-infected cells within the transfected cell population are then identified.

DNA, and siRNAs used throughout the present study were determined by comparing the cell numbers and overall cell appearance of treated cells to mock-treated controls.

Establishment of HCI parameters for control viruses and pseudovirus infections: For control viruses and pseudoviruses, the virus inoculums and viral staining were adjusted to the cell density that was optimal for CCHFV, 40,000 cells per well for 293T cells, and either 40,000 or 80,000 cells per well for A549 cells. The goal was to identify assay conditions for each control virus or pseudovirus that would yield a Z' value between 0.5 and 1, which indicates high quality assays (Zhang, 1999). For VSV-eGFP in A549 cells there was little variability (%CV ranging from 6-14%) at MOI of 0.6 to 2.5, and the Z' values were 0.8 for these MOIs (**Fig. 12A**). As an MOI of 1 also yielded an excellent Z' value of 0.9 and a %CV of 3% in 293T cells (data not shown), this MOI was used for VSV-eGFP in all assays in my research (**Fig. 13C**). The virus titer for the VACV-eGFP was lower than expected once it was calculated. However an MOI of 0.04, which was a one to one dilution of virus in medium, had an acceptable Z' value of 0.6 and a %CV of 14%. For experiments performed in our study a larger number of cells (fields) were analyzed per well to decrease the standard deviation between replicates. Assays for EBOV and EBOV-eGFP were developed previously in Vero cells and 293T cells [173, 181]. After confirming that we could reproduce acceptable results using the parameters of the previously published conditions, we used these for my work with EBOV controls (**Fig. 13A**). For the NiV pseudovirus control, we only tested a 1:10 dilution of the stock preparation in 293T cells, as this was the maximum amount of virus that could be used in the HCI assay (Chapter 5), and this dilution had an excellent Z' value of 0.8 (**Fig. 13C**).

A.



B.

CCHFV in 293T cells

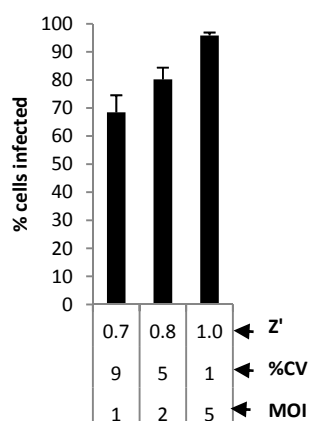
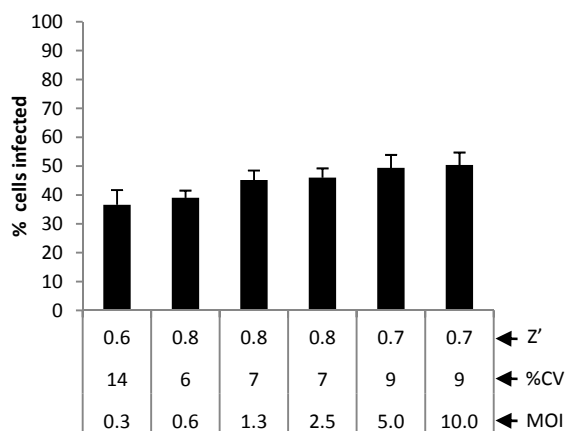


Figure 11. HCI parameters in A549 and 293 T cells. A. The seeding density of A549 cells and the MOI of CCHFV were examined to determine the optimal conditions for HCI. A549 cells were plated for a final cell count of 40,000 or 80,000 cells per well in a 96 well plate. The cells were infected with CCHFV at MOIs of 0.5 to 5 in triplicate, incubated for 24 hours and then fixed and stained for CCHFV N as described in the Materials and Methods. The optimal conditions were chosen as a balance between the percent of infected cells and low variability between replicates as determined by the standard deviation. **B.** Optimization of CCHFV in 293T cells, based on 40,000 cells per well in a 96 well plate. The cells were infected with an MOI of 1, 2, and 5, and treated as in A.

A.

VSV-eGFP in A549 cells



B.

VACV-eGFP in A549 cells

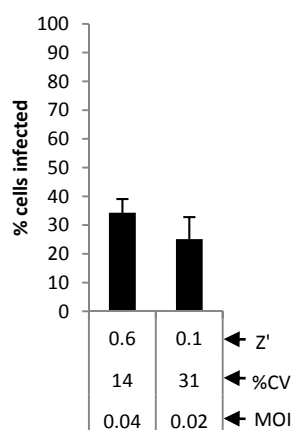
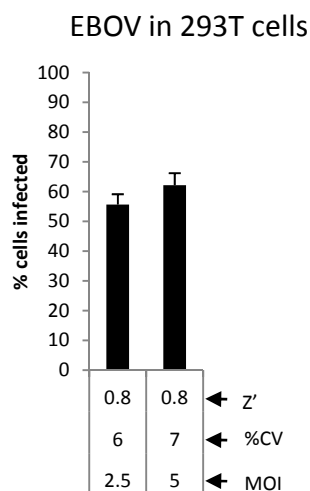
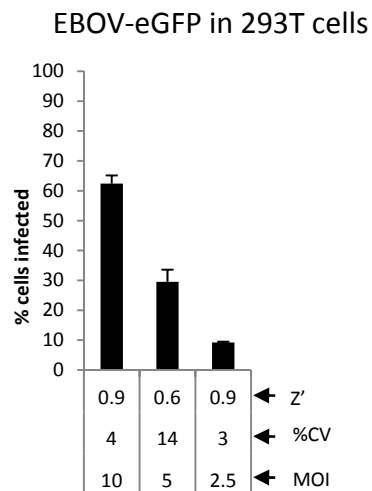


Figure 12. The effect of MOI on VSV-eGFP and VACV-eGFP infection in A549 cells. Cells were infected with a density of 80,000 cells per well in a 96 well plate with the MOI shown in the bottom row of each graph in triplicate. The cells were infected for 16 hours with VSV-eGFP or 24 hours with VACV-eGFP, then fixed and the nuclei and cells were stained as described in the Materials and Methods and read on the Operetta instrument.

A.



B.



C.

Virus or Pseudovirus	MOI or dilution	% cells infected	Hours of infection	%CV	Z'
VSV-eGFP	MOI 1	63.8	16	3	0.9
NiV pseudovirus	1:10 dilution	14.1	16	5	0.8

Figure 13. Parameters of control virus HCI in 293T cells. A. EBOV and B. EBOV-eGFP conditions tested in 293T cells of 40,000 cells per well were infected with the MOI indicated, and incubated for 48 hours prior to fixation. C. Summary of VSV-eGFP and NiV pseudotype testing and MOI used for experiments in 293T cells.

Analysis of results and conclusions

We sought to determine if we could develop a reliable and objective HCI assay for the study of CCHFV entry because of the statistical power and objectivity that this type of assay offers. In this chapter, I reported the results of various conditions that we tested to develop a reliable HCI assay that could be used for measuring entry events during CCHFV replication. First, we had to determine if we could increase the CCHFV virus stock titer to enable us to use HCI for this study. By testing several cell lines and determining the optimal growth and harvesting conditions we were able to obtain CCHFV at a high enough titer to optimize a HCI assay for studying CCHFV entry. To ensure appropriate experimental controls of viruses with known entry pathways, we also tested the HCI with those viruses or pseudoviruses. Even with the automation of HCI equipment, the use of multiple viruses for the same experiment presents enormous challenges, as the infection periods for the optimal replication of each virus differs. Among the pitfalls encountered because of this is variability in cell densities due to the differing incubation times. For example, if the cells become too dense it becomes problematic to properly segment the cells for analysis, while too few cells do not permit adequate data capture. In addition, we also needed to address the variables introduced when the cells were treated with drugs or transfected with siRNA or DNA. For example, variables included identifying cell densities for maximal transfection efficiency, timing for the knockdown of a target protein (siRNA) or protein over-expression (DNA), in relation to timing for optimal virus infectivity. We found that there was more flexibility in the range of cell densities and MOIs for CCHFV and VSV-GFP that produced robust assays than was previously reported for EBOV and EBOV-eGFP. I have presented

parameters that yield statistically valid data for CCHFV and control virus infections, we continued to evaluate the effects of these sorts of variables for every experiment described in the remainder of this thesis.

In conclusion, we found that the optimization of HCI assays for each virus was both challenging and tedious, and required many repetitions of the same experimental conditions to yield reliable assays. This in part is due to the need to practice the techniques so that the operator is skilled, as well as to become thoroughly familiar with the characteristics of each virus tested. Nevertheless, these automated assays provided several advantages throughout my studies, as they allowed for larger assays, with a greater number of replicates and larger number of cells than could have been analyzed manually. The HCI assays developed for each virus, therefore, provided statistical power as determined by the excellent Z' -values obtained for each optimized assay. These assays were then used throughout the rest of the work presented here to minimize the subjectivity of the data described in Chapters 4 and 5. The assays developed here can also be used for future work with CCHFV, such as high throughput screening to identify potential anti-viral drugs.

Chapter 4: Clathrin-dependent entry of CCHFV

Introduction

Clathrin mediated endocytosis (CME) is one of the most common cell entry mechanisms used by enveloped viruses. This complex process involves an initial binding of virus to a host receptor, followed by formation of clathrin coated pits on the cytoplasmic face of the membrane. Numerous regulatory or accessory proteins have been identified that participate in the formation of the clathrin-coated vesicles, which invaginate and pinch off from the host membrane. As described in Chapter 1, the only previous entry study for CCHFV (or any nairovirus) presented data that was consistent with CME entry. However, because clathrin is involved in other cell processes besides CME, some of the traditional tests used to identify an association between clathrin and viral replication provide suggestive but not conclusive evidence for CME entry. We used three approaches to further elucidate the role of CME in CCHFV entry. The first approach was a traditional study in which we tried to visually confirm CCHFV and clathrin co-localization. This approach provided limited useful information because it was not possible to infect cells with sufficient amounts of virus to show convincing co-localization with clathrin. Nevertheless, the data acquired from these studies provide suggestive albeit limited support to the findings obtained in the other two approaches so I have included them in the Results of this chapter.

The second approach involved siRNA depletion of the second most abundant protein in clathrin vesicles, AP-2. This protein, unlike clathrin, is not known to be involved in functions other than those related to CME, as discussed in Chapter 1, so its

association with CCHFV replication provides a relatively specific measure of CCHFV entry through CME.

The third and most conclusive approach that we used to study the CME entry pathway for CCHFV involved treating cells with Pitstop 2, an amphiphilic compound that specifically and reversibly binds to the terminal domain of the clathrin heavy-chain. Binding of Pitstop 2 blocks the ability of clathrin to bind to other ligands, this inhibits clathrin-coated vesicle trafficking in the cell. These three approaches together demonstrate that CME is likely the primary cellular entry mechanism for CCHFV.

Results

Clathrin and CCHFV co-localization: We attempted to directly visualize CCHFV and clathrin interactions, by performing confocal microscopy-based co-localization studies in CCHFV-infected A549 and HepG2 cells. We chose A549 cells in order to be consistent with studies involving the HCI assay used in the other two approaches presented in this chapter. Further, we repeated the studies in HepG2 cells because this liver cell line is not only permissive for CCHFV replication, but it also has a thicker cell body than A549 cells which allows for acquisition of ample Z-stacks (images on multiple planes).

To conduct the confocal co-localization studies, samples were synchronized for infection by incubating cells with virus on ice. The cells were then slowly warmed to 37°C to allow virus entry. In the first studies that we performed in A549 cells, we fixed cells at time points ranging from 1 minute to 30 minutes after warming. As a positive control, we used transferrin labeled with FITC, a glycoprotein that is known to concentrate in clathrin-coated vesicles following receptor mediated endocytosis. The

cells were examined by confocal microscopy using a 60X water objective, and Z-stacks were taken of the cells to identify co-localization of viral protein, or transferrin, with clathrin within a single plane when the red and green images were merged. We were readily able to detect co-localization of transferrin and clathrin at all of the time points, examples of the two intermediate time points are shown in figure 14A. In contrast, there were only rare instances of co-localization of CCHFV protein with clathrin, which are indicated by the white arrows in figure 14B, in A549 cells beginning at 15 minutes, and the majority of the virus particles remained on the cell surface even at 30 minutes (**Fig. 14B**). To further attempt to visually identify CCHFV in association within the CME pathway, we repeated the confocal studies in HepG2 cells and extended the time for co-localization observations to 60 minutes after warming. In these cells, we were able to visualize 1 to 2 co-localization events per cell by 30 minutes after warming, and the number of events increased slightly at 45 minutes after warming (representative 45 minute and 60 minute time-points are shown in **Fig. 15**).

As an additional control, which was intended to be a negative control, co-localization of CCHFV and caveolin was examined in HepG2 cells. The infected cells were fixed at 15 minutes, 30 minutes, 45 minutes, and 60 minutes post warming. At 60 minutes post warming, several virions appeared to co-localize with caveolin (**Fig.16**). These results were initially confounding. However, as described at the end of this chapter, the low level of virus and the relatively late apparent co-localization with caveolin might indicate association in EE compartments rather than in caveolin coated vesicles.

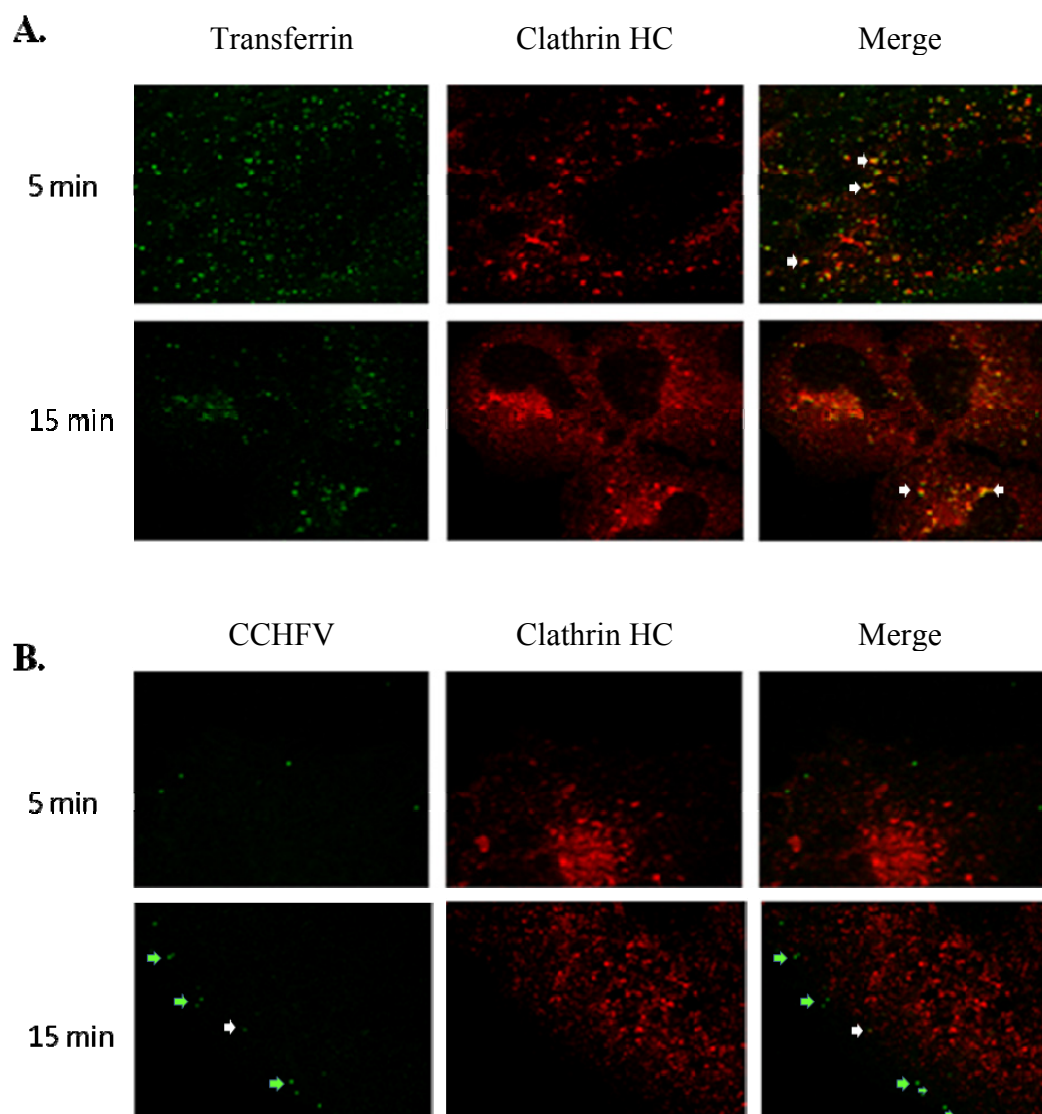


Figure 14. Co-localization of CCHFV and transferrin with clathrin in A549 cells. A549 cells were seeded in 24 well plates and then were incubated on ice with FITC labeled transferrin or with CCHFV for 30-60 minutes. Cells were then slowly warmed to 37°C, and washed and fixed with formalin at 1, 5, 15, or 30 minutes after warming. IFA was performed to detect CCHFV G_c or clathrin heavy chain (HC) as described in the Materials and Methods. Results from the two intermediary time points are shown as examples of typical observations. **A.** FITC-transferrin (green) and clathrin HC (red) at 5 minutes, and 15 minutes after warming. White arrows indicate examples of co-localization. **B.** CCHFV G_c and clathrin HC at 5 minutes, and 15 minutes after warming. Very little co-localization was observed, and the majority of detectable virions appeared to be at or near the cell surface (green). Green arrows indicate examples of virus at the cell surface, the single white arrow indicates co-localization. All images are from a single Z-plane per cell.

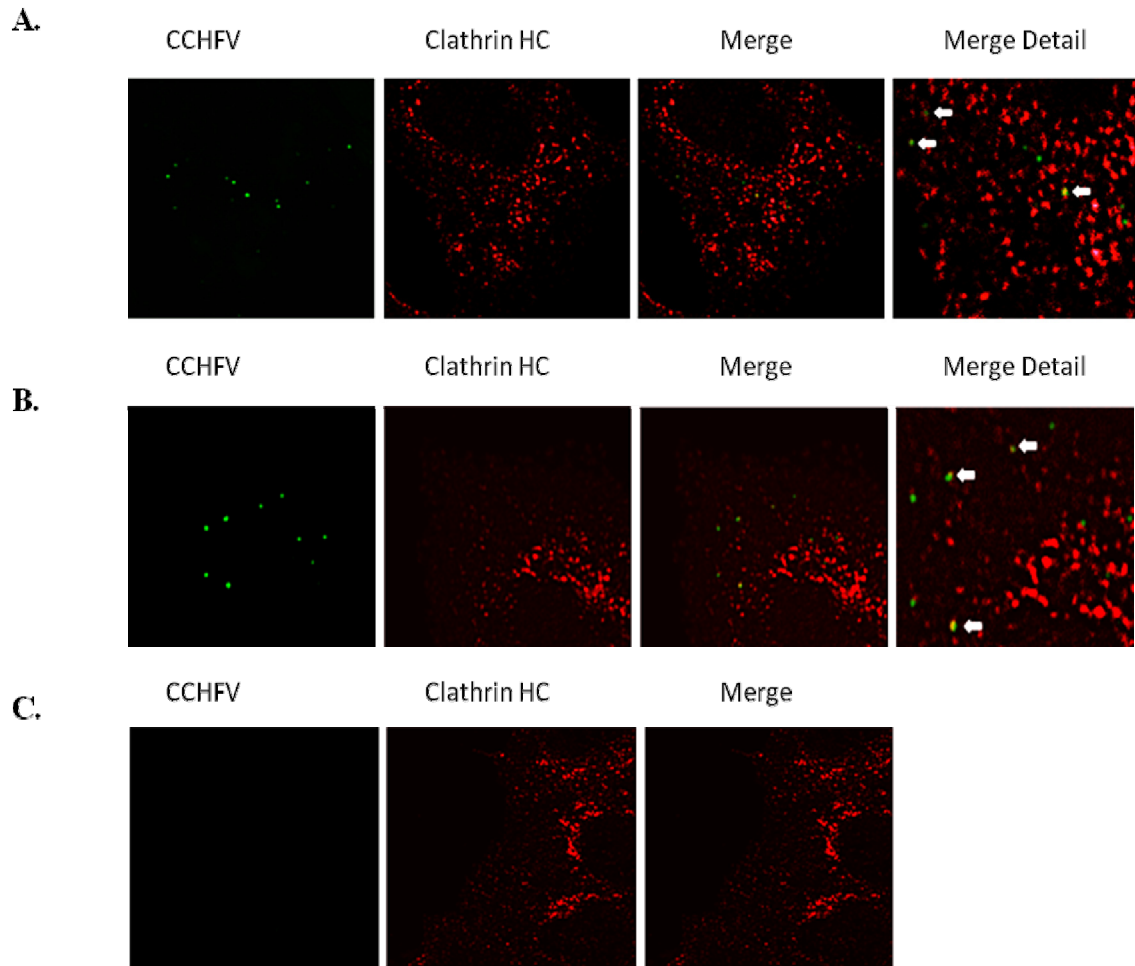


Figure 15. Co-localization of CCHFV and clathrin heavy-chain in HepG2 cells.

HepG2 cells in 24 well plates were infected with CCHFV on ice for 15 minutes. Cells were then slowly warmed to 37°C, and washed and fixed in 10% buffered formalin at time-points between 15 and 60 minutes post warming. IFA staining was performed to detect CCHFV G_C (green) or the clathrin HC (red). The white arrows indicate co-localization between the virus and clathrin heavy-chain. Merge detail panel shows a 5-fold enlargement of the Merge panel. **A.** CCHFV and clathrin HC at 45 minutes after warming. **B.** CCHFV and clathrin HC at 60 minutes post warming. **C.** Non-infected control at 45 minutes after warming.

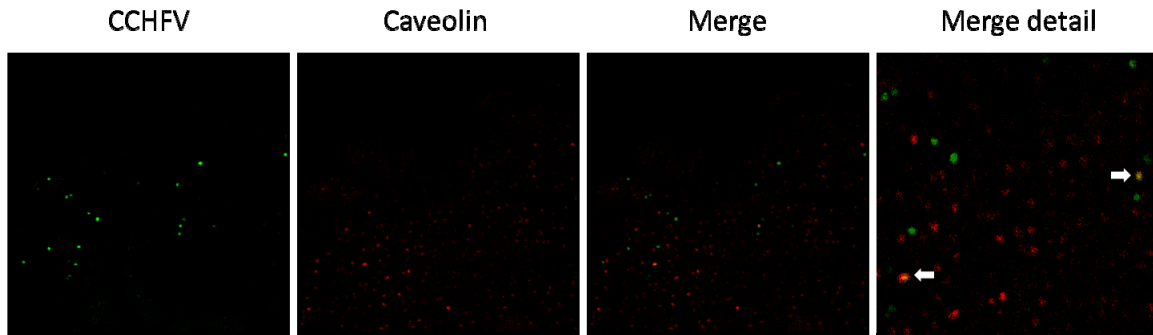


Figure 16. CCHFV has minimal co-localization with caveolin in HepG2 cells at 60 minutes post infection. HepG2 cells were infected with CCHFV and fixed as described in Figure 15, and stained for CCHFV G_C (green) or caveolin-1 (red). Co-localization in the last panel is indicated by the white arrows.

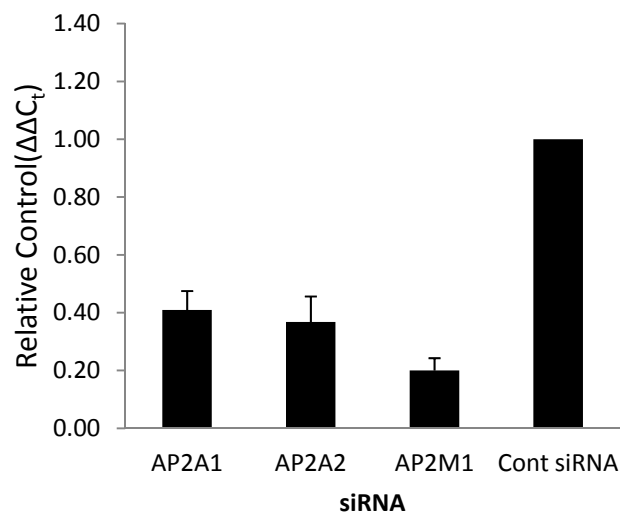
AP-2 association with CCHFV replication. The second approach that we used to study the role of CME in CCHFV entry involved depleting cells of AP-2 with siRNAs. As AP-2 is not known to be involved in host cell processes other than CME, an association with this protein provides strong evidence for use of the CME pathway (Blondeau et al., 2004). AP-2 is a heterotetramer of two large adaptins (α -type subunit AP2A1 or AP2A2 and a β -type subunit AP2B1), one medium adaptin (μ -type subunit AP2M1) and one small adaptin (σ -type adaptin AP2S1). For these studies, we transfected A549 cells with siRNAs directed against the two α isoforms (AP2A1 and AP2A2), or the μ (APM1) subunits of AP-2. Cells were transfected for 48 hours followed by infection with CCHFV. We measured the effect of each siRNA on virus replication by using the HCI assay that was described in Chapter 3. To confirm that the siRNAs specifically decreased the targeted mRNA production in the cells, we measured the mRNA level of each AP-2 subunit in uninfected cells at 48 hours post transfection by qRT-PCR.

We found that each siRNA decreased the target mRNA significantly (**Fig. 17A**). Treatment of cells with these siRNAs resulted in a statistically significant reduction in CCHFV infection (**Fig. 17B**). As virus controls, we also measured the siRNA knockdown effects on VACV-GFP or VSV-GFP replication. Both VACV and VSV serve as AP-2 independent controls. As already indicated, VACV does not use CME and even though VSV does enter by CME it does not require the presence of AP-2; but instead it may require another adaptor protein that has yet to be identified [110]. The AP-2 specific siRNAs had no effect on VACV-GFP or VSV-GFP infections (**Fig. 17B**).

Pitstop 2 effect on CCHFV replication. The final approach that we used to demonstrate that CCHFV enters host cells via CME involved treatment of cells with Pitstop 2, which

binds to the terminal domain of the clathrin heavy-chain. This compound prevents the interaction of the clathrin heavy chain with its ligands so that clathrin coated vesicle dynamics are perturbed, resulting in vesicles that can form but they remain bound to the plasma membrane [114]. In addition to testing the effects of Pitstop 2 on CCHFV replication, we also tested it with a known clathrin-dependent virus, VSV-eGFP, and with a known clathrin-independent virus, VACV-eGFP [110, 182, 183]. For these studies, A549 cells were pre-treated with dilutions of Pitstop 2 for 15 minutes, and then the virus inoculum was added in the presence of the drug and incubated for 1 hour. The inoculum was removed and the drug was added back for the remainder of the incubation, which ranged from 6 to 24 hours for the various viruses. The cells were fixed and stained as described in the Materials and Methods and the effect of the drug on each virus was measured using the HCI assay described in Chapter 3. Cellular cytotoxicity due to the drug was also measured for each virus to rule this out as a cause of reduced viral replication. Pitstop 2 was not cytotoxic at the lower concentrations tested and was only mildly cytotoxic at the higher concentrations tested (**Fig. 18**). Pitstop 2 treatment significantly decreased CCHFV infection in a dose-dependent manner (**Fig. 18A**). The replication of the VSV control virus was also dramatically reduced in the presence of Pitstop 2 but the compound had little effect on VACV infection (**Fig. 18B**).

A.



B.

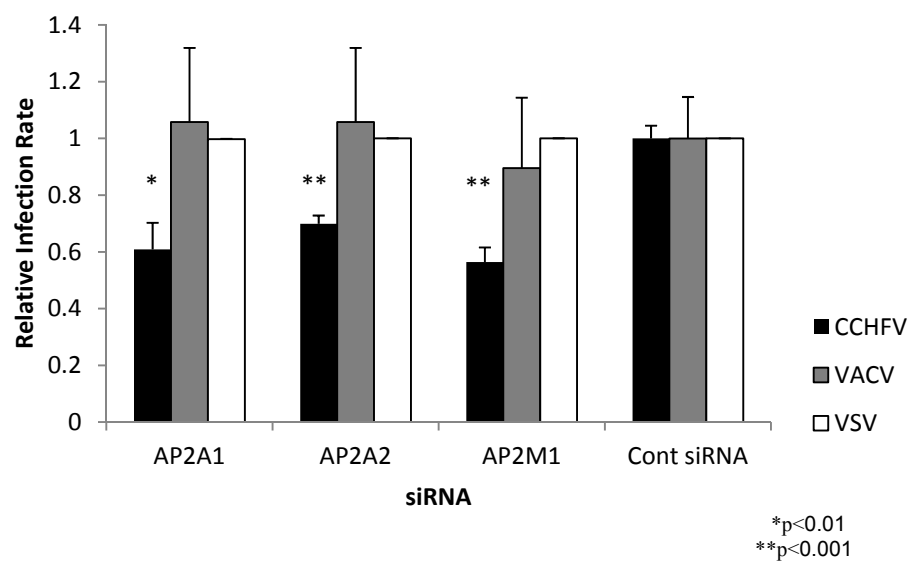
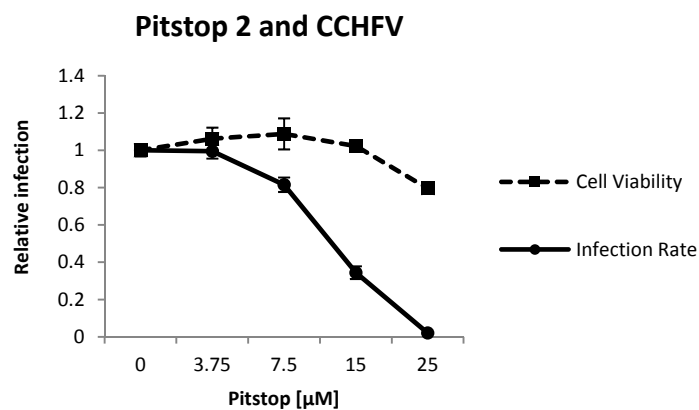
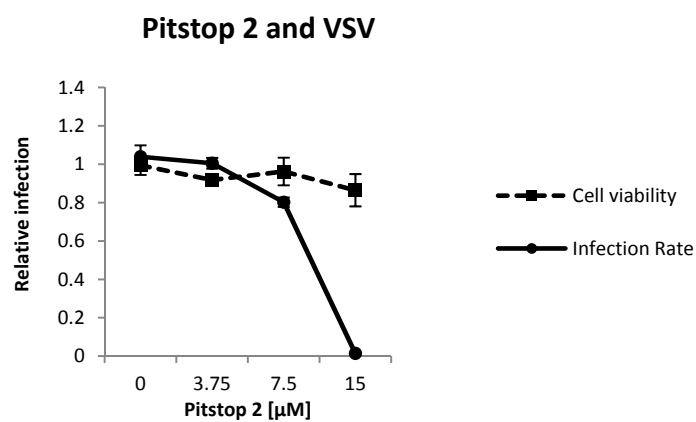


Figure 17. CCHFV uses AP-2 to enter A549 cells. The AP2A1 and AP2A2 siRNA target the two isoforms of the α subunit of AP-2, the AP2M1 siRNA targets the μ subunit of AP-2. A549 cells were transfected with each siRNA in replicates of three and infected with virus 48 hours later. The data shown is from a single experiment, and the data shown for CCHFV is representative of three separate experiments. **A.** qRT-PCR results of the mRNA knockdown mediated by the siRNA at 48 hours post transfection. The negative control siRNA samples were set to 1 and the relative RNA levels of each siRNA were calculated from the cycle threshold (C_t) using the $\Delta\Delta C_t$ method, which corrects the difference between the negative siRNA control and the other siRNAs based on an internal gene control. Cont siRNA (negative control siRNA). **B.** A549 cells transfected with AP2A1, AP2A2, or AP2M1 siRNA were infected with CCHFV, VACV-GFP, or VSV-GFP. The percent of infected cells was normalized to the negative siRNA control (Control siRNA).

A.



B.



C.

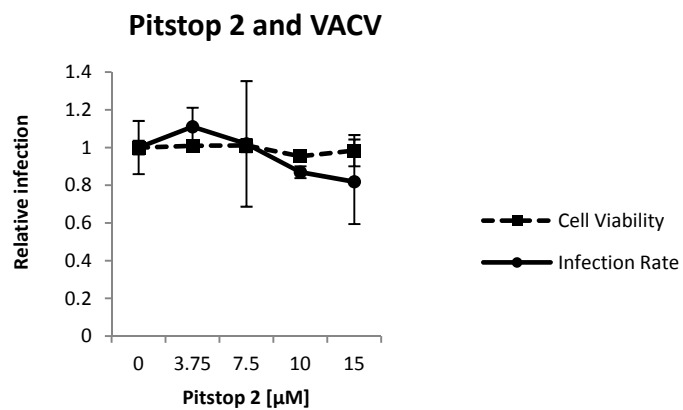


Figure 18. CCHFV entry is mediated by the clathrin-dependent pathway. A549 cells were treated at 37°C with each concentration of Pitstop 2 or a DMSO matched control in triplicate, and infected as described in the Materials and Methods. The percentage of infected cells were identified by HCI and normalized to the DMSO matched control. At least 6,000 cells were scored per experimental point. The change in cell count was determined by comparing the overall cell number per experimental point to the DMSO matched controls, which showed no toxicity when compared to a media control alone. The data shown for is representative of two experiments, the data shown for CCHFV and VSV were conducted in the same experiment. **A.** Cell count and infectivity of CCHFV in the presence of Pitstop 2. **B.** Cell count and infectivity of VSV-eGFP in the presence of Pitstop 2. **C.** Cell count and infectivity of VACV-eGFP in the presence of Pitstop 2.

Analysis of Results and Conclusions

When we initiated the studies on entry events for CCHFV no other reports of studies identifying these events had yet appeared in the literature. However, during my studies, another group published a study examining CCHFV entry events [127]. As described in Chapter 1, and as will be discussed in Chapter 7, the methods used for that work provided results that were suggestive but not conclusive that CCHFV uses CME for entry. Similar studies with other viruses serve to illustrate how relying on one method to define the entry mechanism of a virus can lead to incorrect results. For example EBOV pseudotypes were first reported to be dependent on caveolae for entry into human cells (293T, and HeLa) utilizing co-localization studies and caveolae inhibitors [184]. Later EBOV GP lentivirus pseudotypes were reported to require CME for entry into HeLa and Vero E6 cells utilizing CME inhibitors (chlorpromazine and sucrose), dominant negative EPS15, and siRNA to clathrin. The data was confirmed in the report with EBOV-GFP, utilizing chlorpromazine only [185]. EBOV GP lentivirus pseudoviruses were reported to require AP-2, eps15, and DAB2 for entry into human osteosarcoma cells (HOS) and human mammary epithelial cells (HMEC) [186]. The entry mechanism of EBOV was then refuted by several reports that indicated that the virus entry mechanism was macropinocytosis. Using EBOV-like particles, EBOV-GP-VSV pseudoviruses, and biologically contained EBOV (lacking VP30) it was reported that EBOV uses macropinocytosis and not CME as the mechanism of entry in Vero and Huh7 cells [187]. Another report used EBOV-like particles and EBOV-GFP and confirmed macropinocytosis as the mechanism of entry using Vero and 293T cells [157]. Another report using EBOV-like particles indicated that CME was an alternative means of entry

to macropinocytosis, and suggested the entry mechanism may be cell-dependent; however, this remains to be determined [188]. Similarly, two different entry mechanisms have been reported for UUKV via CME or a clathrin-independent mechanism, depending on the presence or absence of the DC-SIGN receptor [75, 128]. These two examples underscore the need to study virus entry mechanisms with a variety of techniques, and numerous cell lines. Here, we have applied three different approaches that in combination provide additional evidence for CME entry by CCHFV.

The first approach, involved using confocal microscopy to visualize CCHFV and clathrin co-localization. These experiments were not as successful as we had hoped due to the low amount of CCHFV that could be observed within cells. However, in my control experiments we readily observed co-localization of transferrin and clathrin, indicating that the method itself is functional. Despite repeated attempts to improve CCHFV yields from cell cultures, and several efforts aimed at concentrating virus for use in infections (data not presented), we were not able to increase the amount of virus within individual cells to a level that would allow clearly defined co-localization between CCHFV proteins and clathrin. Nevertheless, in HepG2 cells, we were able to visualize a few co-localization events for CCHFV and clathrin, but the data alone are insufficient to demonstrate CME entry. Although several virions also co-localized with caveolin at a late time point (60 minutes) as well, this does not necessarily indicate that the caveolin pathway plays a role in CCHFV entry. Caveolin is also present in domains of EE vesicles, and at 60 minutes post warming it is likely that virus has entered these compartments of the cell [189]. Work presented by Simon et al. has provided some evidence that caveolin does not play a role in CCHFV entry [127]. They found that

depleting caveolin with siRNA had no impact on virus entry; however, as these investigators did not include caveolae-dependent controls the data are difficult to interpret. It is possible that the co-localization of CCHFV and caveolin is due to overlap with the EE compartments rather than entry via a caveolin-dependent manner, but the role of caveolin in CCHFV entry cannot be ruled out by the results of our present study.

To further assess the role of CME in CCHFV entry, we used siRNAs directed against another resident protein of clathrin coated vesicles, AP-2. These experiments provide additional supportive evidence that CCHFV is associated with CME entry. Previous studies utilizing siRNA to knockdown AP-2 have reported that double transfections (48 hours apart) are needed to obtain maximal knockdown of AP-2 subunit proteins [110, 111, 186]. Two of these studies also showed that all of the subunits of AP-2 are down regulated when only the α or μ subunits are targeted by siRNA [110, 111]. It should be noted however that negative control viruses were not included in these last two studies to ensure that there were no off target effects resulting from the double transfections. We employed a single transfection method which appeared sufficient to reduce levels of each target mRNA 48 hours after transfection. We also observed a statistically significant decrease in infectivity of CCHFV with all three siRNAs directed against the AP-2 complex and no impact on the control viruses. The data presented in this chapter are representative of three experiments utilizing these siRNAs. All three experiments with the AP-2 specific siRNAs resulted in similar levels of decrease in CCHFV infectivity. Future experiments utilizing the double knockdown protocol to obtain even greater knockdown of AP-2 protein levels can be done to determine if that

further reduces CCHFV infection but with the data presented it is clear that AP-2 plays a role in CCHFV entry via clathrin-coated vesicles

Further evidence for CME entry by CCHFV came from results obtained by inhibiting clathrin-coated vesicle trafficking using Pitstop 2. To our knowledge this approach has not been previously tested against any bunyavirus, and it is a new way of showing that CME disruption also inhibits the ability of CCHFV to replicate. Because the method is new, there were some experimental details that required extensive and repeated consideration and testing to develop an optimal assay using this compound. For example, we found that a higher concentration of Pitstop 2 was required to completely block CCHFV replication as compared to VSV replication. In discussions with the corresponding author of the group that designed the compound and published the mechanism of action (personal communication with Volker Haucke [114], we discovered that the activity of Pitstop 2 is greatly reduced in high concentrations of FBS. Because the VSV stock was more diluted more than the CCHFV stock in order to achieve the MOIs that were optimal for each HCI assay, there was a final concentration of 0.75% FBS in the CCHFV inoculums, but only a 0.03% concentration of FBS in the VSV inoculums. Consequently, it was likely that a higher concentration of the drug was needed to produce the same level of activity against CCHFV as with the VSV-eGFP. In support of this theory, preliminary experiments with Pitstop 2 diluted in medium containing 10% FBS had a significant decrease in the activity against VSV and CCHFV (data not shown). To fully explore this, additional studies including adding 0.75% FBS to the VSV inoculums could be performed.

Chapter 5: Endosomal Trafficking of CCHFV

Introduction

In this chapter I describe studies aimed at determining the early trafficking events leading to CCHFV membrane fusion. After cargo is internalized within clathrin-coated vesicles it is then sorted into endosomes that become increasingly acidic as the organelles develop from early endosome (EE) to late endosome (LE) (reviewed in [90]). Many enveloped viruses depend on the acidic environment of endosomes to trigger conformational changes in their own envelope proteins that result in exposure of previously hidden fusion peptides. This process is essential for viral replication by initiating the fusion of viral and endosomal membranes so that the viral genetic material can be deposited in the host cell cytoplasm.

We used three distinct methods to study the endosomal trafficking events of CCHFV. In the single study describing CCHFV entry it was found that a lysosomal agent, bafilomycin A, and a weak base, ammonium chloride (NH_4Cl), inhibited CCHFV replication [127]. We treated cells with a weak base, NH_4Cl , which prevents acidification of endosomal vesicles (reviewed in [146]). Using this method, we confirmed that CCHFV requires an acidic environment for infectivity. We also compared the dose response of CCHFV to NH_4Cl with EE and LE dependent viruses, the dose response of CCHFV was indicative of EE dependence. Next, we tested the pH sensitivity of CCHFV. These results determined that the threshold of pH inactivation, which was pH 6.0, was also consistent with EE fusion. Finally, we used dominant negative versions of an EE-localized protein, Rab5, or a LE-localized protein, Rab7, to interrupt the trafficking of EE and LE during CCHFV infection. The dominant negative Rab

experiments also indicated that CCHFV fuses in EE. Taken together, the results for each of the experiments indicate that membrane fusion of CCHFV likely occurs in the EE.

Results

CCHFV has an acid-dependent entry step. The weak base NH_4Cl has been shown to concentrate in endocytic vesicles and neutralize their otherwise acidic environment [190]. Consequently, treating cells with NH_4Cl is a commonly used method for determining if a virus has an acid-dependent fusion requirement. In addition, the relative sensitivity that a virus displays to NH_4Cl can also provide clues as to whether fusion with EE or LE occurs since viruses that require the lower pH environment of LE as compared to EE are generally more sensitive to NH_4Cl treatment. We assessed the sensitivity of CCHFV replication to vacuolar neutralization. For comparison, we also measured the effects of NH_4Cl treatment on VSV-eGFP, which has been reported to fuse in the EE, and EBOV-eGFP, which has been shown to fuse in LE [157]. We treated 293T cells various concentrations (1-25mM) NH_4Cl in replicates of 6 for 60 minutes and then infected CCHFV or control viruses. The plates were fixed and analyzed using the HCl assays described in Chapter 6. We observed variable cytotoxicity at the highest concentration of NH_4Cl (25mM) for all viruses (EBOV – 35%, VSV-16%, CCHFV – 20%) and none below 25mM. EBOV-eGFP was more sensitive to the effects of lower concentrations of NH_4Cl treatment than VSV-eGFP (**Fig. 19**), results which are consistent with their LE and EE fusion steps respectively. CCHFV was inactivated at an intermediate concentration of NH_4Cl as compared to the control viruses but appeared to be more similar to VSV than to EBOV, particularly at NH_4Cl concentrations below 6.25 mM.

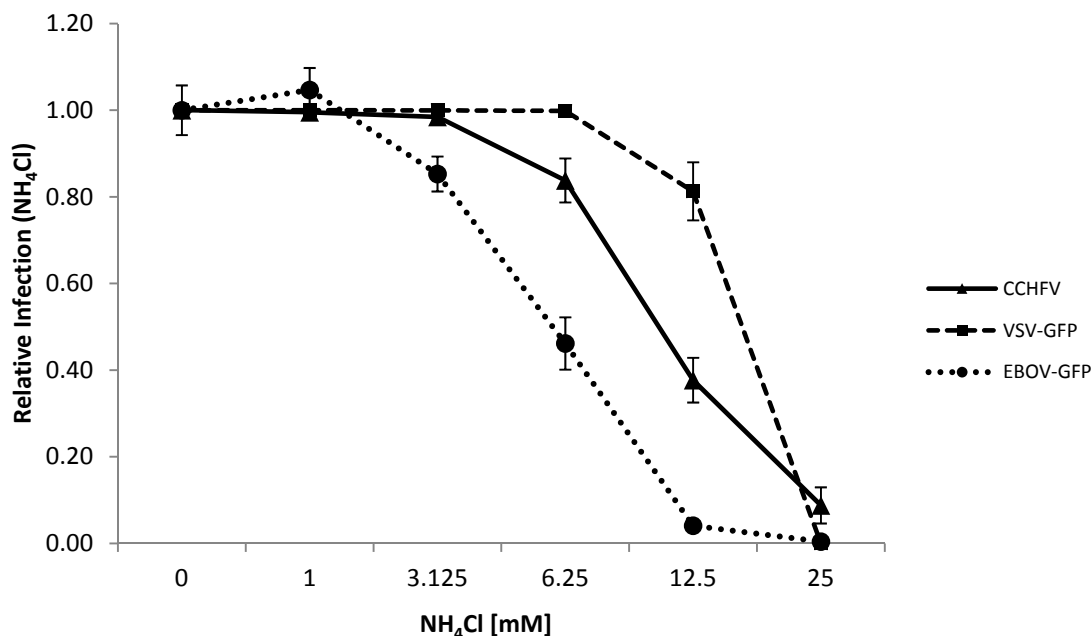


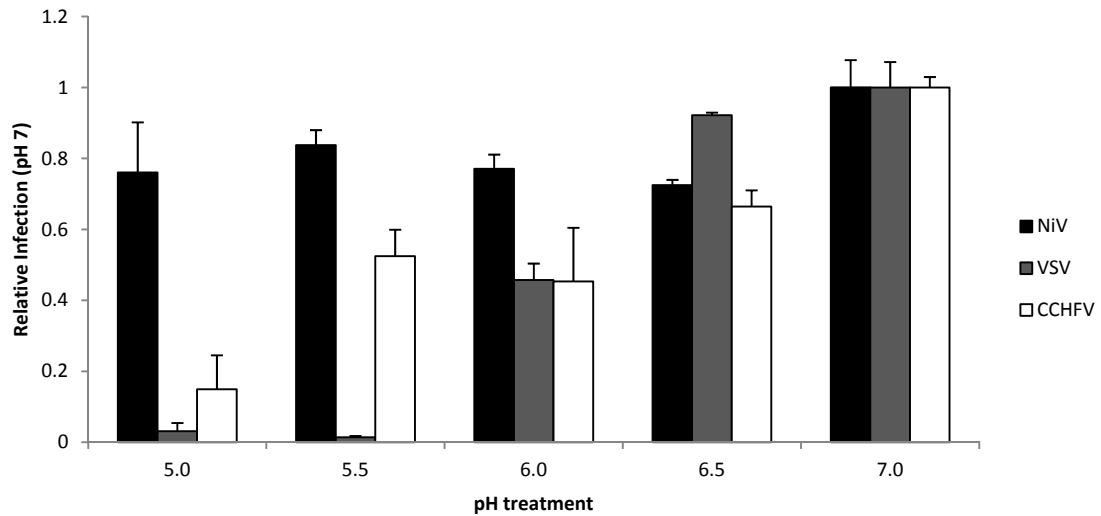
Figure 19. CCHFV entry is acid-dependent. 293T cells were pre-treated with NH₄Cl at various doses for 60 minutes prior to infection, in replicates of six, with VSV, CCHFV, or EBOV-GFP and incubated for 16, 24, and 48 hours respectively. The cells were fixed in 10% formalin, and CCHFV N and eGFP was detected as described in the Materials and Methods. The percent of infection was determined in each experimental point utilizing HCl, and normalized to the mock-treated control for each virus.

These results confirm that CCHFV has an acid-dependent entry step and suggest that fusion occurs in EE [127].

Low pH sensitivity and CCHFV fusion. To more clearly define whether CCHFV utilizes EE or LE fusion of CCHFV, we used a pH sensitivity assay in which we incubated the viruses in buffers ranging from pH 5.0 to 7.0. These pH values mimic conditions that would be encountered in the EE and the LE. Next, the solution containing the virus was neutralized to pH 7.2 to 7.4, which is the pH of EMEM medium. Finally, we determined the effect of the pH changes on the virus by infecting cells with virus that had been exposed to each pH. As control viruses, we similarly treated VSV-GFP and Nipah virus (NiV), which are pH-dependent and -independent viruses respectively, and then assessed their infectivity. We then performed a HCl assay for each virus to determine the changes in infectivity. The pH that is critical for CCHFV fusion should promote the conformational change in the glycoprotein that is responsible for fusion; therefore, it is no longer in the correct conformation to bind to the receptor and infectivity should be hindered.

For CCHFV we observed a statistically significant decline in infectivity at pH 6.5, and a much more substantial decline after treatment at pH 6.0 or 5.5 as compared to pH 6.5 or 7.0 (**Fig. 20**). Consistent with earlier studies showing that the pH threshold for conformational changes in the VSV G protein to promote fusion with endosomal membranes is 6.2 [151, 191], there was a substantial decline in VSV infectivity at pH 6.0 and complete inhibition of infectivity at pH 5.5. In contrast, NiV remained infectious even at pH 5.0 (**Fig. 20**). These results support those obtained by NH₄Cl treatment suggesting that CCHFV fuses with EE for entry to the host cell cytoplasm.

A.



B.

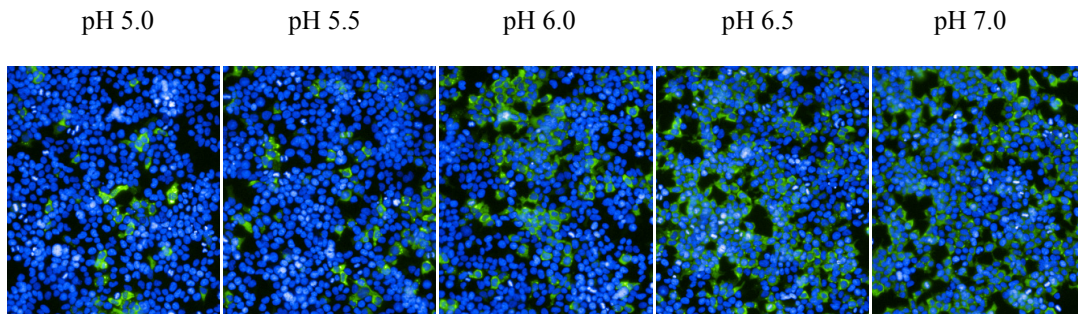


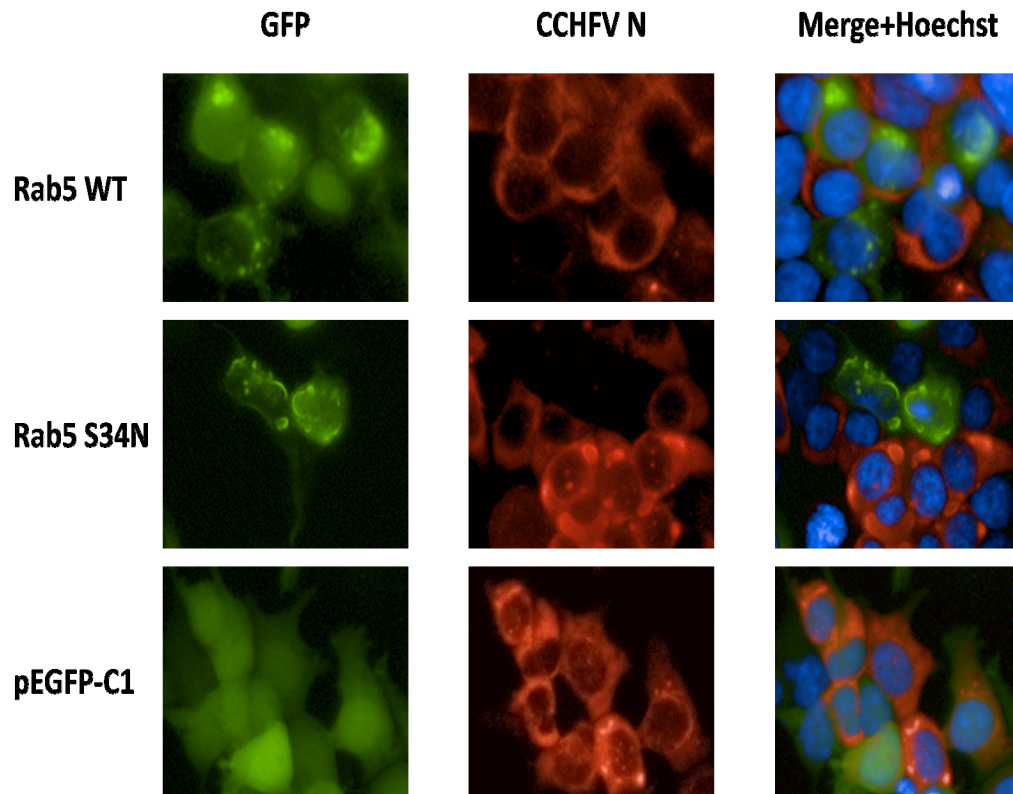
Figure 20. Threshold of pH inactivation. A. CCHFV, NiV, and VSV were pre-treated with buffers of various pH as indicated and then were neutralized to a pH of 7.2-7.4 as described in the Materials and Methods. 293T cells were then infected with each pre-treated virus in replicates of 6. The data shown is representative of three experiments. A. Infectivity was assessed using the HCI described in Chapter 3, and data acquired from greater than 20,000 cells were analyzed per experimental point and normalized to the pH 7.0 treated virus. The data shown is representative of three experiments B. 20x magnification images from the high-content imaging system is demonstrates that treatments did not compromise cells. CCHFV N is shown in green, with the nuclei stained with Hoechst (blue).

CCHFV and Rab5 GTPase. To confirm that CCHFV uses EE-dependent entry to the cytoplasm, we next performed studies using a dominant negative Rab 5 protein to inhibit native Rab5 functions. we transfected 293T cells with a plasmid expressing GFP only (pEGFP-C1) or expressing either an eGFP tagged wild type (Rab5 WT) or a dominant negative mutant of Rab5 (Rab5 S34N), then infected the cells with CCHFV 24 hours later. EBOV was used as a Rab5-dependent control virus as it requires both the EE specific Rab5 GTPase as well as the LE specific Rab7 GTPase for entry [157].

We observed that cells transfected with the Rab5 WT (green) or with the pEGFP-C1 plasmid expressing only eGFP (green) also showed evidence of CCHFV N (red) (**Fig. 21A**). In contrast, the majority of Rab5 S34N transfected cells (green) were not infected with CCHFV (red). Using the HCI assay described in Chapter 3 to quantify these findings, we found that CCHFV infection decreased by 57% in the Rab5 S34N transfected cells when compared to the pEGFP-C1 control (**Fig. 21B**). Conversely, the Rab5 WT construct increased CCHFV infection by 55% (**Fig. 21B**). This increase in virus with Rab5 WT has been shown previously with other EE dependent viruses such as VSV [160]. Likewise, consistent with earlier studies [157], EBOV infection decreased by 68% when comparing Rab5 S34N with the pEGFP- C1 control, and EBOV infection was also increased by the addition of the Rab5 WT (**Fig. 21B**). These data indicate that CCHFV requires passage at least through the EE for cell entry.

CCHFV and Rab7 GTPase. We conducted a similar experiment to the Rab5 GTPase experiment described above using a dominant negative version of the LE-specific Rab7 GTPase to determine if CCHFV also traffics through the LE compartment. Similar to the Rab5 DN, Rab7 T22N cannot bind GTP and the Rab7 protein remains

A.



B.

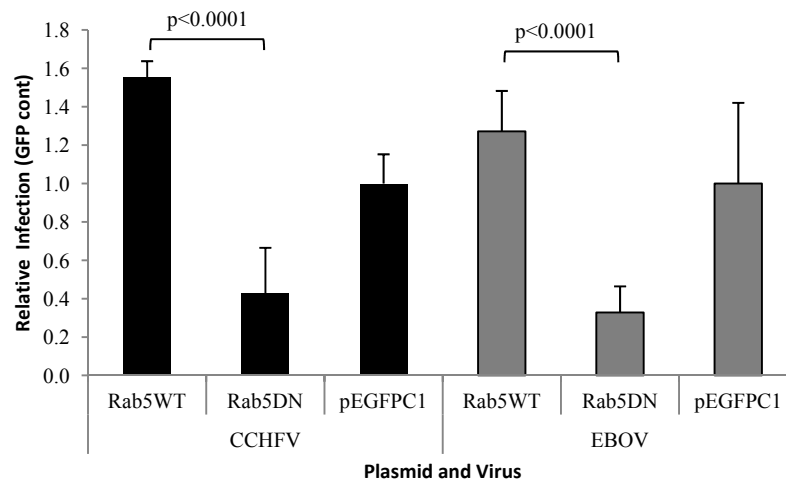
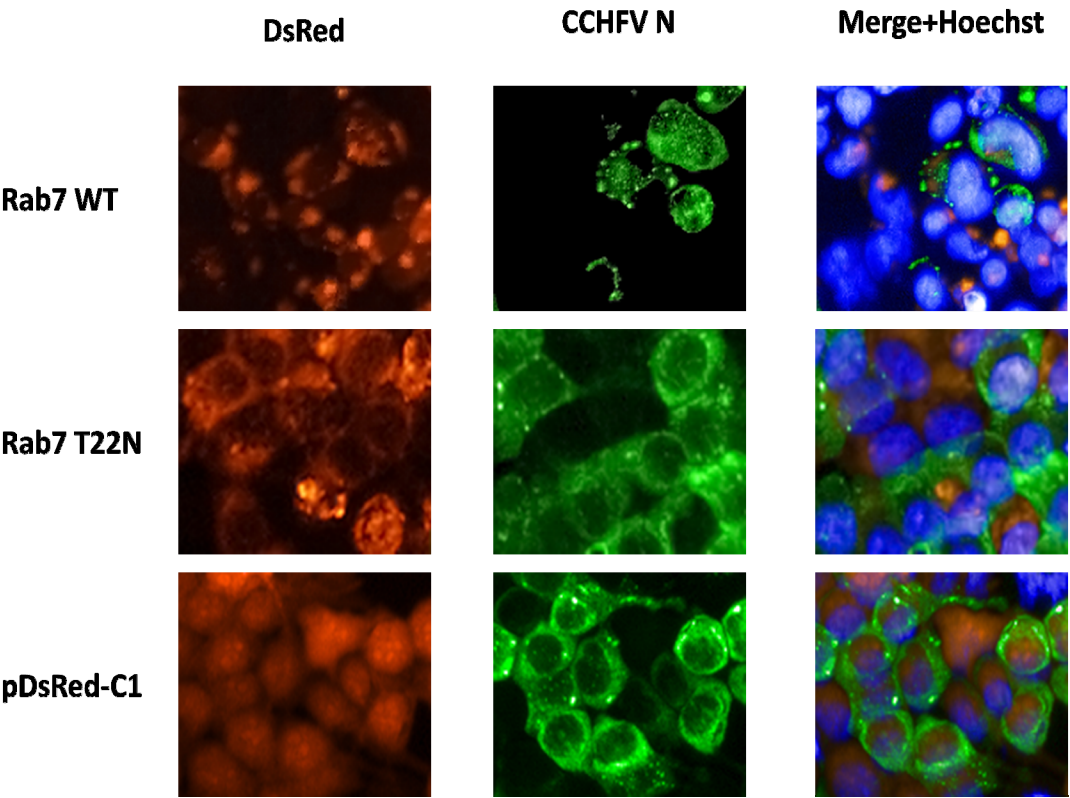


Figure 21. CCHFV is Rab 5 dependent. 293T cells were transiently transfected with Rab5-GFP S34N, Rab5-GFP wild type, or a pEGFP-C1 in replicates of six and then infected with CCHFV or EBOV 24 hours later. **A.** 20x magnification images from the HCI system, CCHFV N is shown in red, Rab5 WT and DN in green, with the nuclei stained with Hoechst (blue). **B.** The analyzed data from the high-content imager, greater than 19,000 cells were analyzed per experimental point.

A.



B.

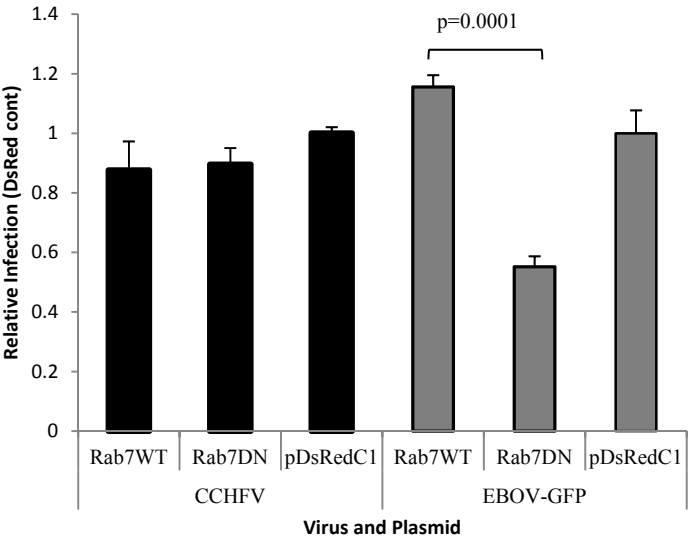


Figure 22. CCHFV is not Rab 7 dependent. 293T cells were transiently transfected with Rab7-DsRed T22N, Rab7-DsRed wild type, or a pDsRed in replicates of six and infected with CCHFV or EBOV-eGFP 24 hours later. **A.** 10x magnification images from the HCI system, CCHFV N is shown in green, Rab7 WT and DN in red, with the nuclei stained with Hoechst (blue). **B.** The analyzed data from the high-content imager, greater than 50,000 cells were analyzed per experimental point.

inactive [170, 192]. We found that cells transfected with Rab7 WT in DsRed-C1 (red), Rab7 T22N in DsRed-C1(red), or the DsRed-C1 empty plasmid (red) were also infected with CCHFV (green) (**Fig. 22A**). Quantifying the results by HCI, we found that there was no statistically significant change in CCHFV infection in cells transfected with any of the constructs (**Fig. 22B**). Consistent with earlier findings, EBOV-eGFP infection was decreased in Rab7 T22N expressing cells in comparison to the pDsRed-C1 control, $p=0.0001$ (**Fig. 22B**) [157]. These data indicate that CCHFV does not require LE trafficking for entry.

Analysis of Results and Conclusions

My studies showing that CCHFV has an acid-dependent entry step is in agreement with results from an earlier study, which demonstrated that the virus was sensitive to lysomotropic agents [127]. Our data showed a dose response of CCHFV inhibition to NH_4Cl , which more closely resembled the dose response of an EE dependent virus than that of a LE dependent virus. In the work presented in this Chapter, we further defined this entry step by identifying the pH threshold of CCHFV inactivation. The data indicated that CCHFV is sensitive to treatment with pH 6.0, which implicated that the pH within the EE compartment was sufficient to trigger a conformational change in the viral glycoproteins.

To further elucidate the role of endocytic vesicles in CCHFV entry we used a method of dissecting EE and LE compartments with dominant negative proteins to disrupt the functions of Rab GTPases that are known to be associated with these compartments. The inhibition of CCHFV infectivity with the dominant negative Rab5

protein, but not with the dominant negative Rab7 protein provides the first evidence that CCHFV likely enters cells by fusing in the EE compartment.

In experiments using 293T cells, we had to be wary of the ease at which these cells are removed from the wells in the 96 well plates during transfection, infection, fixation, and staining as this can skew HCI analysis. Careful review of the HCI images was required for all experiments involving this cell line, particularly when there were large deviations in cell number and percent of infected cells between replicates. Additionally, 293T cells monolayers can easily overgrow and the cells start to overlap, which is not ideal for HCI analysis. This cell line, therefore, required more testing and image review than A549 cells to achieve optimal conditions for HCI. The reasons for the inclusion of 293T cells in this study, they transfect well with plasmid DNA and the NiV pseudotypes did not infect A549 cells, outweighed the pitfalls described above.

Chapter 6: Additional CCHFV entry studies

Introduction

In Chapters 4 and 5, I described research that led to confirmatory and novel information about two key steps in CCHFV replication: (1) clathrin-mediated endocytosis; and, (2) viral uncoating in early endosomes. In addition to those studies, we also performed work aimed at furthering the understanding of another entry step, receptor binding. Although certain viruses use only a single molecular species as a receptor (e.g. phleboviruses, [128]), others are able to use two or more molecular species equally well (e.g. SARS coronavirus, [193, 194]), and still others require the presence of multiple surface components (e.g. hepatitis C virus, reviewed in [195]). Because the data suggests CCHFV enters cells via CME, and it has been shown to infect many cell types, we hypothesized that the virus likely binds to a receptor that is common to most cells or it has more than one receptor.

To explore this hypothesis, we first performed an experiment to determine if CCHFV entry requires the presence of protein for cell binding. We next attempted to uncover specific receptor(s) by identifying cell lines that do not support CCHFV replication and then using a bioinformatics approach to compile a list of surface proteins found on the permissive but not the non-permissive cells. Of course, we recognize that there are many reasons why these cells might not be permissive for CCHFV replication other than the absence of a specific receptor. The absence of a host cell molecule necessary for CCHFV replication or the presence of a host molecule that inhibits replication could serve as blocks to prevent virus replication in these cells. An example of an inhibition of viral replication after entry is that HIV-1 replication can be blocked by a

cytoplasmic species-specific restriction factor TRIM5 α [196]. TRIM5 α interacts with the viral capsid lattice and causes a premature disassembly of the virus and blocks reverse transcription of the viral genome. In addition, TRIM5 α cooperates with other host factors to activate the innate immune response within the cell. TRIM5 α expressed in rhesus monkey cells is much more efficient at blocking HIV-1 infection in comparison to human TRIM5 α , and human TRIM5 α polymorphisms and expression levels can influence human infection and disease progression (reviewed in [197, 198]). Even if it is surmised that the proteins that we identified are not related to receptor binding, to my knowledge this is the first reporting of cell lines that do not support CCHFV replication. The list of permissive cells also includes cell lines that have not been reported as able to support CCHFV replication. The information is novel and the cell lines might prove useful for studying other aspects of viral replication in addition to attachment.

In this chapter, I also briefly describe studies in which we created soluble CCHFV glycoprotein fragments that were tagged with an Fc domain. We anticipated using these constructs to perform co-precipitation studies with cell membranes from permissive cells in order to identify cellular proteins that bind to CCHFV glycoproteins. Before we were able to perform the co-precipitation studies, however, another group reported use of this same approach and identified nucleolin as a putative receptor for CCHFV, with G_C proposed as the attachment protein [72]. At the time of that publication, we had already generated and partially characterized a soluble Fc-tagged G_N expression product, and we were working on establishing conditions for its purification. We were also attempting to generate an F_C-tagged G_C ectodomain. However, although we were able to express the protein it was not soluble. Consequently, we terminated further work using this approach

in order to focus on the work detailed in Chapters 3-5. Nevertheless, the tagged G_N ectodomain that we produced differs slightly from the published constructs as it includes a flexible linker, which is required for binding to 293T cells. This construct might prove useful for future studies such as ongoing proteomics work on CCHFV replication.

Results

CCHFV binding to cells is sensitive to trypsin. To determine if CCHFV binding to host cells requires exposed protein components), we treated 293T cells with the serine proteinase trypsin to remove cell surface proteins and then incubated them with CCHFV at an MOI of 10 for 90 minutes at 4°C to allow virus to bind but not internalize. Unbound virus was removed by washing as described in Materials and Methods, and the cells were lysed and viral nucleic acid quantified using qRT-PCR. CCHFV bound to untreated 293T cells, but did not bind to the trypsin-treated cells (**Fig. 23**). These data indicate that trypsin-sensitive molecules are required for CCHFV attachment. Most likely, this indicates that the viral receptor is a protein, but it does not rule out that attachment depends on a protein-associated component, such as carbohydrate.

Identifying human cell lines that are non-permissive for CCHFV. We attempted to identify potential cellular protein receptors for CCHFV by comparing proteins expressed in permissive and non-permissive cells. We obtained a library of 59 human cancer cell lines from the National Cancer Institute (NCI) and screened them for their ability to support CCHFV replication. This well-characterized library and has been used since 1988 by the NCI to screen more than 100,000 compounds for anti-cancer activity and includes cells derived from leukemias, melanomas, and cancers of the central nervous system.

These cells are also of renal, prostate, breast, and lung origin (**Table 1**) [199]. Some of the lines were difficult to maintain in culture; however, but we were able to propagate and screen CCHFV replication in 55 of the 59 cell lines (**Table 1**). Two rounds of testing were conducted to identify cells lines permissive for CCHFV infection as determined by IFA. CER cells were used as a positive control as they are very permissive for CCHFV replication. For the first round of testing, cells were infected with an MOI of 1 for 48 hours and then fixed and stained for CCHFV N as described in the Materials and Methods. The cells were visually scored as either positively or negatively infected by detecting CCHFV N protein using microscopy. Nine cell lines were negative for CCHFV N in this first round of testing: COLO 205, HCT-15, NCI-H460, LOX-IMVI, MOLT-4, CCRF-CEM, RPMI 8226, MDA-MB-435, HL-60 (**Table 1**).

A second round of testing was performed on the nine cell lines initially found to be non-permissive for infection. We extended the infection incubations to three, five and seven days to rule out a delay in replication as a cause for the initial absence of CCHFV N. In this second

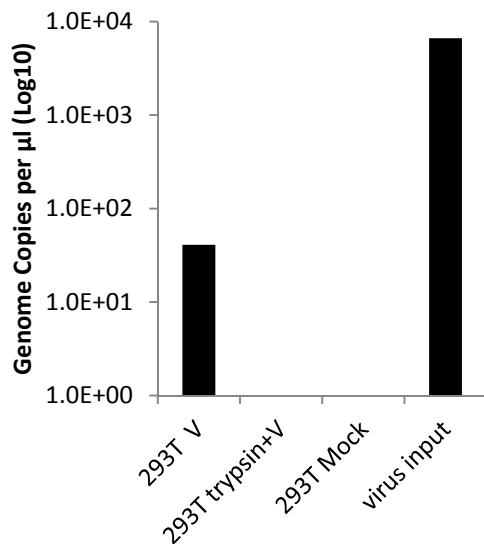


Figure 23. Trypsin treatment decreases CCHFV attachment to 293T cells. 293T cells were treated with trypsin prior to incubation with CCHFV at 4°C, unbound virus was washed away, and the bound virus or the virus in the original inoculums was quantified by qRT-PCR. 293T V (239T cells untreated and incubated with virus), 239T trypsin+V (293T cells treated with trypsin and incubated with virus), 293T Mock (no trypsin and no virus), virus input (the virus inoculum).

<i>Designation</i>	<i>Tumor Origin/Cell Type</i>	<i>Growth</i>	<i>Hour Post infection +IFA</i>
MOLT-4	Peripheral Blood - T Lymphoblast	Suspension	
CCRF-CEM	Peripheral Blood - T Lymphoblast	Suspension	
HL-60 (TB)	promyeloblast	Suspension	
NCI-H460	Lung - epithelial	Adherent	72 hr
LOX-IMVI	Melanoma	Adherent	72 hr
COLO 205	Ascites Fluid - epithelial	Adherent	72 hr
HCT-15	Colon - epithelial	Adherent	72 hr
RPMI 8226	Peripheral Blood - B-lymphocyte	Suspension	72 hr
MDA-MB-435	Breast	Adherent	72 hr
SK-0V-3	Ovary - epithelial	Adherent	48 hr
OVCAR-3	Ovary - epithelial	Adherent	48 hr
SK-MEL-5	Axillary Node Metastasis	Adherent	48 hr
U251	CNS	Adherent	48 hr
SF-295	CNS	Adherent	48 hr
SNB-75	CNS	Adherent	48 hr
SF-539	CNS	Adherent	48 hr
SNB-19	CNS	Adherent	48 hr
SF-268	CNS	Adherent	48 hr
SW-620	Colon - epithelial	Adherent	48 hr
HCT-116	Colon - epithelial	Adherent	48 hr
EKVX	Lung	Adherent	48 hr
HOP 62	Lung	Adherent	48 hr
HOP 92	Lung	Adherent	48 hr
NCI-H226	Lung - epithelial	Adherent	48 hr
A549	Lung - epithelial	Adherent	48 hr
NCI-H23	Lung	Adherent	48 hr
NCI-H522	Lung	Adherent	48 hr
MALME-3M	Lung Metastasis	Adherent	48 hr
BT-549	Lymph Node	Adherent	48 hr
NCI/ADR-RES	Pleural Effusion	Adherent	48 hr
K-526	Pleural Effusion - lymphoblast	Suspension	48 hr
MCF-7	Pleural Effusion	Adherent	48 hr
MDA-MB-231	Pleural Effusion	Adherent	48 hr
T-47D	Pleural Effusion	Adherent	48 hr
DU-145	Prostate	Adherent	48 hr
PC-3	Prostate	Adherent	48 hr
HT-29	Recto-Sigmoid colon	Adherent	48 hr
UO-31	Renal	Adherent	48 hr
CAKI-1	Renal	Adherent	48 hr
RXF-393	Renal	Adherent	48 hr
ACHN	Renal	Adherent	48 hr
786-0	Renal	Adherent	48 hr
TK-10	Renal	Adherent	48 hr

<i>Designation</i>	<i>Tumor Origin/Cell Type</i>	<i>Growth</i>	<i>Hour Post infection +IFA</i>
SN12C	Renal	Adherent	48 hr
A498	Renal	Adherent	48 hr
IGR-OV1	Right Ovary	Adherent	48 hr
SK-MEL-2	Skin Metastasis-Thigh	Adherent	48 hr
OVCAR-5	Adenocarcinoma	Adherent	48 hr
OVCAR-8	Adenocarcinoma	Adherent	48 hr
SK-MEL-28	Malignant melanoma	Adherent	48 hr
UACC-62	Malignant melanoma	Adherent	48 hr
UACC-257	Malignant melanoma	Adherent	48 hr
OVCAR-4	Adenocarcinoma	Adherent	48 hr
M14	Amelanotic melanoma	Adherent	48 hr
HCC 2998	Adenocarcinoma	Adherent	48 hr

Table 1. NCI-59 cell line library and CCHFV replication. The cell-lines listed in the table were examined visually by IFA and microscopy for CCHFV replication. The first round of IFA screening was performed 24 hours post infection, and nine cell lines were negative for CCHFV N staining. A second screen was performed on all nine negative cell lines, and three (listed in red in the table) continued to be negative for CCHFV N protein on days three, five and seven after infection.

round of testing, six of the nine cell lines were positive by three days post infection: COLO 205, HCT-15, NCI-H460, LOX-IMVI, RPMI 8226, and MDA-MB-435, but three cell lines remained negative for CCHFV replication: CCRF-CEM, MOLT-4, and HL-60. One of the cell lines, HL-60, displayed weak fluorescence in some cells, which appeared different from the positive controls, so an additional flow cytometry test was performed to confirm that HL-60 was non-permissive for CCHFV replication (**Fig. 24A**). Because two of the three non-permissive cell lines were T-lymphocytes (Molt-4 and CCRF-CEM), we wanted to determine if this might be a common feature of this type of cells. Consequently, we tested another T-lymphocyte cell line, Jurkat cells for CCHFV permissiveness. All three of these T-lymphocyte cell lines showed no evidence of CCHFV replication (**Fig. 24B**); therefore, it is possible that T-lymphocytes in general cannot support CCHFV replication.

Bioinformatics-screen of cell lines to identify candidate receptors. Work by others provided two microarray mRNA expression data sets for the entire cell-line panel that we tested [199]. The data sets were compiled from the Affymetrix chips HG-U95 (approximately 60,000-feature set) and HG-95 (approximately 30,000 feature set) and are available in the Gene Expression Omnibus (<http://www.ncbi.nlm.nih.gov/geo/>). To analyze the data with regard to CCHFV replication, we uploaded these microchip data sets into the Ingenuity Systems Pathway Analysis (IPA) Software, which is a curated database of published interactions among millions of biomolecules. Through IPA the data from the thousands of genes contained on each chip was identified, sorted by cellular location, the expression level above background based on the chip controls was assessed, and the cell lines were cross referenced for each gene to determine the level of expression

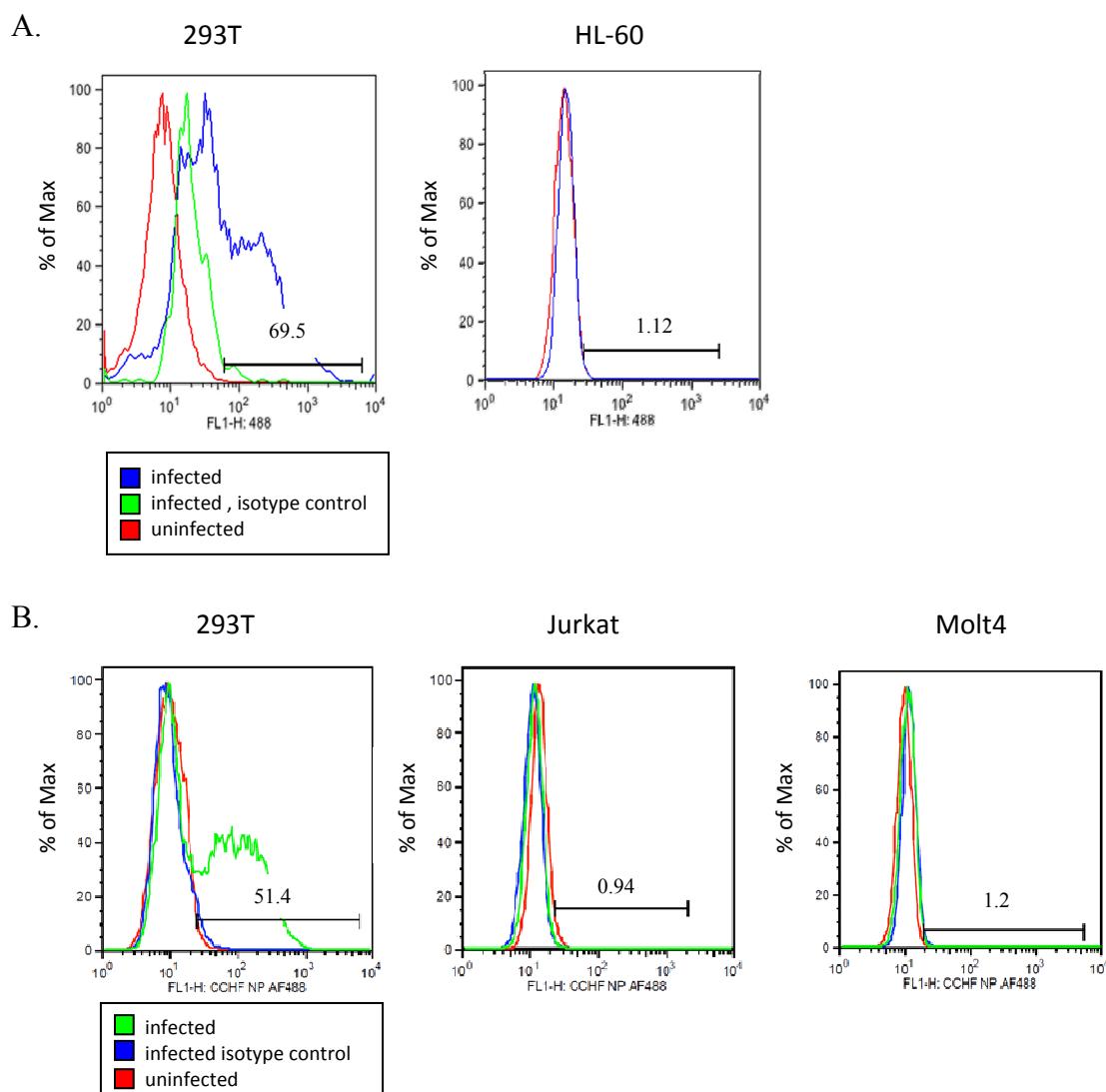


Figure 24. Flow cytometry confirmation of non-permissive cell lines for CCHFV infection. Flow cytometry was performed using an Alexa-488 conjugated mouse monoclonal 9D5 antibody to detect CCHFV N protein as described in the Materials and Methods. **A.** To confirm that HL-60 cells did not support CCHFV replication, they were further tested using flow cytometry as compared to a highly permissive line, 293T. No evidence of replication in the HL-60 cells was observed with this method. **B.** As described in the text, an additional T-lymphocyte line (Jurkat cells), which was not present in the cancer cell line panel, was tested by flow cytometry to gain additional information about the ability of human T cells to support CCHFV replication. Comparing the results of the Jurkat cells to those obtained with the permissive 293T cells, or one of the cancer cell T-cell lines (Molt-4) demonstrated that Jurkat cells also do not support CCHFV replication.

Gene symbol	Gene name
ACTR2	actin-related protein 2 homolog (yeast)
AGRN	Agrin
B2M	beta-2-microglobulin
CALM1	calmodulin 1
CD59	CD59 molecule, complement regulatory protein
CD63	CD63 molecule
CD9	CD9 molecule
CNIH4	cornichon homolog 4 (Drosophila)
CTNNA1	cadherin-associated protein
CTTN	Cortactin
DSP	Desmoplakin
EPCAM	Epithelial cell adhesion molecule
HNRNPM	Heterogeneous nuclear ribonucleoprotein M
JUP	Junction plakoglobin
LAMP1	lysosomal-associated membrane protein 1
LDLR	low density lipoprotein receptor
MCAM	melanoma cell adhesion molecule
PLXNB2	Plexin-B2
PPAP2C	Lipid phosphate phosphohydrolase 2
PTPRF	Receptor-type tyrosine-protein phosphatase F
SPTBN1	Spectrin beta chain, brain 1
STOM	stomatin
TFRC	Transferrin receptor
VAPA	vesicle-associated membrane protein

Table 2. List of 25 common plasma membrane proteins genes expressed in permissive cells with low or no expression in non-permissive cells. Two transcript data sets were used in the present study to perform a bioinformatics screen comparing plasma membrane protein expression between permissive and non-permissive cells. The data used were from transcript profile data sets from Affymetrix HG-U95 and HG-U133A chips published previously [192], which were uploaded and analyzed using IPA.

as either above or below background. Using IPA features, we performed a bioinformatics screen to identify proteins common to the permissive cell lines but absent in the non-permissive cell lines. A list of the highest expressing genes that were unique to the permissive cell lines was compiled for each data set and the 25 proteins with the highest expression from all permissive cell lines from both data sets is included in **Table 2**.

Development of soluble Fc-tagged G_N . The final approach that we explored for identifying a putative receptor for CCHFV was to use Fc-tagged ectodomains of G_N and G_C to perform immunoprecipitation studies with plasma membrane proteins from permissive cells. This approach has been used successfully by others in our laboratory to identify candidate receptors for other viruses [200].

We added in a C-terminal flexible linker (GGGGSGGGG) to the gene region of G_N encoding the ectodomain (amino acids 1 to 171 of matured G_N), which was cloned into the pFUSE-Fc vector and expressed in 293T cells. The flexible linker was found to be necessary, as the original G_N -pFUSE-Fc clone was constructed without the flexible linker did not bind to 293T cells (data not shown). This earlier construct was therefore not likely to co-precipitate cellular proteins as the Fc region probably occluded the binding site. The resulting soluble G_N -Fc with the flexible linker expression product was released in the supernatant of transfected 293T as confirmed by western blot (**Fig. 25B**).

To prepare the protein for use in the anticipated co-precipitation studies, we used fast protein liquid chromatography (FPLC) with a Protein A column for affinity purification of the Fc-tagged G_N expression product. We eluted products with either 3M $MgCl_2$ (**Fig. 25A**) or 0.1M glycine (data not shown) and detected proteins in the eluted

fractions by silver staining (**Fig. 25A**) and western blotting (**Fig. 25B**). Both elution methods were used initially as it was anticipated that the low pH treatment, which is commonly used for eluting antibodies from protein A columns, might cause a conformational change in the glycoprotein. The fractions containing the eluted protein were combined, the protein was concentrated, and the elution buffers were exchanged for PBS using Centricon-20 filters. We then assessed the ability of the purified proteins to bind to 293T cells, by flow cytometry. We found that the MgCl_2 -eluted protein bound to 293T cells, while the glycine-eluted protein did not (**Fig. 25C, D**). The failure of the glycine-eluted protein, which had a pH of less than 3, to bind to 293T cells is not surprising, as a low pH would presumably trigger the conformational change required for endosomal fusion. This resulting conformation might not be suitable for receptor binding.

As we attempted to establish conditions under which we could purify sufficient quantities of stable protein for use in the planned co-precipitation studies, this same approach was used by others to identify nucleolin as a candidate receptor for CCHFV infection [72]. Consequently, as discussed below, we did not continue with this approach for verifying the published results.

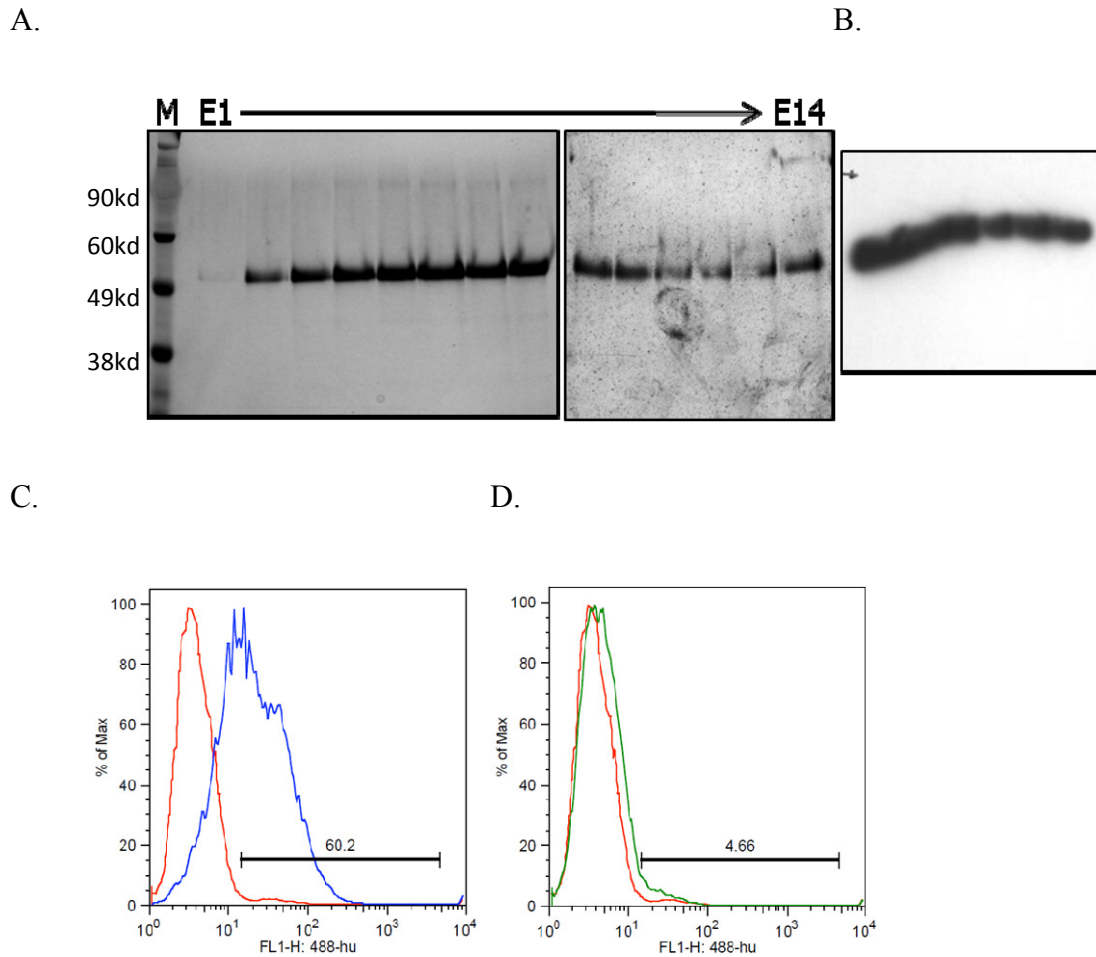


Figure 25. CCHFV GN-Fc production and binding to 293T cells. A. Silver stain of the eluted fraction from an FPLC Protein A column obtained using increasing concentrations of MgCl_2 . B. Western blot (right) of fractions 9 through 14 with rabbit anti- G_N polyclonal antibody (4093) confirming the presence of G_N . C. Flow cytometry histograms showing that MgCl_2 eluted G_N -Fc (blue line) binds to 293T cells, which was detected using an Alexa-488 goat anti-human antibody, as compared to mock treated cells (red line). D. Flow cytometry histograms showing that glycine eluted G_N -Fc (green line), detected as in (C) does not bind to 293T cells as compared to mock treated cells (red line).

Analysis of Results and Conclusions

The data presented in this chapter include the demonstration that protein or protein-associated surface components are necessary for CCHFV attachment, a list of cell surface molecules from cells that do not support CCHFV replication, and a description of the development of Fc-tagged CCHFV ectodomain proteins. Although this research did not lead to the identification of a specific receptor for CCHFV, the information obtained provides several avenues for further work toward identifying replication properties of CCHFV. For example, this is the first description of four cell lines (three of which are T-lymphocytes) that do not support CCHFV replication. It is also the first description of CCHFV replication in a large number of cell lines that had not been previously evaluated.

The cell line study also resulted in a list of proteins found on permissive but not on non-permissive cells that could be further tested as candidate receptors. For example, competition assays could be performed using antibodies directed against each candidate receptor to determine if blocking the protein inhibits viral infection. Conversely a competition experiment using soluble forms of the putative receptor to bind CCHFV particles and block membrane receptor binding could be performed. These types of experiments would define the requirement for these proteins for CCHFV infection. In addition, trans-complementation studies, in which genes for the candidate receptors are introduced into non-permissive cell lines, would show whether the absence of the protein is the only reason that CCHFV cannot infect the cell line.

Finally, we did not complete the development and testing of Fc-tagged G_N and G_C ectodomain constructs because as we were attempting to re-clone my G_C construct to generate a soluble product, as well as optimize the purification of the G_N expression

product, a report appeared in which this same approach was used by another group. This group found that the G_C ectodomain expression product co-precipitated nucleolin, implicating it as a host receptor for CCHFV. However the G_N ectodomain expression product did not precipitate any specific plasma membrane cellular protein [72]. In the preliminary binding studies, we did find that the G_N ectodomain expression product bound to 293T cells so it is possible that the use of this construct in precipitation experiments could uncover other cell surface factors involved in CCHFV attachment. However, because it would have taken considerable work to prepare enough of the soluble G_N to continue these studies, and because we had not yet generated a soluble G_C product, we decided not to continue with this approach for receptor identification. Nevertheless, these constructs and the purification methods that I describe might prove valuable in either future receptor studies or in other types of proteomic studies with CCHFV.

Chapter 7: Discussion

Preface

As viruses are dependent on cellular machinery for replication, an understanding of the initial virus-host interactions is crucial for developing effective means to prevent or resolve infections at these early stages. Attachment, entry and uncoating events all provide opportunities for antiviral intervention. Few studies of the entry mechanisms used by viruses in the family *Bunyaviridae* have been reported to date, and only a single study has been published for CCHFV or any other nairovirus. That study implicated CME in viral entry. Although CME is the best studied entry pathway, macropinocytosis and caveolar endocytosis are two other major pathways used by enveloped viruses. Other less well defined clathrin-and caveolae independent pathways have also been described. For bunyaviruses, CME appears to be the most common mechanism of entry so far but it is not the only mechanism. For example, the phlebovirus UUKV was reported to use non-coated vesicles for entry as well as CME, and these entry mechanisms are cell-line dependent [75, 128].

CME is a complicated process with numerous steps and accessory proteins involved in the formation of the clathrin-coated pits and linking of cargo. Once internalized, the viral cargo is delivered to endosomes where low pH usually triggers conformational changes in viral proteins leading to membrane fusion (reviewed in [164, 195]) [201]. The mechanism of endosomal maturation, from EE to LE and then to lysosomes, is also very complex and has a vast network of integral players that direct the maturation of EE vesicles. The maturation of the EE vesicles occurs through the exchange of components within the lumen and the vesicle membrane, such as the

recruitment of hydrolases to the EE during the maturation process to become LE, which is controlled by bidirectional vesicles from the trans-Golgi network (reviewed in [202]). An understanding of the endosomal compartment from which viral genetic content is released into cells could also provide clues for developing broad anti-viral therapeutics. Accordingly, the overall goal of this project was to define specific early entry events for CCHFV.

Experimental results in the context of the project aims.

The first specific aim of this project sought to substantiate previously reported data suggesting that CCHFV enters host cells through CME [127]. The earlier study demonstrated reduced CCHFV infection in cells treated with chlorpromazine and sucrose, which disrupt clathrin coated pit formation, and with siRNAs against the clathrin heavy chain, which depletes clathrin in the cells. Both methods provide suggestive evidence for CME but both treatments also negatively impact other trafficking processes. That is, chlorpromazine also interferes with the biogenesis of phagosomes and macropinosomes, and hypertonic sucrose not only reduces clathrin-coated pits, but also reduces the presence of non-coated invaginations [116, 117]. The use of siRNAs can likewise result in inconclusive findings, because clathrin isn't exclusively involved in CME. Clathrin is also involved in the transport of vesicles from the *trans*-Golgi network (TGN) to other parts of the cell. Clathrin also plays a role in mitosis, by direct binding of the clathrin heavy chain to microtubules or microtubule-associated proteins, which stabilizes the mitotic spindle (reviewed in [90]). In addition, because clathrin is such an abundant protein in cells it is necessary to use large concentrations of siRNAs to realize a measureable depletion in the levels of clathrin within the cell. At high concentrations

off-target effects of the siRNAs are common and can vary in different cell types [123]. Such off target effects might have been the reason for the observation in the previous CCHFV study in which the investigators found that in Vero E6 cells the control siRNAs reduced CCHFV replication, as measured by N protein production, to the same extent as the clathrin-specific siRNAs [127]. Therefore, to meet the goals of this first specific aim we wanted to use methods that would provide less ambiguity and obtain data that would either support or refute CME entry by CCHFV. To disrupt clathrin pit formation, we used the inhibitor Pitstop 2, which functions by reversibly interrupting the interaction of the clathrin heavy chain terminal domain and its accessory proteins [114]. Because the interaction is reversible, the use of Pitstop 2 can prevent long term negative effects on other cell processes involving clathrin. The data showed that Pitstop 2 completely inhibited CCHFV infection, while having no significant effect on clathrin-independent viruses, indicating that CCHFV enters cells through CME.

To further meet the goal of specific aim 1, we investigated depletion of the second most common protein found in clathrin-coated pits, AP-2. AP-2 is part of an adaptor complex that works at the plasma membrane to recruit and link cargo to clathrin-coated pits and it is not known to be involved in cell functions other than as a cargo adaptor [90]. Our results showed that siRNA to AP-2 complex proteins significantly reduced CCHFV infection but did not reduce infection by two control viruses: VSV, which uses CME but does not require AP-2; and VACV, which does not use CME. These data indicate that CCHFV uses CME entry. Additionally, these findings are the first evidence suggesting that AP-2 is likely to be the cargo adaptor for CCHFV internalization.

The second specific aim of this project was to identify endosomal trafficking requirements for CCHFV entry into the cytosol for replication. The hypothesis was that CCHFV is acid-dependent and requires trafficking through EE and possibly LE for fusion and uncoating. A previous report suggested that CCHFV was pH dependent as NH_4Cl and bafilomycin treatment of cells decreased CCHFV infection [127]. We confirmed that CCHFV entry is pH-dependent with an inactivation threshold consistent with EE dependency. Additional evidence that CCHFV requires EE but not LE for uncoating was obtained by showing that Rab5 GTPase but not Rab7 GTPase was necessary for CCHFV entry. Together the results support the hypothesis that CCHFV is an early-penetrating member of the family *Bunyaviridae*.

Contributions to the field of bunyavirus entry

Receptor binding is the first step in viral entry to host cells. The host receptor used by a virus will dictate the endocytic mechanism and route of trafficking the virus takes (reviewed in [195]). The work from our studies did not result in the discovery of a specific receptor for CCHFV but it is possible that the four cell lines that we identified as being unable to support CCHFV replication might allow for such additional experiments. This approach has been used successfully to identify a factor that enhances EBOV uptake, Axl, as well as identifying the receptor for Hendra and Nipah virus, ephrin-B2 [203, 204]. One issue that may suggest that our approach was not successful in identifying receptor negative cells for CCHFV is that nucleolin was not among the 25 most highly expressed proteins that were unique to the replication permissive cells. This finding is inconsistent with a recent study in which the CCHFV G_C ectodomain expression product was shown to co-precipitated nucleolin, implicating nucleolin as a

host receptor for CCHFV [72]. The absence of nucleolin in the list generated in our work does not necessarily negate our approach, however, in that viruses can use more than one receptor (as discussed in Chapter 6). Moreover, the surface expression of nucleolin is upregulated in cancer cell lines in comparison to primary cells [205]. Other receptors could be used by CCHFV in addition to nucleolin; therefore, the presence of nucleolin on both the permissive and non-permissive cancer cells might have resulted in it not being detected as a unique receptor by the method that we used. The upregulation of nucleolin might have biased not only our cell-line comparison studies, but also the co-precipitation study by Xiao et al. Therefore, it is still possible that the block in infection in these cancer cell lines is related to the absence of an appropriate receptor.

Internalization is the second step in cell entry, and our work supports CME as the CCHFV entry mechanism in the cell lines that we tested. This does not rule out the possibility that a different method could be used in different types of cells, as this appears to be the case with EBOV and UUKV as discussed in Chapter 4.

It is my hope that the contributions that my work has made to the study of internalization by CCHFV will provide a path forward for other types of studies that lead to an overall understanding of how CCHFV replicates, and will point toward potential means to control CCHFV infections. Precedence for this comes from entry studies with other viruses. For example, as discussed in Chapter 1 a study to examine kinases involved in CME used VSV as the cargo for the pathway, and numerous kinases were found to be involved in regulating CME viral entry [98]. These kinases are likely to be involved in general CME as well, as they were confirmed to also be involved in regulating transferrin uptake via CME. Knowing the importance of these kinases for

regulating CME allows further studies to determine if they can be exploited as antiviral targets. Such studies could be performed using general kinase inhibitors such as erlotinib and dasatinib, both of which are already under investigation as possible treatments to prevent the CME entry of hepatitis C virus as these drugs inhibit receptor kinase activity [206]. Our studies indicate that CCHFV enters through CME, so perhaps similar studies with kinases that regulate CME can be explored as potential anti-viral therapeutics for CCHFV as well as other bunyaviruses. Similarly, the knowledge that CCHFV requires endosomal acidification for entry might also lead to therapeutic studies in which acidification is circumvented. For example, drugs that prevent acidification like chloroquine, an anti-malaria drug, could also be tested as a short term prophylactic or treatment for CCHFV. This drug is being investigated as a treatment for the alphavirus Chikungunya virus as it presumably prevents entry of the virus through inhibiting endosomal acidification [207].

Unanswered questions

What are the individual contributions of G_N and G_C in attachment and fusion?

Acidification within the endocytic vesicles promotes a conformational change in G_N and/or G_C in bunyaviruses, which facilitates fusion of the viral and cellular membranes and allows the viral genome and polymerase access to the cytoplasm [52, 65, 66, 70].

The question still remains as to the exact role of each of the glycoproteins in attachment and fusion. Predictive modeling studies suggest that bunyaviruses contain structural similarities to viral proteins that employ a class II fusion mechanism and also predicts that G_C contains a class II fusion loop [161, 162]. To date, crystal structures have not been solved for any of the bunyavirus glycoproteins to provide actual evidence for this

hypothetical model. Although reverse genetics systems have been developed for some of the bunyaviruses (e.g., Bunyamwera virus and Rift Valley fever virus), there is currently no reverse genetics system or cell-cell fusion assay available for the study of CCHFV fusion outside of BSL-4 containment. A reverse genetics system would be extremely valuable for dissecting the contributions of each of the CCHFV proteins for entry. Likewise, the development of a reliable cell-cell fusion assay would provide a valuable tool for further exploring the mechanism of attachment and fusion of the individual glycoproteins of the virus. As discussed in Chapter 6, we developed a soluble form of G_N that could be used in future studies to examine the involvement of this glycoprotein in virus entry, such as determining binding partners in host cells.

What are the receptors for CCHFV in various cell types? To date, nucleolin has been the only receptor implicated in CCHFV attachment [72]. Surface proteins that can serve as cellular receptors are known to differ on various cell types or even within the same cell line depending on the passage history [128, 199, 204]. In our studies, three out of four non-permissive cell lines identified were T-lymphocytes. Previous work also showed that CCHFV does not appear to replicate in primary T-cells [208]. The reason(s) for the non-permissiveness of T cells is not known and was not determined in our work. One possibility is that CCHFV does not need to adapt to these cells to hide from the immune system because it causes an acute infection, with high mortality, indicating that it outcompetes the host immune response. In contrast, many viruses that do infect T lymphocytes, such as human T-cell lymphotropic virus, hepatitis C, and Epstein-Barr virus cause chronic rather than acute infections, [209-211]. Another possibility is that these highly differentiated T cells do not have an appropriate receptor for CCHFV. The

permissive and non-permissive cell lines identified in this study will provide tools to explore these questions more fully.

Limitations of the study

The work presented here adds to the understanding of CCHFV entry into mammalian cells, but there are limitations to the study. First of all my work, as well as most published work on CCHFV, was conducted using the lab-adapted IbAr 10200 strain of CCHFV, which is the prototype strain used for the study of CCHFV [56, 57, 72, 127, 212, 213]. IbAr 10200 was isolated from ticks in Nigeria in 1966 and has an undocumented laboratory passage history, and it has never been identified in a human case of CCHF. Further study with non-cell culture adapted strains from ticks and humans might reveal additional or different receptor usage, such as was found with the alphavirus Sindbis virus [214]. In that study, cell culture passage of Sindbis virus resulted in mutations that altered the receptor binding affinity and use of an alternate receptor. Another example is cell culture adapted dengue 2 virus, which was found to use a different form of the heparin sulfate receptor than did primary virus isolates from patients [215]. Not only has receptor binding been found to differ between cell culture passaged and non-passaged viruses, so have entry events. For example, the cell culture passaged JHM strain of murine hepatitis coronavirus (MHV) requires carcinoembryonic antigen family of cell adhesion molecules (CEACAM1) for fusion with the spike glycoprotein, while the wild type virus does not [216]. Cell culture variants of MHV type 4 become pH dependent, while the wild type virus is capable of fusing with cells at a neutral pH. As few as three amino acid changes were identified within the surface glycoprotein that can alter the pH dependence of this virus [217]. Although it would be interesting to do

similar studies with primary human or tick isolates of CCHFV, all of the available antibodies to detect CCHFV viral proteins were generated against the IbAr 10200 strain. These antibodies had no cross-reactivity with a primary isolate from a CCHFV patient and only minimal cross reactivity to the only other cell-culture adapted strains that we were able to propagate (UG3010 and Drosdov strains) (data not shown). Future work examining the entry mechanism of diverse strains of CCHFV isolates would require strain specific antibodies as well as optimizing growth conditions to achieve higher titers of virus, as was done for strain IbAr 10200 in this study.

Another limitation of the study was the observed mild cytotoxicity of the specific inhibitor of clathrin pit formation, Pitstop 2. At the time of our study, only the initial report describing Pitstop 2 use for inhibiting HIV entry had been published [114]. In that report there was little cytotoxicity in HeLa cells when they were exposed to up to 100 μ M of the drug for eight hours. In our study in A549 cells there was visible cytotoxicity in the cells at concentrations above 15 μ M within 7 hours of exposure to Pitstop 2. Shorter durations of exposure to Pitstop 2, even at high concentrations, did not cause cytotoxicity, but those shorter times were ineffective at reducing viral infectivity. Moreover, once the Pitstop 2 is removed from the cell culture medium, the drug activity is quickly reversed and viruses within the clathrin-coated pits at the surface can undergo endocytosis and replicate. To prevent this delayed entry, it was necessary to have Pitstop 2 in the medium throughout the incubation with each virus, from 7 to 24 hours depending on the virus. Despite this limitation related to cytotoxicity at higher concentrations, it was clear that Pitstop 2 specifically inhibited CCHFV replication but did not specifically inhibit the non CME-dependent control virus.

Future directions of research

Additional components of CME can also be examined to further define factors within the CME pathway that are important for CCHFV entry and trafficking. Examples of such components include EPS15, dynamin, EPSIN, and SNX 9. Our work showed that CCHFV likely uses AP-2 complex proteins as a cargo adaptor for CME; however, this does not preclude the use of other factors as well. In addition, CCHFV entry by macropinocytosis and caveolae-dependent pathways, as well as clathrin-independent pathways cannot be excluded by results from the data presented. Although macropinocytosis and caveolae-dependent mechanisms have not been implicated in entry of any bunyavirus to date, a clathrin-independent entry mechanism can be used by UUKV [75]. For CCHFV, siRNA knockdown of caveolin-1 was reported to have no effect on CCHFV replication [127]. This report did not include a caveolin dependent virus control to ensure the level of knockdown was sufficient to inhibit entry, thus these results do not conclusively show that caveolin is not involved in CCHFV entry. Studies similar to those that we performed with the dominant negative Rab5 and Rab7 proteins could also be performed with dominant negative caveolin-1 plasmids to block this entry pathway. To investigate macropinocytosis, cells could be treated with the drug blebbistatin, which prevents membrane ruffling thus macropinocytosis [182]. Additionally, the effect on CCHFV replication by over-expression of a dominant negative protein involved in filapodial extensions during macropinocytosis, such as Rho GTPases CDC42, could be used to determine if macropinocytosis is involved in CCHFV entry [182].

We have presented evidence that CCHFV is acid dependent and requires the EE for entry into host cells. This work, however, does not address additional modification within the endosome that might be required for fusion of CCHFV within the EE membrane. For example, in addition to low pH, EBOV and the SARS coronavirus require endoproteolytic cleavage for fusion [133, 134]. We would argue that the low pH trigger alone is probably sufficient for CCHFV fusion because several diverse members of the family can undergo direct plasma membrane fusion and produce productive infections with a low pH trigger alone. These viruses include the orthobunyaviruses LACV and California encephalitis virus, the phleboviruses UUKV and RVFV, and the hantavirus HTNV [67, 69, 75, 86]. Similar fusion bypass experiments could be performed with CCHFV to attempt to determine if low pH is sufficient to promote fusion of the viral and host membranes and allow for a productive infection. Such assays are generally conducted by binding virus to cells on ice, followed by briefly incubating the cells and virus with low pH buffers at 37°C and then replacing the low pH buffers with a neutral buffer containing NH₄Cl to prevent endosomal acidification. If low pH is sufficient for fusion, the virus should enter and replicate within cells that are treated with the pH necessary to promote fusion.

For the first time, we also reported on four negative cell lines for CCHFV, three of which are T-lymphocyte cell lines. Although it has not been determined if these cell lines are non-permissive at the point of entry, or if another step in virus replication viral is blocked, these cell lines represent potentially valuable tools to examine possible receptors or other replication processes for CCHFV. A protease protection assay is one type of experiment that could be performed to attempt to determine if the absence of a

receptor is involved in the cells' inability to support CCHFV replication. In this assay, the cells would be infected with virus and incubated at 37°C to allow endocytosis to occur, followed by protease treatment to cleave external virus. The virus that entered the cells would then be quantified by RT-PCR. If virus enters the non-permissive cells, the blockage is not at the point of entry, and would occur later in the replication cycle of the virus. If the virus does not enter the cell, it is likely that the cell lacks a receptor or attachment factor that is required for CCHFV entry. In our work, we used *in silico* methods to identify twenty-five cell surface proteins that could be investigated as potential receptors for CCHFV using the non-permissive cells. Studies that could be conducted include expressing genes for the putative receptors in the non-permissive cells and determining if this renders them permissive for CCHFV replication.

We also performed co-localization studies with CCHFV and clathrin but these data were inconclusive. The most likely reason for the failure of these studies is that we did not have sufficient amounts of virus within cells to measure co-localization events. Published confocal microscopy or electron microscopy co-localization studies typically report the use an MOI of 100 to 5000 for this very reason [75, 86, 87, 110, 128]. As we were unable to increase the titer of CCHFV to achieve this MOI, another approach might be to use Pitstop 2 to halt CCHFV in clathrin-coated pits at the cell surface for use in co-localization studies with clathrin. Another possible reason for the failure of our co-localization studies might simply be a matter of incorrect timing. Clathrin uptake within cells is typically a rapid process. But the reported time for uptake of viruses, and even of various bunyaviruses into clathrin coated vesicles varies. For example the uptake of UUKV and VSV into clathrin-coated pits and clathrin-coated vesicles occurred in 2-3

minutes or 10 minutes respectively [75, 110, 128]. For HTNV however, clathrin co-localization was not observed until about 30 minutes post-warming, and LACV co-localized at 20 minutes post-warming [86, 87]. Therefore, in addition to increasing the titer of CCHFV for co-localization studies, additional time points could be examined.

Future work should be done to study the entry mechanism of CCHFV pertaining to natural transmission by investigating strains that have not been adapted to cell culture as well as infection in primary cells. These studies, however, would be more informative if there was more known about the tropism of the virus in infected animals and humans, so that the appropriate cell types could be studied. Due the sporadic nature of human CCHFV infection, and a limited of clinical pathology facilities in endemic areas, there is little information regarding the viral tropism and pathology resulting from CCHFV infection. Some of this information could be gleaned from studies using animals, but as of now, there are no immunocompetent animal models of disease. There are two immune-suppressed mouse models that provide limited insight into the temporal course of CCHFV infection and its tropism [43, 44]. One day post infection the virus is detected in the blood of these mice, and disseminated to the lung, liver, and spleen in most mice by two days post infection, and by day three over half of the mice have detectable virus in the brain [43]. Human data comes almost entirely from autopsies performed on fatal cases, and those data indicate that the target organs in humans include the liver and the kidneys, but the pathology of CCHFV largely remains a mystery [5]. It is suspected that the virus infects endothelial cells, but there is no direct evidence for this, and the endothelial damage seen in CCHF patients could be due to a bystander effect [21, 218]. The virus infects a wide variety of cultured cells, as discussed in Chapter 6, but this might

be due to the presence of receptor commonly found on transformed cells, such as nucleolin, and may not be relevant to the virus tropism in nature. There is one publication in which the researchers infected primary blood mononuclear cells (PBMC) with CCHFV and found that monocyte derived dendritic cells were the only circulating human cells that could support CCHFV infection [208]. The data in this publication are limited as the PBMCs were from only four donors, and although a productive infection was not seen in T-cells, a small amount of viral RNA was detected in these cells at 24 and 48 hours post infection. It is possible that these infected cells represent a small population of infected (possibly stimulated) T-cells. Future work with the T-cell lines we identified as non-permissive for the virus could be used to address this question, as well as primary T-lymphocytes, by comparing the infection of stimulated and unstimulated cells.

Finally, future work could be conducted to try to define cell entry events of CCHFV in tick cells. Since the discovery of CCHFV, very little work has been done to examine viral replication in the tick vector due to the need to work with the virus in BSL4 containment, the lack of specific pathogen-free tick colonies, and the expertise to maintain ticks through *in vivo* feedings in BSL-4. A recent study has reported that several *Hyalomma* spp tick cell lines support CCHFV replication, and these cells could be used for *in vitro* studies of CCHFV entry [219].

Conclusions

As viruses are dependent on the cellular machinery for entry and transport in the cell as well as replication, understanding how viruses exploit the endocytic pathways can provide information that will assist in determining targets for intervention to prevent virus infection. Although clathrin-mediated endocytosis is a complex pathway, numerous components of the pathway have now been defined and can be studied with regard to viral entry. As discussed in Chapter 1 the mechanisms of endosomal maturation, from EE to LE and then to lysosomes, is also very complex and has a vast network of integral players that direct the maturation [202]. Again, despite this complexity, there are numerous potential interactions that have been identified and can be investigated to determine how they are involved in viral entry. It is my hope that the additional insight into the entry mechanism of CCHFV in this study will provide a starting point for the development of anti-CCHFV therapeutics.

References

1. Chumakov, M.P., et al., [New data on the viral agent of Crimean hemorrhagic fever]. *Vopr Virusol*, 1968. **13**(3): p. 377.
2. Chumakov, M.P., S.E. Smirnova, and E.A. Tkachenko, *Relationship between strains of Crimean haemorrhagic fever and Congo viruses*. *Acta Virol*, 1970. **14**(1): p. 82-5.
3. Hoogstraal, H., *The epidemiology of tick-borne Crimean-Congo hemorrhagic fever in Asia, Europe, and Africa*. *J Med Entomol*, 1979. **15**(4): p. 307-417.
4. Casals, J., *Antigenic similarity between the virus causing Crimean hemorrhagic fever and Congo virus*. *Proc Soc Exp Biol Med*, 1969. **131**(1): p. 233-6.
5. Whitehouse, C.A., *Crimean-Congo hemorrhagic fever*. *Antiviral Res*, 2004. **64**(3): p. 145-60.
6. Darwish, M.A., et al., *Results of a preliminary seroepidemiological survey for Crimean-Congo hemorrhagic fever virus in Egypt*. *Acta Virol*, 1978. **22**(1): p. 77.
7. Vorou, R., I.N. Pierrotsakos, and H.C. Maltezou, *Crimean-Congo hemorrhagic fever*. *Curr Opin Infect Dis*, 2007. **20**(5): p. 495-500.
8. Leblebicioglu, H., *Crimean-Congo haemorrhagic fever in Eurasia*. *Int J Antimicrob Agents*, 2010. **36 Suppl 1**: p. S43-6.
9. Diseases, N.I.o.A.a.I., *Biodefense and Emerging Infectious Diseases. NIAID Category A, B, and C Priority Pathogens*, D.o.H. security, Editor. 2012, National Institute of Allergy and Infectious Diseases.
10. Dohm, D.J., et al., *Transmission of Crimean-Congo hemorrhagic fever virus by Hyalomma impeltatum (Acari:Ixodidae) after experimental infection*. *J Med Entomol*, 1996. **33**(5): p. 848-51.
11. Saidi, S., J. Casals, and M.A. Faghih, *Crimean hemorrhagic fever-Congo (CHF-C) virus antibodies in man, and in domestic and small mammals, in Iran*. *Am J Trop Med Hyg*, 1975. **24**(2): p. 353-7.
12. Woodall, J.P., M.C. Williams, and D.I. Simpson, *Congo virus: a hitherto undescribed virus occurring in Africa. II. Identification studies*. *East Afr Med J*, 1967. **44**(2): p. 93-8.
13. Causey, O.R., et al., *Congo virus from domestic livestock, African hedgehog, and arthropods in Nigeria*. *Am J Trop Med Hyg*, 1970. **19**(5): p. 846-50.
14. Yen, Y.C., et al., *Characteristics of Crimean-Congo hemorrhagic fever virus (Xinjiang strain) in China*. *Am J Trop Med Hyg*, 1985. **34**(6): p. 1179-82.
15. Shepherd, A.J., et al., *Field and laboratory investigation of Crimean-Congo haemorrhagic fever virus (Nairovirus, family Bunyaviridae) infection in birds*. *Trans R Soc Trop Med Hyg*, 1987. **81**(6): p. 1004-7.
16. Shepherd, A.J., P.A. Leman, and R. Swanepoel, *Viremia and antibody response of small African and laboratory animals to Crimean-Congo hemorrhagic fever virus infection*. *Am J Trop Med Hyg*, 1989. **40**(5): p. 541-7.
17. Smirnova, S.E., *A comparative study of the Crimean hemorrhagic fever-Congo group of viruses*. *Arch Virol*, 1979. **62**(2): p. 137-43.
18. Fagbami, A.H., et al., *Experimental Congo virus (Ib -AN 7620) infection in primates*. *Virologie*, 1975. **26**(1): p. 33-7.
19. Shepherd, A.J., R. Swanepoel, and P.A. Leman, *Antibody response in Crimean-Congo hemorrhagic fever*. *Rev Infect Dis*, 1989. **11 Suppl 4**: p. S801-6.
20. Swanepoel, R., et al., *Experimental infection of ostriches with Crimean-Congo haemorrhagic fever virus*. *Epidemiol Infect*, 1998. **121**(2): p. 427-32.
21. Ergonul, O., *Crimean-Congo haemorrhagic fever*. *Lancet Infect Dis*, 2006. **6**(4): p. 203-14.

22. Estrada-Pena, A., et al., *The trend towards habitat fragmentation is the key factor driving the spread of Crimean-Congo haemorrhagic fever*. Epidemiol Infect, 2009. **138**(8): p. 1194-203.
23. Antoniadis, A. and J. Casals, *Serological evidence of human infection with Congo-Crimean hemorrhagic fever virus in Greece*. Am J Trop Med Hyg, 1982. **31**(5): p. 1066-7.
24. Sidira, P., et al., *Seroepidemiological study of Crimean-Congo haemorrhagic fever in Greece, 2009-2010*. Clin Microbiol Infect, 2011. **18**(2): p. E16-9.
25. Papa, A., et al., *A case of Crimean-Congo haemorrhagic fever in Greece, June 2008*. Euro Surveill., 2008. **13**(33).
26. Papa, A., et al., *Emergence of Crimean-Congo haemorrhagic fever in Greece*. Clin Microbiol Infect, 2009. **16**(7): p. 843-7.
27. Patel, A.K., et al., *First Crimean-Congo hemorrhagic fever outbreak in India*. J Assoc Physicians India, 2012. **59**: p. 585-9.
28. Mourya, D.T., et al., *Detection, isolation and confirmation of Crimean-Congo hemorrhagic fever virus in human, ticks and animals in Ahmadabad, India, 2010-2011*. PLoS Negl Trop Dis, 2012. **6**(5): p. e1653.
29. ProMED-mail, *Crimean-Congo Hemorrhagic fever - India: (Gujarat) Nosocomial*, in ProMED-mail 2012, ProMED-mail
30. Bodur, H., et al., *Subclinical infections with Crimean-Congo hemorrhagic fever virus, Turkey*. Emerg Infect Dis, 2012. **18**(4): p. 640-2.
31. Gale, P., et al., *Impact of climate change on risk of incursion of Crimean-Congo haemorrhagic fever virus in livestock in Europe through migratory birds*. J Appl Microbiol, 2011. **112**(2): p. 246-57.
32. Ergonul, O., *Treatment of Crimean-Congo hemorrhagic fever*. Antiviral Res, 2008. **78**(1): p. 125-31.
33. Cevik, M.A., et al., *Clinical and laboratory features of Crimean-Congo hemorrhagic fever: predictors of fatality*. Int J Infect Dis, 2008. **12**(4): p. 374-9.
34. Swanepoel, R., et al., *The clinical pathology of Crimean-Congo hemorrhagic fever*. Rev Infect Dis, 1989. **11 Suppl 4**: p. S794-800.
35. Schmaljohn, C.S. and S.T. Nichol, *Bunyaviridae*, in *Fields Virology*, K.D.a.H. PM, Editor. 2007, Lippincott Williams & Wilkins: Philadelphia. p. 1741-1789.
36. Maltezou, H.C. and A. Papa, *Crimean-Congo hemorrhagic fever: epidemiological trends and controversies in treatment*. BMC Med, 2011. **9**: p. 131.
37. Karti, S.S., et al., *Crimean-Congo hemorrhagic fever in Turkey*. Emerg Infect Dis, 2004. **10**(8): p. 1379-84.
38. Cagatay, A., et al., *Haemophagocytosis in a patient with Crimean Congo haemorrhagic fever*. J Med Microbiol, 2007. **56**(Pt 8): p. 1126-8.
39. Tasdelen Fisgin, N., et al., *Initial high rate of misdiagnosis in Crimean Congo haemorrhagic fever patients in an endemic region of Turkey*. Epidemiol Infect, 2009. **138**(1): p. 139-44.
40. Ergonul, O., *DEBATE (see Elaldi N et al, Efficacy of oral ribavirin treatment in Crimean-Congo haemorrhagic fever: a quasi-experimental study from Turkey. Journal of Infection 2009; 58: 238-244): Biases and misinterpretation in the assessment of the efficacy of oral ribavirin in the treatment of Crimean-Congo hemorrhagic fever*. J Infect, 2009. **59**(4): p. 284-6; author reply 286-9.
41. Keshtkar-Jahromi, M., et al., *Crimean-Congo hemorrhagic fever: current and future prospects of vaccines and therapies*. Antiviral Res, 2011. **90**(2): p. 85-92.

42. Papa, A., E. Papadimitriou, and I. Christova, *The Bulgarian vaccine Crimean-Congo haemorrhagic fever virus strain*. Scand J Infect Dis, 2010. **43**(3): p. 225-9.
43. Bente, D.A., et al., *Pathogenesis and immune response of Crimean-Congo hemorrhagic fever virus in a STAT-1 knockout mouse model*. J Virol, 2010. **84**(21): p. 11089-100.
44. Bereczky, S., et al., *Crimean-Congo hemorrhagic fever virus infection is lethal for adult type I interferon receptor-knockout mice*. J Gen Virol, 2010. **91**(Pt 6): p. 1473-7.
45. Spik, K., et al., *Immunogenicity of combination DNA vaccines for Rift Valley fever virus, tick-borne encephalitis virus, Hantaan virus, and Crimean Congo hemorrhagic fever virus*. Vaccine, 2006. **24**(21): p. 4657-66.
46. WHO (2001) *Crimean-Congo hemorrhagic fever* Fact Sheet N°208 **Volume**,
47. Mohamed, M., et al., *Epidemiologic and Clinical Aspects of a Rift Valley Fever Outbreak in Humans in Tanzania, 2007*. The American Journal of Tropical Medicine and Hygiene, 2010. **83**(2 Suppl): p. 22-27.
48. Ergunay, K., et al., *Sandfly fever virus activity in central/northern Anatolia, Turkey: first report of Toscana virus infections*. Clin Microbiol Infect, 2010. **17**(4): p. 575-81.
49. Sargianou, M., et al., *Hantavirus infections for the clinician: From case presentation to diagnosis and treatment*. Crit Rev Microbiol, 2012.
50. Davies, F.G., *Nairobi sheep disease*. Parassitologia, 1997. **39**(2): p. 95-8.
51. Yadav, P.D., et al., *Genomic analysis reveals Nairobi sheep disease virus to be highly diverse and present in both Africa, and in India in the form of the Ganjam virus variant*. Infection, Genetics and Evolution, 2011. **11**(5): p. 1111-1120.
52. Overby, A.K., et al., *Insights into bunyavirus architecture from electron cryotomography of Uukuniemi virus*. Proc Natl Acad Sci U S A, 2008. **105**(7): p. 2375-9.
53. Hardestam, J., et al., *Ex vivo stability of the rodent-borne Hantaan virus in comparison to that of arthropod-borne members of the Bunyaviridae family*. Appl Environ Microbiol, 2007. **73**(8): p. 2547-51.
54. Storms, M.M., et al., *The nonstructural NSm protein of tomato spotted wilt virus induces tubular structures in plant and insect cells*. Virology, 1995. **214**(2): p. 485-93.
55. Sanchez, A.J., M.J. Vincent, and S.T. Nichol, *Characterization of the glycoproteins of Crimean-Congo hemorrhagic fever virus*. J Virol, 2002. **76**(14): p. 7263-75.
56. Bergeron, E., M.J. Vincent, and S.T. Nichol, *Crimean-Congo hemorrhagic fever virus glycoprotein processing by the endoprotease SKI-1/S1P is critical for virus infectivity*. J Virol, 2007. **81**(23): p. 13271-6.
57. Altamura, L.A., et al., *Identification of a novel C-terminal cleavage of Crimean-Congo hemorrhagic fever virus PreGN that leads to generation of an NSM protein*. J Virol, 2007. **81**(12): p. 6632-42.
58. Sanchez, A.J., et al., *Crimean-congo hemorrhagic fever virus glycoprotein precursor is cleaved by Furin-like and SKI-1 proteases to generate a novel 38-kilodalton glycoprotein*. J Virol, 2006. **80**(1): p. 514-25.
59. Sonnhammer, E.L., G. von Heijne, and A. Krogh, *A hidden Markov model for predicting transmembrane helices in protein sequences*. Proc Int Conf Intell Syst Mol Biol, 1998. **6**: p. 175-82.
60. Huiskonen, J.T., et al., *Electron cryo-microscopy and single-particle averaging of Rift Valley fever virus: evidence for GN-GC glycoprotein heterodimers*. J Virol, 2009. **83**(8): p. 3762-9.
61. Battisti, A.J., et al., *Structural studies of Hantaan virus*. J Virol, 2010. **85**(2): p. 835-41.
62. Freiberg, A.N., et al., *Three-dimensional organization of Rift Valley fever virus revealed by cryoelectron tomography*. J Virol, 2008. **82**(21): p. 10341-8.

63. Sherman, M.B., et al., *Single-particle cryo-electron microscopy of Rift Valley fever virus*. Virology, 2009. **387**(1): p. 11-5.
64. Jacoby, D.R., et al., *Expression of the La Crosse M segment proteins in a recombinant vaccinia expression system mediates pH-dependent cellular fusion*. Virology, 1993. **193**(2): p. 993-6.
65. Plassmeyer, M.L., et al., *California serogroup Gc (G1) glycoprotein is the principal determinant of pH-dependent cell fusion and entry*. Virology, 2005. **338**(1): p. 121-32.
66. Plassmeyer, M.L., et al., *Mutagenesis of the La Crosse Virus glycoprotein supports a role for Gc (1066-1087) as the fusion peptide*. Virology, 2007. **358**(2): p. 273-82.
67. Ogino, M., et al., *Cell fusion activities of Hantaan virus envelope glycoproteins*. J Virol, 2004. **78**(19): p. 10776-82.
68. Shi, X., et al., *Functional analysis of the Bunyamwera orthobunyavirus Gc glycoprotein*. J Gen Virol, 2009. **90**(Pt 10): p. 2483-92.
69. Hacker, J.K. and J.L. Hardy, *Adsorptive endocytosis of California encephalitis virus into mosquito and mammalian cells: a role for G1*. Virology, 1997. **235**(1): p. 40-7.
70. Pekosz, A. and F. Gonzalez-Scarano, *The extracellular domain of La Crosse virus G1 forms oligomers and undergoes pH-dependent conformational changes*. Virology, 1996. **225**(1): p. 243-7.
71. Haferkamp, S., et al., *Intracellular localization of Crimean-Congo Hemorrhagic Fever (CCHF) virus glycoproteins*. Virol J, 2005. **2**: p. 42.
72. Xiao, X., et al., *Identification of a putative Crimean-Congo hemorrhagic fever virus entry factor*. Biochem Biophys Res Commun, 2011. **411**(2): p. 253-8.
73. Gavrilovskaya, I.N., et al., *Cellular entry of hantaviruses which cause hemorrhagic fever with renal syndrome is mediated by beta3 integrins*. J Virol, 1999. **73**(5): p. 3951-9.
74. Gavrilovskaya, I.N., et al., *beta3 Integrins mediate the cellular entry of hantaviruses that cause respiratory failure*. Proc Natl Acad Sci U S A, 1998. **95**(12): p. 7074-9.
75. Lozach, P.Y., et al., *Entry of bunyaviruses into mammalian cells*. Cell Host Microbe, 2010. **7**(6): p. 488-99.
76. Gonzalez-Scarano, F., et al., *Characterization of monoclonal antibodies against the G1 and N proteins of LaCrosse and Tahyna, two California serogroup bunyaviruses*. Virology, 1982. **120**(1): p. 42-53.
77. Grady, L.J., et al., *Monoclonal antibodies against La Crosse virus*. J Gen Virol, 1983. **64** (Pt 8): p. 1699-704.
78. Sundin, D.R., et al., *A G1 glycoprotein epitope of La Crosse virus: a determinant of infection of Aedes triseriatus*. Science, 1987. **235**(4788): p. 591-3.
79. Pekosz, A., et al., *Tropism of bunyaviruses: evidence for a G1 glycoprotein-mediated entry pathway common to the California serogroup*. Virology, 1995. **214**(2): p. 339-48.
80. Pekosz, A., et al., *Protection from La Crosse virus encephalitis with recombinant glycoproteins: role of neutralizing anti-G1 antibodies*. J Virol, 1995. **69**(6): p. 3475-81.
81. Ludwig, G.V., et al., *Enzyme processing of La Crosse virus glycoprotein G1: a bunyavirus-vector infection model*. Virology, 1989. **171**(1): p. 108-13.
82. Gruenberg, J., *Viruses and endosome membrane dynamics*. Curr Opin Cell Biol, 2009. **21**(4): p. 582-8.
83. Schelhaas, M., *Come in and take your coat off - how host cells provide endocytosis for virus entry*. Cell Microbiol, 2010. **12**(10): p. 1378-88.
84. Futter, C.E., et al., *In polarized MDCK cells basolateral vesicles arise from clathrin-gamma-adaptin-coated domains on endosomal tubules*. J Cell Biol, 1998. **141**(3): p. 611-23.

85. Brodsky, F.M., et al., *Biological basket weaving: formation and function of clathrin-coated vesicles*. Annu Rev Cell Dev Biol, 2001. **17**: p. 517-68.
86. Hollidge, B.S., et al., *Orthobunyavirus entry into neurons and other mammalian cells occurs via clathrin-mediated endocytosis and requires trafficking into early endosomes*. J Virol, 2012.
87. Jin, M., et al., *Hantaan virus enters cells by clathrin-dependent receptor-mediated endocytosis*. Virology, 2002. **294**(1): p. 60-9.
88. Santos, R.I., et al., *Oropouche virus entry into HeLa cells involves clathrin and requires endosomal acidification*. Virus Res, 2008. **138**(1-2): p. 139-43.
89. Mettlen, M., et al., *Cargo- and adaptor-specific mechanisms regulate clathrin-mediated endocytosis*. J Cell Biol, 2010. **188**(6): p. 919-33.
90. McMahon, H.T. and E. Boucrot, *Molecular mechanism and physiological functions of clathrin-mediated endocytosis*. Nat Rev Mol Cell Biol, 2011. **12**(8): p. 517-33.
91. McMahon, H.T., *Endocytosis: an assembly protein for clathrin cages*. Curr Biol, 1999. **9**(9): p. R332-5.
92. Henne, W.M., et al., *FCHo proteins are nucleators of clathrin-mediated endocytosis*. Science, 2010. **328**(5983): p. 1281-4.
93. Pechstein, A., et al., *Regulation of synaptic vesicle recycling by complex formation between intersectin 1 and the clathrin adaptor complex AP2*. Proc Natl Acad Sci U S A, 2010. **107**(9): p. 4206-11.
94. Edeling, M.A., et al., *Molecular switches involving the AP-2 beta2 appendage regulate endocytic cargo selection and clathrin coat assembly*. Dev Cell, 2006. **10**(3): p. 329-42.
95. Edeling, M.A., C. Smith, and D. Owen, *Life of a clathrin coat: insights from clathrin and AP structures*. Nat Rev Mol Cell Biol, 2006. **7**(1): p. 32-44.
96. Teckchandani, A., et al., *The clathrin adaptor Dab2 recruits EH domain scaffold proteins to regulate integrin β 1 endocytosis*. Molecular Biology of the Cell, 2012.
97. Hinshaw, J.E., *Dynamin and its role in membrane fission*. Annu Rev Cell Dev Biol, 2000. **16**: p. 483-519.
98. Pelkmans, L., et al., *Genome-wide analysis of human kinases in clathrin- and caveolae/raft-mediated endocytosis*. Nature, 2005. **436**(7047): p. 78-86.
99. Mitsunari, T., et al., *Clathrin adaptor AP-2 is essential for early embryonal development*. Mol Cell Biol, 2005. **25**(21): p. 9318-23.
100. Schang, L.M., *First demonstration of the effectiveness of inhibitors of cellular protein kinases in antiviral therapy*. Expert Rev Anti Infect Ther, 2006. **4**(6): p. 953-6.
101. Schang, L.M., *Herpes simplex viruses in antiviral drug discovery*. Curr Pharm Des, 2006. **12**(11): p. 1357-70.
102. Schang, L.M., M.R. St Vincent, and J.J. Lacasse, *Five years of progress on cyclin-dependent kinases and other cellular proteins as potential targets for antiviral drugs*. Antivir Chem Chemother, 2006. **17**(6): p. 293-320.
103. Kontzias, A., et al., *Kinase inhibitors in the treatment of immune-mediated disease*. F1000 Med Rep, 2012. **4**: p. 5.
104. Xie, L., et al., *Kinome-wide siRNA screening identifies molecular targets mediating the sensitivity of pancreatic cancer cells to Aurora kinase inhibitors*. Biochem Pharmacol, 2011. **83**(4): p. 452-61.
105. Vela, E.M., et al., *Genistein, a general kinase inhibitor, as a potential antiviral for arenaviral hemorrhagic fever as described in the Pirital virus-Syrian golden hamster model*. Antiviral Res, 2010. **87**(3): p. 318-28.

106. Nacken, W., C. Ehrhardt, and S. Ludwig, *Small molecule inhibitors of the c-Jun N-terminal kinase (JNK) possess antiviral activity against highly pathogenic avian and human pandemic influenza A viruses*. Biol Chem, 2012. **393**(6): p. 525-34.
107. Kolokoltsov, A.A., et al., *Inhibition of Lassa virus and Ebola virus infection in host cells treated with the kinase inhibitors genistein and tyrphostin*. Arch Virol. **157**(1): p. 121-7.
108. Blondeau, F., et al., *Tandem MS analysis of brain clathrin-coated vesicles reveals their critical involvement in synaptic vesicle recycling*. Proc Natl Acad Sci U S A, 2004. **101**(11): p. 3833-8.
109. Pearce, B.M., C.J. Smith, and D.J. Owen, *Clathrin coat construction in endocytosis*. Curr Opin Struct Biol, 2000. **10**(2): p. 220-8.
110. Johannsdottir, H.K., et al., *Host cell factors and functions involved in vesicular stomatitis virus entry*. J Virol, 2009. **83**(1): p. 440-53.
111. Motley, A., et al., *Clathrin-mediated endocytosis in AP-2-depleted cells*. J Cell Biol, 2003. **162**(5): p. 909-18.
112. Hung, W.S., et al., *The endocytic adaptor protein Disabled-2 is required for cellular uptake of fibrinogen*. Biochim Biophys Acta, 2012.
113. Boucrot, E., et al., *Roles of AP-2 in clathrin-mediated endocytosis*. PLoS One, 2010. **5**(5): p. e10597.
114. von Kleist, L., et al., *Role of the clathrin terminal domain in regulating coated pit dynamics revealed by small molecule inhibition*. Cell, 2011. **146**(3): p. 471-84.
115. Wang, L.H., K.G. Rothberg, and R.G. Anderson, *Mis-assembly of clathrin lattices on endosomes reveals a regulatory switch for coated pit formation*. J Cell Biol, 1993. **123**(5): p. 1107-17.
116. Elferink, J.G., *Chlorpromazine inhibits phagocytosis and exocytosis in rabbit polymorphonuclear leukocytes*. Biochem Pharmacol, 1979. **28**(7): p. 965-8.
117. Watanabe, S., et al., *Calmodulin antagonists inhibit the phagocytic activity of cultured Kupffer cells*. Lab Invest, 1988. **59**(2): p. 214-8.
118. Vercauteren, D., et al., *The use of inhibitors to study endocytic pathways of gene carriers: optimization and pitfalls*. Mol Ther, 2009. **18**(3): p. 561-9.
119. Hansen, S.H., K. Sandvig, and B. van Deurs, *Clathrin and HA2 adaptors: effects of potassium depletion, hypertonic medium, and cytosol acidification*. J Cell Biol, 1993. **121**(1): p. 61-72.
120. Carpentier, J.L., et al., *Potassium depletion and hypertonic medium reduce "non-coated" and clathrin-coated pit formation, as well as endocytosis through these two gates*. J Cell Physiol, 1989. **138**(3): p. 519-26.
121. Bradley, J.R., D.R. Johnson, and J.S. Pober, *Four different classes of inhibitors of receptor-mediated endocytosis decrease tumor necrosis factor-induced gene expression in human endothelial cells*. J Immunol, 1993. **150**(12): p. 5544-55.
122. Synnes, M., et al., *Fluid phase endocytosis and galactosyl receptor-mediated endocytosis employ different early endosomes*. Biochim Biophys Acta, 1999. **1421**(2): p. 317-28.
123. Vankoningsloo, S., et al., *Gene expression silencing with 'specific' small interfering RNA goes beyond specificity - a study of key parameters to take into account in the onset of small interfering RNA off-target effects*. FEBS J, 2008. **275**(11): p. 2738-53.
124. Deborde, S., et al., *Clathrin is a key regulator of basolateral polarity*. Nature, 2008. **452**(7188): p. 719-23.
125. Royle, S.J., N.A. Bright, and L. Lagnado, *Clathrin is required for the function of the mitotic spindle*. Nature, 2005. **434**(7037): p. 1152-7.

126. Hollidge, B.S., et al., *Orthobunyavirus Entry into Neurons and Other Mammalian Cells Occurs via Clathrin-Mediated Endocytosis and Requires Trafficking into Early Endosomes*. J Virol, 2012. **86**(15): p. 7988-8001.
127. Simon, M., C. Johansson, and A. Mirazimi, *Crimean-Congo hemorrhagic fever virus entry and replication is clathrin-, pH- and cholesterol-dependent*. J Gen Virol, 2009. **90**(Pt 1): p. 210-5.
128. Lozach, P.Y., et al., *DC-SIGN as a receptor for phleboviruses*. Cell Host Microbe, 2011. **10**(1): p. 75-88.
129. Murphy, R.F., S. Powers, and C.R. Cantor, *Endosome pH measured in single cells by dual fluorescence flow cytometry: rapid acidification of insulin to pH 6*. J Cell Biol, 1984. **98**(5): p. 1757-62.
130. Sipe, D.M., A. Jesurum, and R.F. Murphy, *Absence of Na⁺,K⁺-ATPase regulation of endosomal acidification in K562 erythroleukemia cells. Analysis via inhibition of transferrin recycling by low temperatures*. J Biol Chem, 1991. **266**(6): p. 3469-74.
131. Sieczkarski, S.B. and G.R. Whittaker, *Differential requirements of Rab5 and Rab7 for endocytosis of influenza and other enveloped viruses*. Traffic, 2003. **4**(5): p. 333-43.
132. Zaitseva, E., et al., *Dengue virus ensures its fusion in late endosomes using compartment-specific lipids*. PLoS Pathog. **6**(10): p. e1001131.
133. Chandran, K., et al., *Endosomal proteolysis of the Ebola virus glycoprotein is necessary for infection*. Science, 2005. **308**(5728): p. 1643-5.
134. Simmons, G., et al., *Inhibitors of cathepsin L prevent severe acute respiratory syndrome coronavirus entry*. Proc Natl Acad Sci U S A, 2005. **102**(33): p. 11876-81.
135. Marsh, M. and A. Helenius, *Virus entry: open sesame*. Cell, 2006. **124**(4): p. 729-40.
136. Mothes, W., et al., *Retroviral entry mediated by receptor priming and low pH triggering of an envelope glycoprotein*. Cell, 2000. **103**(4): p. 679-89.
137. Stenmark, H., *Rab GTPases as coordinators of vesicle traffic*. Nat Rev Mol Cell Biol, 2009. **10**(8): p. 513-25.
138. Stenmark, H., et al., *Inhibition of rab5 GTPase activity stimulates membrane fusion in endocytosis*. EMBO J, 1994. **13**(6): p. 1287-96.
139. Stenmark, H., et al., *Distinct structural elements of rab5 define its functional specificity*. EMBO J, 1994. **13**(3): p. 575-83.
140. Semerdjieva, S., et al., *Coordinated regulation of AP2 uncoating from clathrin-coated vesicles by rab5 and hRME-6*. J Cell Biol, 2008. **183**(3): p. 499-511.
141. Rink, J., et al., *Rab conversion as a mechanism of progression from early to late endosomes*. Cell, 2005. **122**(5): p. 735-49.
142. Flores-Rodriguez, N., et al., *Roles of dynein and dynactin in early endosome dynamics revealed using automated tracking and global analysis*. PLoS One, 2011. **6**(9): p. e24479.
143. Le Blanc, I., et al., *Endosome-to-cytosol transport of viral nucleocapsids*. Nat Cell Biol, 2005. **7**(7): p. 653-64.
144. Lin, S.X., G.G. Gundersen, and F.R. Maxfield, *Export from pericentriolar endocytic recycling compartment to cell surface depends on stable, detyrosinated (glu) microtubules and kinesin*. Mol Biol Cell, 2002. **13**(1): p. 96-109.
145. Maritzen, T. and V. Haucke, *Gadkin: A novel link between endosomal vesicles and microtubule tracks*. Commun Integr Biol, 2010. **3**(4): p. 299-302.
146. Mercer, J., M. Schelhaas, and A. Helenius, *Virus entry by endocytosis*. Annu Rev Biochem, 2010. **79**: p. 803-33.

147. Vonderheit, A. and A. Helenius, *Rab7 associates with early endosomes to mediate sorting and transport of Semliki forest virus to late endosomes*. PLoS Biol, 2005. **3**(7): p. e233.
148. Chu, J.J., P.W. Leong, and M.L. Ng, *Analysis of the endocytic pathway mediating the infectious entry of mosquito-borne flavivirus West Nile into Aedes albopictus mosquito (C6/36) cells*. Virology, 2006. **349**(2): p. 463-75.
149. Bernard, E., et al., *Endocytosis of chikungunya virus into mammalian cells: role of clathrin and early endosomal compartments*. PLoS One, 2010. **5**(7): p. e11479.
150. Quirin, K., et al., *Lymphocytic choriomeningitis virus uses a novel endocytic pathway for infectious entry via late endosomes*. Virology, 2008. **378**(1): p. 21-33.
151. White, J., K. Matlin, and A. Helenius, *Cell fusion by Semliki Forest, influenza, and vesicular stomatitis viruses*. J Cell Biol, 1981. **89**(3): p. 674-9.
152. Takikawa, S., et al., *Cell fusion activity of hepatitis C virus envelope proteins*. J Virol, 2000. **74**(11): p. 5066-74.
153. Bossart, K.N., et al., *Functional expression and membrane fusion tropism of the envelope glycoproteins of Hendra virus*. Virology, 2001. **290**(1): p. 121-35.
154. Shinn-Thomas, J.H., V.L. Scranton, and W.A. Mohler, *Quantitative assays for cell fusion*. Methods Mol Biol, 2008. **475**: p. 347-61.
155. Helenius, A., et al., *On the entry of Semliki forest virus into BHK-21 cells*. J Cell Biol, 1980. **84**(2): p. 404-20.
156. Clemente, R. and J.C. de la Torre, *Cell entry of Borna disease virus follows a clathrin-mediated endocytosis pathway that requires Rab5 and microtubules*. J Virol, 2009. **83**(20): p. 10406-16.
157. Saeed, M.F., et al., *Cellular entry of ebola virus involves uptake by a macropinocytosis-like mechanism and subsequent trafficking through early and late endosomes*. PLoS Pathog, 2010. **6**(9): p. e1001110.
158. Rojek, J.M., et al., *Different mechanisms of cell entry by human-pathogenic Old World and New World arenaviruses*. J Virol, 2008. **82**(15): p. 7677-87.
159. Kim, C. and J.M. Bergelson, *Echovirus 7 entry into polarized intestinal epithelial cells requires clathrin and Rab7*. MBio, 2012. **3**(2).
160. Pasqual, G., et al., *Old world arenaviruses enter the host cell via the multivesicular body and depend on the endosomal sorting complex required for transport*. PLoS Pathog, 2011. **7**(9): p. e1002232.
161. Garry, C.E. and R.F. Garry, *Proteomics computational analyses suggest that the carboxyl terminal glycoproteins of Bunyaviruses are class II viral fusion protein (beta-penetrenes)*. Theor Biol Med Model, 2004. **1**: p. 10.
162. Tischler, N.D., et al., *Hantavirus Gc glycoprotein: evidence for a class II fusion protein*. J Gen Virol, 2005. **86**(Pt 11): p. 2937-47.
163. Vaney, M.C. and F.A. Rey, *Class II enveloped viruses*. Cell Microbiol. **13**(10): p. 1451-9.
164. Sapir, A., et al., *Viral and Developmental Cell Fusion Mechanisms: Conservation and Divergence*. Developmental Cell, 2008. **14**(1): p. 11-21.
165. Filone, C.M., et al., *Development and characterization of a Rift Valley fever virus cell-cell fusion assay using alphavirus replicon vectors*. Virology, 2006. **356**(1-2): p. 155-64.
166. Towner, J.S., et al., *Generation of eGFP expressing recombinant Zaire ebolavirus for analysis of early pathogenesis events and high-throughput antiviral drug screening*. Virology, 2005. **332**(1): p. 20-7.
167. Khetawat, D. and C.C. Broder, *A functional henipavirus envelope glycoprotein pseudotyped lentivirus assay system*. Virol J, 2010. **7**: p. 312.

168. Wilson, J.A., et al., *Epitopes Involved in Antibody-Mediated Protection from Ebola Virus*. Science, 2000. **287**(5458): p. 1664-1666.
169. Zhang, J.H., T.D. Chung, and K.R. Oldenburg, *A Simple Statistical Parameter for Use in Evaluation and Validation of High Throughput Screening Assays*. J Biomol Screen, 1999. **4**(2): p. 67-73.
170. Choudhury, A., et al., *Rab proteins mediate Golgi transport of caveola-internalized glycosphingolipids and correct lipid trafficking in Niemann-Pick C cells*. J Clin Invest, 2002. **109**(12): p. 1541-50.
171. Ramos-Vara, J.A. and M.E. Beissenherz, *Optimization of immunohistochemical methods using two different antigen retrieval methods on formalin-fixed paraffin-embedded tissues: experience with 63 markers*. J Vet Diagn Invest, 2000. **12**(4): p. 307-11.
172. Garrison, A.R., et al., *Development of a TaqMan minor groove binding protein assay for the detection and quantification of Crimean-Congo hemorrhagic fever virus*. Am J Trop Med Hyg, 2007. **77**(3): p. 514-20.
173. Panchal, R.G., et al., *Development of high-content imaging assays for lethal viral pathogens*. J Biomol Screen, 2010. **15**(7): p. 755-65.
174. Panchal, R.G., et al., *Identification of an antioxidant small-molecule with broad-spectrum antiviral activity*. Antiviral Res, 2011. **93**(1): p. 23-9.
175. Filone, C.M., et al., *Rift valley fever virus infection of human cells and insect hosts is promoted by protein kinase C epsilon*. PLoS One, 2010. **5**(11): p. e15483.
176. Ljosa, V. and A.E. Carpenter, *Introduction to the quantitative analysis of two-dimensional fluorescence microscopy images for cell-based screening*. PLoS Comput Biol, 2009. **5**(12): p. e1000603.
177. Brass, A.L., et al., *Identification of host proteins required for HIV infection through a functional genomic screen*. Science, 2008. **319**(5865): p. 921-6.
178. Ibig-Rehm, Y., et al., *High-content screening to distinguish between attachment and post-attachment steps of human cytomegalovirus entry into fibroblasts and epithelial cells*. Antiviral Research, 2011. **89**(3): p. 246-256.
179. Krishnan, M.N., et al., *RNA interference screen for human genes associated with West Nile virus infection*. Nature, 2008. **455**(7210): p. 242-5.
180. Shariff, A., et al., *Automated image analysis for high-content screening and analysis*. J Biomol Screen. **15**(7): p. 726-34.
181. Spurgers, K.B., et al., *Identification of essential filovirion-associated host factors by serial proteomic analysis and RNAi screen*. Mol Cell Proteomics. **9**(12): p. 2690-703.
182. Mercer, J. and A. Helenius, *Vaccinia virus uses macropinocytosis and apoptotic mimicry to enter host cells*. Science, 2008. **320**(5875): p. 531-5.
183. Sun, X., et al., *Role of clathrin-mediated endocytosis during vesicular stomatitis virus entry into host cells*. Virology, 2005. **338**(1): p. 53-60.
184. Empig, C.J. and M.A. Goldsmith, *Association of the caveola vesicular system with cellular entry by filoviruses*. J Virol, 2002. **76**(10): p. 5266-70.
185. Bhattacharyya, S., et al., *Ebola virus uses clathrin-mediated endocytosis as an entry pathway*. Virology, 2010. **401**(1): p. 18-28.
186. Bhattacharyya, S., T.J. Hope, and J.A. Young, *Differential requirements for clathrin endocytic pathway components in cellular entry by Ebola and Marburg glycoprotein pseudovirions*. Virology, 2011. **419**(1): p. 1-9.
187. Nanbo, A., et al., *Ebolavirus is internalized into host cells via macropinocytosis in a viral glycoprotein-dependent manner*. PLoS Pathog, 2010. **6**(9): p. e1001121.

188. Aleksandrowicz, P., et al., *Ebola virus enters host cells by macropinocytosis and clathrin-mediated endocytosis*. J Infect Dis, 2011. **204 Suppl 3**: p. S957-67.
189. Aoki, T., et al., *Internalization of caveolae and their relationship with endosomes in cultured human and mouse endothelial cells*. Anatomical Science International, 2007. **82**(2): p. 82-97.
190. Galloway, C.J., et al., *Acidification of macrophage and fibroblast endocytic vesicles in vitro*. Proc Natl Acad Sci U S A, 1983. **80**(11): p. 3334-8.
191. Carneiro, F.A., A.S. Ferradosa, and A.T. Da Poian, *Low pH-induced conformational changes in vesicular stomatitis virus glycoprotein involve dramatic structure reorganization*. J Biol Chem, 2001. **276**(1): p. 62-7.
192. Bucci, C., et al., *Rab7: a key to lysosome biogenesis*. Mol Biol Cell, 2000. **11**(2): p. 467-80.
193. Li, W., et al., *Angiotensin-converting enzyme 2 is a functional receptor for the SARS coronavirus*. Nature, 2003. **426**(6965): p. 450-4.
194. Jeffers, S.A., et al., *CD209L (L-SIGN) is a receptor for severe acute respiratory syndrome coronavirus*. Proc Natl Acad Sci U S A, 2004. **101**(44): p. 15748-53.
195. Grove, J. and M. Marsh, *The cell biology of receptor-mediated virus entry*. J Cell Biol, 2011. **195**(7): p. 1071-82.
196. Stremlau, M., et al., *The cytoplasmic body component TRIM5alpha restricts HIV-1 infection in Old World monkeys*. Nature, 2004. **427**(6977): p. 848-53.
197. Grutter, M.G. and J. Luban, *TRIM5 structure, HIV-1 capsid recognition, and innate immune signaling*. Curr Opin Virol, 2012. **2**(2): p. 142-50.
198. Luban, J., *TRIM5 and the Regulation of HIV-1 Infectivity*. Mol Biol Int, 2012. **2012**: p. 426840.
199. Shankavaram, U.T., et al., *Transcript and protein expression profiles of the NCI-60 cancer cell panel: an integromic microarray study*. Mol Cancer Ther, 2007. **6**(3): p. 820-32.
200. Radoshitzky, S.R., et al., *Transferrin receptor 1 is a cellular receptor for New World haemorrhagic fever arenaviruses*. Nature, 2007. **446**(7131): p. 92-6.
201. Gibbons, D.L., et al., *Conformational change and protein-protein interactions of the fusion protein of Semliki Forest virus*. Nature, 2004. **427**(6972): p. 320-5.
202. Huotari, J. and A. Helenius, *Endosome maturation*. EMBO J, 2011. **30**(17): p. 3481-500.
203. Brindley, M.A., et al., *Tyrosine kinase receptor Axl enhances entry of Zaire ebolavirus without direct interactions with the viral glycoprotein*. Virology, 2011. **415**(2): p. 83-94.
204. Bonaparte, M.I., et al., *Ephrin-B2 ligand is a functional receptor for Hendra virus and Nipah virus*. Proc Natl Acad Sci U S A, 2005. **102**(30): p. 10652-7.
205. Hovanessian, A.G., et al., *Surface expressed nucleolin is constantly induced in tumor cells to mediate calcium-dependent ligand internalization*. PLoS One. **5**(12): p. e15787.
206. Lupberger, J., et al., *EGFR and EphA2 are host factors for hepatitis C virus entry and possible targets for antiviral therapy*. Nat Med. **17**(5): p. 589-95.
207. Khan, M., et al., *Assessment of in vitro prophylactic and therapeutic efficacy of chloroquine against Chikungunya virus in vero cells*. J Med Virol. **82**(5): p. 817-24.
208. Connolly-Andersen, A.M., et al., *Creaman Congo hemorrhagic fever virus infects human monocyte-derived dendritic cells*. Virology, 2009. **390**(2): p. 157-62.
209. Kondo, Y., et al., *Hepatitis C virus infects T cells and affects interferon-gamma signaling in T cell lines*. Virology, 2007. **361**(1): p. 161-73.
210. Gallo, R.C., et al., *The human T-cell leukemia virus family, adult T cell leukemia, and AIDS*. Haematol Blood Transfus, 1985. **29**: p. 317-25.
211. Neuhiel, B., et al., *Glycoprotein gp110 of Epstein-Barr virus determines viral tropism and efficiency of infection*. Proc Natl Acad Sci U S A, 2002. **99**(23): p. 15036-41.

212. Erickson, B.R., et al., *N-linked glycosylation of Gn (but not Gc) is important for Crimean Congo hemorrhagic fever virus glycoprotein localization and transport*. Virology, 2007. **361**(2): p. 348-55.
213. Flick, R., et al., *Reverse genetics for crimean-congo hemorrhagic fever virus*. J Virol, 2003. **77**(10): p. 5997-6006.
214. Klimstra, W.B., K.D. Ryman, and R.E. Johnston, *Adaptation of Sindbis virus to BHK cells selects for use of heparan sulfate as an attachment receptor*. J Virol, 1998. **72**(9): p. 7357-66.
215. Okamoto, K., et al., *Dengue virus strain DEN2 16681 utilizes a specific glycochain of syndecan-2 proteoglycan as a receptor*. J Gen Virol, 2011. **93**(Pt 4): p. 761-70.
216. Krueger, D.K., et al., *Variations in disparate regions of the murine coronavirus spike protein impact the initiation of membrane fusion*. J Virol, 2001. **75**(6): p. 2792-802.
217. Gallagher, T.M., C. Escarmis, and M.J. Buchmeier, *Alteration of the pH dependence of coronavirus-induced cell fusion: effect of mutations in the spike glycoprotein*. J Virol, 1991. **65**(4): p. 1916-28.
218. Ergonul, O., *Clinical and pathological features of Crimean-Congo hemorrhagic fever virus*. 2007: Springer.
219. Bell-Sakyi, L., et al., *Tick Cell Lines for Study of Crimean-Congo Hemorrhagic Fever Virus and Other Arboviruses*. Vector Borne Zoonotic Dis.

